DISS. ETH NO. 19074

Phage-derived human monoclonal antibody fragments to vascular endothelial growth factor-C that block its interaction with VEGF receptor-2 and -3.

A dissertation submitted to
ETH ZURICH

for the degree of
Doctor of Sciences

presented by
Matthias Andreas Rinderknecht
Dipl. Natw. ETH, ETH Zurich
Born March 23, 1979
Citizen of Wallisellen (ZH) and Turgi (AG)

Accepted on the recommendation of

Prof. Dr. Michael Detmar, examiner
Prof. Dr. Dario Neri, co-examiner

2010

Table of Contents

1. Summary

1.1. Summary

Tumor metastasis represents the hallmark of malignancy in cancer and accounts for the majority of cancer deaths. Metastasis of the primary tumor happens via two main routes, the blood vascular and the lymphatic system. For several decades, lymphatic metastasis was considered a rather passive process, where tissue-invading cancer cells encounter preexisting lymphatic vessels and are then taken up and drained to lymph nodes. However, the recent progress in the identification of lymphatic vessel-specific markers, as well as the identification of lymphatic growth factors, have enabled experimental studies in rodents that have provided compelling evidence for an active role of tumor-induced lymphangiogenesis in the promotion of lymph node metastasis. Lymphangiogenesis is the growth of lymphatic vessels from preexisting ones and the extent of lymphangiogenesis in cancers such as malignant melanoma has been shown to be a predictor of disease progression and survival. Vascular endothelial growth factor-C (VEGF-C) is a key mediator of lymphangiogenesis, acting via its receptors VEGF-R2 and VEGF-R3. High expression of VEGF-C in tumors correlates with increased lymphatic vessel density, lymphatic vessel invasion, sentinel lymph node metastasis and poor prognosis. Recently, it was found that in a chemically induced skin carcinoma model, increased VEGF-C drainage from the tumor enhanced lymphangiogenesis in the sentinel lymph node and facilitated metastatic spread of cancer cells via the lymphatics and beyond. Hence, interference with the VEGF-C / VEGF-R3 axis holds promise to block metastatic spread, as recently shown by use of a neutralizing anti-VEGF-R3 antibody and a soluble VEGF-R3 (VEGF-C/D trap).

We have therefore set out to generate an antibody fragment that could inhibit the binding of VEGF-C to its receptors. By antibody phage-display, we panned the

ETH-2 Gold antibody phage-display library against the fully processed mature form of human VEGF-C, ΔNΔC-VEGF-C. We identified 4 single-chain Fragment variable (scFv) clones that bound with high specificity and double to triple digit nanomolar affinity to the fully processed mature form of human VEGF-C. One of the 4 clones was specific only for *Pichia pastoris*-derived human ΔNΔC-VEGF-C, which was used for the panning, while the other 3 clones also bound to mammalian cell-derived human ΔNΔC-VEGF-C. By affinity maturation using degenerate PCR, we subsequently improved the affinity of lead binder VC2 about 4-fold to 22 nM (clone VC2.2.2). VC2.2.2 dose-dependently inhibited the interaction of VEGF-C with VEGF-R2 and VEGF-R3 as shown by BIAcore and ELISA analyses, which hinted to an interaction of VC2.2.2 with the receptor-binding domain on ΔNΔC-VEGF-C. This finding was further corroborated by an epitope mapping experiment using a peptide microarray, where VC2.2.2-scFv bound to an epitope located partly in the VEGF receptor-binding region on ΔNΔC-VEGF-C. We also found that panning against VEGF-C by means of antibody phage-display favored the selection of variable heavy (V_H) domains that contained mutations typical for V_HH domains of camelid heavy chain-only antibodies; these single-nucleotide transitional mutations lead to the substitution of hydrophobic with more hydrophilic amino acid residues in the variable heavy / variable light interface and enhanced the solubility of the V_H as shown by size-exclusion gel-filtration profiles. We could finally show that the anti-VEGF-C V_H is sufficient for binding to VEGF-C, which reduced the size of the potentially VEGF-C-blocking antibody fragment to less than 14.6 kDa. Taken together, we conclude that anti-VEGF-C V_H-based immunoproteins hold promise to block the lymphangiogenic activity of VEGF-C, which would present a significant advance in inhibiting lymphatic-based metastatic spread of certain cancer types.

1.2. Zusammenfassung

Die Metastasierung von Tumoren ist das typische Kennzeichen von bösartigem Krebs und ist für den Grossteil der krebsbedingten Todesfälle verantwortlich. Sie geschieht via zwei Hauptrouten, über das Blutgefässsystem sowie das lymphatische Gefässsystem. Lange Zeit wurde die Metastasierung via Lymphgefässe als passiver Prozess betrachtet, in welchem losgelöste Krebszellen im Gewebe zufällig auf bereits schon existierende lymphatische Gefässe treffen, aufgenommen werden und zu den Lymphknoten transportiert werden. In jüngster Zeit wurden jedoch spezifische Marker und Wachstumsfaktoren für lymphatische Gefässe entdeckt, welche es ermöglicht haben, gezielte Tierversuche in Nagetieren durchzuführen. Diese Experimente haben Beweise dafür erbracht, dass die tumor-induzierte Lymphangiogenese in der Begünstigung der Metastasierung des Tumors zum Lymphknoten hin eine aktive Rolle spielt. Lymphangiogenese beschreibt das Ausknospen und Wachsen von neuen lymphatischen Gefässen aus schon existierenden Lymphgefässen. Das Ausmass der Lymphangiogenese in gewissen Krebsarten wie dem bösartigen Melanom ist ein negativer prognostischer Faktor für das Fortschreiten der Krebserkankung und das Überleben des Patienten. Der Vaskuläre Endotheliale Wachstumsfaktor C (vascular endothelial growth factor-C, VEGF-C) wirkt via die Rezeptoren VEGF-R2 und VEGF-R3 und ist einer der bedeutendsten Promotoren der Lymphangiogenese. Eine vermehrte Expression von VEGF-C in Tumoren korreliert mit erhöhter lymphatischer Gefässdichte, der Invasion von Lymphgefässen, der Metastasierung in die Sentinel-Lymphknoten sowie ungünstiger Prognose. Vor kurzem wurde in einem Tiermodell mit chemisch-induziertem Hautkrebs die Beobachtung gemacht, dass vermehrte Drainage von tumor-sekretiertem VEGF-C die Lymphangiogenese im Sentinel-Lymphknoten

erhöht und die Metastasierung von Krebszellen via Lymphgefässe und schliesslich weiter entfernte Organe fördert. Ein Eingriff in die VEGF-C / VEGF-R3 Achse stellt daher eine vielversprechende Möglichkeit zur Verhinderung der lymphatischen Metastasierung dar. Dies wurde kürzlich gezeigt mithilfe von neutralisierenden Antikörpern gegen VEGF-R3 sowie einem löslichen VEGF-R3 Konstrukt.

Das Ziel dieser Dissertation war es deshalb, ein Antikörper-Fragment gegen VEGF-C zu generieren, welches die Bindung von VEGF-C an seine Rezeptoren verhindern kann. Mittels Antikörper Phagen-Display haben wir die ETH-2 Gold Antikörper Phagen-Display Bibliothek auf spezifisch an humanes ΔNΔC-VEGF-C bindende Antikörperfragmente durchsucht. ΔNΔC-VEGF-C stellt die vollständig prozessierte, wirkungsstärkste Variante von VEGF-C dar. Dabei haben wir 4 Einzelkettenfragment-Klone (single-chain Fragment variable, scFv) gefunden, welche mit hoher Spezifität und zwei- bis dreistelliger nanomolarer Affinität an humanes VEGF-C binden. Einer dieser 4 Klone bindet nur an humanes ΔNΔC-VEGF-C produziert in der Hefe *Pichia pastoris*, welches für die Antikörper-Selektion benutzt wurde. Die übrigen 3 Klone binden auch an humanes ΔNΔC-VEGF-C produziert in Säugerzellen. Durch Affinitäts-Reifung mittels PCR mit degenerierten Primern verbesserten wir die Affinität des Ursprungsklons VC2 ungefähr vierfach auf 22 nM (Klon VC2.2.2). VC2.2.2 inhibiert die Interaktion von VEGF-C mit VEGF-R2 und VEGF-R3 dosisabhängig, wie wir mit Oberflächenplasmonresonanz und ELISA zeigen konnten. Diese blockierende Wirkung weist auf eine Interaktion von VC2.2.2 mit der rezeptorbindenden Domäne auf ΔNΔC-VEGF-C hin. Ein Experiment zur Epitopkartierung mittels Peptid-Chip untermauerte diese These. VC2.2.2 bindet an ein Epitop, welches teilweise in derjenigen Region auf ΔNΔC-VEGF-C liegt, die an die VEGF Rezeptoren bindet. Ausserdem stellten wir fest, dass das Anreichern von

Antikörperfragmenten gegen VEGF-C mittels Antikörper Phagen-Display die Selektion spezieller Mutationen in der variablen Domäne der schweren Immunglobulinkette (variable heavy domain, V_H) fördert. Wir fanden Mutationen in den V_H, welche typisch für V_HH Domänen der natürlich vorkommenden Schwere-Ketten-Antikörpern von Kameliden sind. Die festgestellten transitionalen Einzelnukleotidmutationen führen dabei zur Substitution von hydrophoben mit hydrophileren Aminosäuren in der Berührungsfläche der leichten und schweren variablen Domäne, was die Löslichkeit der V_H erhöht, wie wir mit Grössenausschlusschromatographie zeigen konnten. Schliesslich konnten wir zeigen, dass die weniger als 14.6 kDa grosse schwere variable Domäne (V_H) von VC2.2.2 für die Bindung an VEGF-C ausreicht. Zusammenfassend halten wir fest, dass Immunoproteine basierend auf der V_H von anti-VEGF-C VC2.2.2 das Potential zur Blockierung der lymphangiogenen Wirkung von VEGF-C haben, was einen signifikanten Fortschritt bei der Verhinderung der lymphatischen Metastasierung gewisser Krebsarten bedeuten würde.

2. Introduction

2.1. Lymphatic system

2.1.1. History, function and constituents of the lymphatic system

The existence of a second vessel system besides the blood vascular circulatory pathway in vertebrates has been noted already in 1627, when the Italian anatomist Gasparo Aselli reported “milky veins” in the mesentery of a well-fed dog (Aselli 1627). Although he described lymphatic vessels in a very accurate way, unknowingly referring to their role in lipid uptake when using the word “milky” in his observation, the function of the lymphatic system remained a mystery to him and others and was not further described for the next three centuries. In the 20th century, the function of the lymphatic system was discovered. Unlike the closed blood vascular circulatory system centrally driven by the heart, the lymphatic system is an open vessel system with no active transport. The blood vasculature transports oxygen and nutrients to the cells and carries away metabolic waste products and carbon dioxide, and also transports hormones and immune cells as well as platelets. The lymphatic system, however, acts as the body’s main drainage system. Interstitial fluid, also called lymph, is a protein-rich exudate that leaks from the blood capillaries into the interstitial space. From there, it enters the lymphatic capillaries through the loosely connected endothelium on their blind-ended tips and further drains to lymph nodes, larger collecting lymphatic capillaries and finally the thoracic duct, from which the lymph is returned to the blood circulation via the left subclavian vein. The transport of the lymph in lymphatic vessels is driven by peristaltic pulsation of neighbouring arteries, the action of skeletal muscles in the proximity and the contraction of smooth muscle cells covering larger lymphatic vessels (Zorzetto *et al.* 1977). Unidirectional flow of the lymph is assured by valves in the lumen of larger

lymphatic vessels (Lynch *et al.* 2007). In the intestine, the lymphatic capillaries within the villi mediate the uptake of dietary lipids and the fat-soluble vitamins A, D, E and K (Cueni *et al.* 2006). The role of the lymphatic system in immune surveillance of the body is accomplished by the lymphoid organs, such as lymph nodes, spleen, tonsils, thymus and Peyer's patches (Alitalo *et al.* 2005; Cueni *et al.* 2006). Immune cells such as activated Langerhans cells from the skin travel through lymphatic vessels to regional lymph nodes, where they can present foreign antigens to other immune cells and start an immune response (Randolph *et al.* 2005).

To optimally fulfill their function, lymphatic capillaries are highly permeable. This is achieved by the lack of a tight basement membrane and pericytes as opposed to the case in blood capillaries. The lymphatic capillaries consist only of a rather loosely jointed single layer of endothelial cells that are on the abluminal side connected to the surrounding extra-cellular matrix by anchoring filaments. These anchoring filaments act as a sensor for interstitial pressure and cause the lymphatics to dilate and get more permeable when the hydrostatic pressure increases (Gerli *et al.* 2000), thereby preventing lymphedema. Larger collecting lymphatic vessels possess a basal membrane and are covered with smooth muscle cells.

2.1.2. Lymphatic growth factors and receptors

VEGF-C and VEGF-D were the first lymphangiogenic growth factors to be identified (Joukov *et al.* 1996; Orlandini *et al.* 1996; Yamada *et al.* 1997; Achen *et al.* 1998). They bind to and activate VEGF-R3, in the adult exclusively expressed on lymphatic endothelial cells (LECs) but not blood vascular endothelial cells (BECs) under normal conditions. Proteolytically processed forms of VEGF-C and VEGF-D increase their affinity for VEGF-R3 and can, in the fully processed form, also bind to

and activate VEGF-R2, which is present on both LECs and BECs. Activation of VEGF-R2 and / or VEGF-R3 leads to LEC proliferation, migration and survival *in vitro* and lymphangiogenesis as well as angiogenesis. VEGF-C and -D can also bind to neuropilin-2 (Nrp-2), a coreceptor of VEGF-R2 and -R3, which is thought to modulate VEGF-R activation (Fig. 2.1) (Favier *et al.* 2006; Karpanen *et al.* 2006).

More recently, hepatocyte growth factor was identified as a potent lymphangiogenic factor *in vitro* and *in vivo*, acting via its receptor c-met (Kajiya *et al.* 2005). The relative contribution of direct versus indirect effects of hepatocyte growth factor—via activation of the VEGF-R3 (Cao *et al.* 2006)—under different *in vivo* conditions remains to be investigated. Angiopoietin-1, a ligand for the endothelial cell-specific receptor Tie2 (Davis *et al.* 1996), was recently shown to also induce lymphangiogenesis after viral or transgenic delivery to the skin of mice (Morisada *et al.* 2005; Tammela *et al.* 2005). The role of angiopoietin-2, another ligand of the Tie2 receptor, in lymphangiogenesis remains at present unclear. However, mice deficient in angiopoietin-2 are characterized by lymphedema and abnormal lymphatic vessel development (Gale *et al.* 2002). A number of additional growth factors with known activities on blood vascular endothelium have recently been found to also promote lymphangiogenesis (Fig. 2.1). These factors include fibroblast growth factor-2 (Kubo *et al.* 2002; Chang *et al.* 2004; Shin *et al.* 2006), platelet-derived growth factors (Cao *et al.* 2004) and insulin-like growth factors (Bjorndahl *et al.* 2005). Very recently, it was shown that the known vasodilator adrenomedullin, acting via calcitonin receptor-like receptor (calcrl) and receptor activity-modifying protein-2 (RAMP2), also promotes lymphangiogenesis (Fritz-Six *et al.* 2008). The relative contribution of each

of these factors towards physiological and pathological lymphangiogenesis remains to be established.

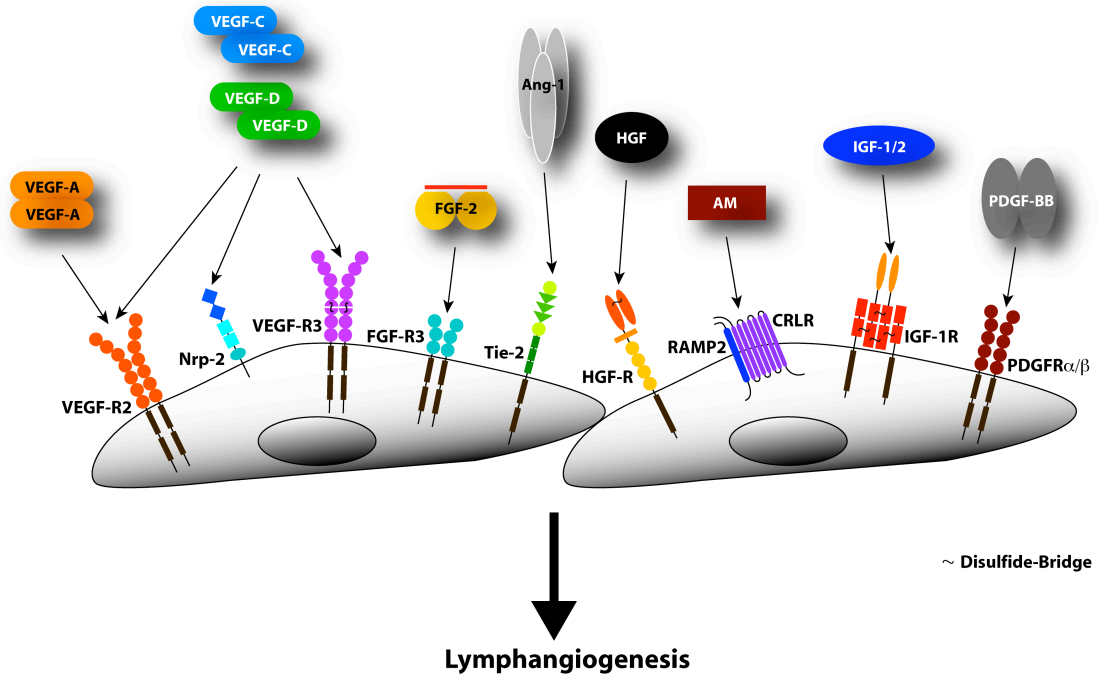

Figure 2.1. Lymphangiogenic growth factors and their cognate receptors. AM, adrenomedullin; Ang-1, angiopoietin-1; CRLR, calcitonin receptor-like receptor; FGF(-R), fibroblast growth factor (receptor); HGF(-R), hepatocyte growth factor (receptor); IGF(-R), insulin-like growth factor (receptor); Nrp2, neuropilin-2; PDGF-BB, platelet-derived growth factor-BB; PDGFR, platelet-derived growth factor receptor; RAMP2, receptor activity modifying protein 2; Tie-2, tunica internal endothelial cell kinase-2; VEGF(-R), vascular endothelial growth factor (receptor). Reprinted from Rinderknecht *et al.* 2008.

2.2. VEGF-C

2.2.1. Discovery

VEGF-C was discovered in 1996 by screening for VEGF-R3 (at that time still called Fms-like tyrosine kinase 4, Flt-4) ligands and cloned from a cDNA library prepared from human prostatic adenocarcinoma cell line PC-3 (Joukov *et al.* 1996). At first, two proteins of 23 kDa (major peak) and 32 kDa (minor peak) were described. Upon cloning of the VEGF-C gene and examination of the 350 amino acid (aa) open reading frame (ORF), it became clear that the newly cloned Flt-4 ligand shares all eight typical cysteine residues (McDonald *et al.* 1993) and several other residues with members of the VEGF/PDGF family of growth factors (Fig. 2.7). The Flt-4 ligand was therefore classified as a new member of the VEGF family and renamed as VEGF-C. The predicted molecular mass for the VEGF-C protein was calculated to be about 36 kDa and it was suggested that VEGF-C might first be translated into a precursor, from which the mature ligand of 23 kDa is derived by proteolytic cleavage. The 23 kDa form of VEGF-C was shown to be able to induce autophosphorylation of VEGF-R3 and also VEGF-R2. One year later, the proteolytic processing of VEGF-C was unraveled (Joukov *et al.* 1997).

2.2.2. Molecular properties

VEGF-C is encoded by the VEGFC gene located near the end of the long arm of chromosome 4, at 4q34. It consists of seven exons (Paavonen *et al.* 1996). VEGF-C is translated as a precursor spanning 419 residues (NP_005420) (Fig. 2.2), residues Met1 to Ala31 form the secretion signal peptide, Phe32 to Arg102 (or Ala111) compose the N-terminal propeptide, Thr103 (or Ala112) to Arg227 form the

fully processed mature ΔNΔC VEGF-C (the VEGF homology domain, VHD) and Ser228 to Ser419 make up the C-terminal propeptide. The intracellular C-terminal processing of the precursor VEGF-C is accomplished by proprotein convertases (PCs) furin, PC5 and PC7 (Siegfried *et al.* 2003). These PCs have dibasic specific recognition sites exhibiting the general motif (K/R)-$(X)_n$-(K/R)↓, where n = 0, 2, 4, or 6, and where K is lysine, R is arginine, and X is any amino acid. The C-terminal end of the VHD consists of such a motif, namely HSIIRR^{227}SL, and it is cleaved after Arg227 (Fig. 2.2). N-terminal processing occurs extracellularly and is mediated by the serine protease plasmin (McColl *et al.* 2003), which can cleave either between Arg102 and Thr103 or between Ala111 and Ala112. Plasmin can also cleave off the C-terminal propeptide, at the same site as PCs.

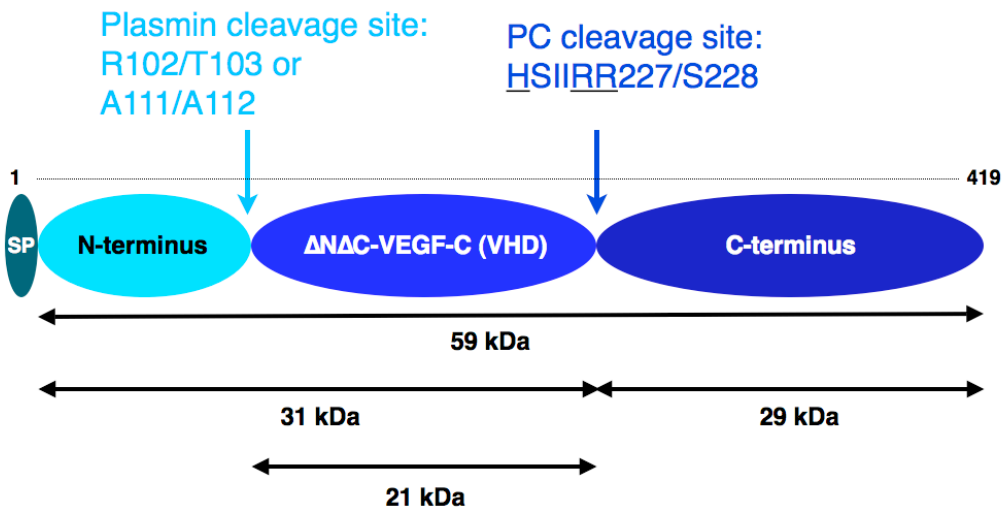

Figure 2.2. VEGF-C proprotein convertase (PC) and plasmin cleavage sites. SP: signal peptide; VHD: VEGF homology domain. The PC recognition motif is underlined. Modified from Siegfried *et al.* 2003.

Three potential N-linked glycosylation sites at asparagine residues 175, 205 and 240 are present, the first two sites are located within the VHD (Fig. 2.3). As a result of glycosylation, the apparent molecular masses of the different VEGF-C forms

are higher than calculated from the aa sequence. The fully processed ΔNΔC VEGF-C migrates e.g. as a 21 kDa band on SDS-PAGE under reducing conditions, while the calculated mass is only 14.1 kDa.

During the secretion and processing stages, VEGF-C is dimerized in an antiparallel fashion by two interchain disulfide bonds at Cys156 and Cys165 (Fig. 2.3), although mature VEGF-C has been described as a mixture of covalently and non-covalently bound dimers (Joukov *et al.* 1996; Jeltsch *et al.* 2006). Several intrachain disulfide bonds form the typical cystine-knot motif common for all VEGFs (Vitt *et al.* 2001; Muller *et al.* 2002). The complex processing and disulfide bond patterns lead to a variety of partially and fully processed VEGF-C isoforms of different sizes (Fig. 2.3).

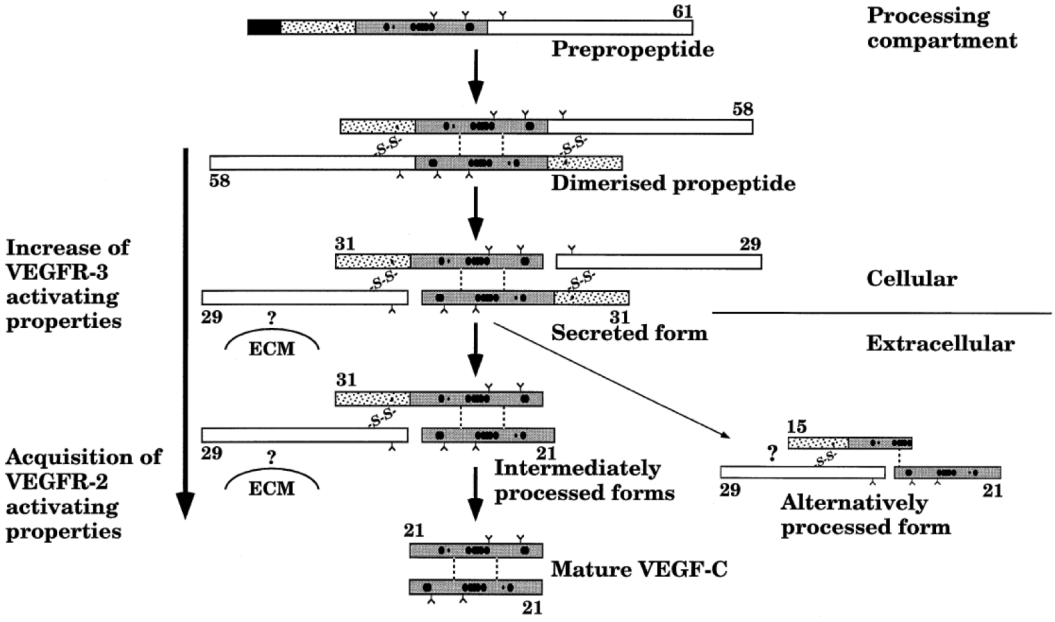

Figure 2.3. Schematic model of the proteolytic processing of VEGF-C. The regions of the VEGF-C polypeptide are marked as follows: signal sequence, black box; VEGF homology domain, grey box; N-terminal and C-terminal propeptides, dotted and open boxes, respectively. Sites of N-linked glycosylation are marked with a "Y". Numbers indicate molecular mass (kDa) of the corresponding polypeptide in reducing conditions. Disulfide bonds are marked as -S-S-; non-covalent bonds as

dotted lines. The hypothetical binding of the C-terminal domain to the extracellular matrix (ECM), and the proposed structure of the alternatively processed VEGF-C are indicated with question marks. The proteolytic generation of a small fraction of disulfide-linked 21 kDa forms is not indicated in the figure. Several intermediate forms are also omitted to simplify the scheme. Reprinted from Joukov *et al.* 1997.

Recently, the three-dimensional crystal structure of ΔNΔC-VEGF-C in complex with one of its receptors, VEGF-R2, was solved by X-ray diffraction (Leppanen *et al.* 2010). The receptor-binding domains of VEGF-C were mapped to two sites consisting of three loops and part of the N-terminal helix on VEGF-C (Fig. 2.4 A). Site 1 is composed of the N-terminal helix alpha1 (His113 – Thr129, residues in contact with VEGF-R2 are Asp123, Trp126, Arg127 and Gln130) and the loop L2 (Asn167 – Leu171, residues in contact are Asn167, Ser168, Glu169, Gly170 and Leu171). Site 2 consists of the loops L1 (Asp139 – Pro155, residues in contact with VEGF-R2 are Thr148, Asn 149, Phe151 and Lys153) and L3 (Ile188 – Pro196, residues in contact are Phe186, Ile188, Val190, Pro191, Leu192, Ser193, Gly195 and Pro196), held together by hydrogen bonding. Site 1 is provided by one VEGF-C monomer, while site 2 comes from the antiparallel second VEGF-C monomer (Leppanen *et al.* 2010) (Fig. 2.4 B). They combine to make contact to two closely spaced sites on VEGF-R2, located on domains D2 and D3 (Fig. 2.5).

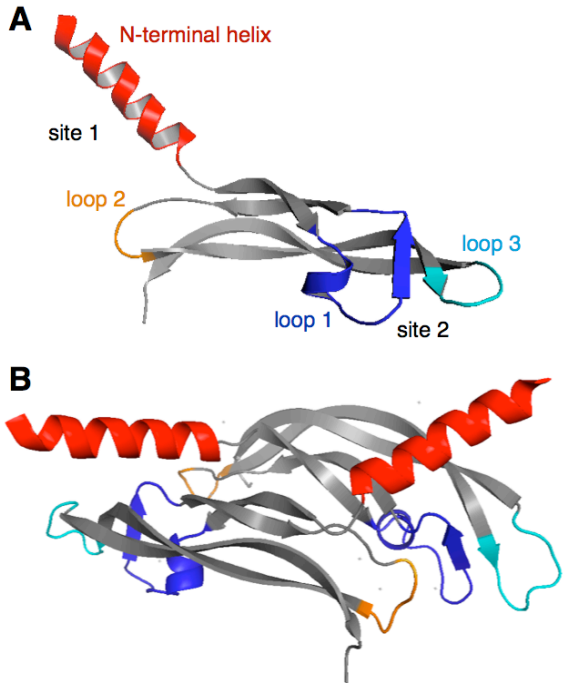

Figure 2.4. VEGF-R binding sites on VEGF-C. Binding sites are defined as in Leppanen *et al.* 2010, projected on the pdb file 2X1X (www.pdb.org). A: monomer. B: antiparallel dimer. Original artwork.

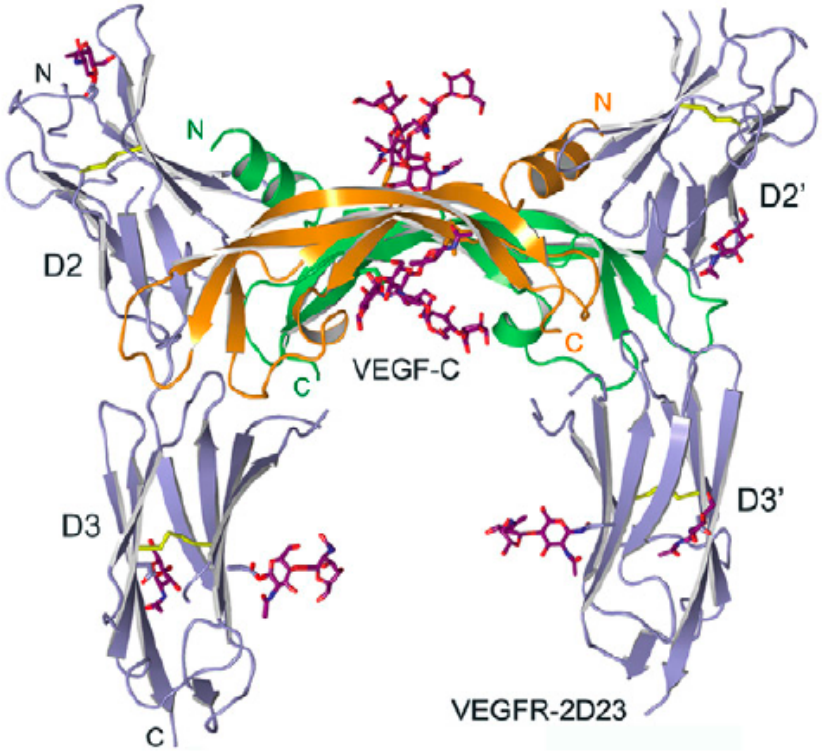

Figure 2.5: Structure of the VEGF-C/VEGFR-2D23 complex. The VEGF-C homodimer is shown in orange and green, and the two VEGFR-2 receptor chains are colored in light blue. The sugar moieties and the disulfide bonds are shown in purple and yellow sticks, respectively. VEGF-C binds to the VEGFR-2 interface between domains 2 and 3. Reprinted from Leppanen *et al.* 2010.

The receptor-binding domains to both VEGF-R2 and VEGF-R3 have also earlier been analyzed by mutational analysis of VEGF-C and these data correlate well with the structural results for VEGF-R2. The VEGF-C sites and residues responsible for binding to VEGF-R3 are essentially the same as those making contact with VEGF-R2 (Jeltsch *et al.* 2006).

Besides binding to VEGF-Rs, VEGF-C can also bind to the b1b2 domain (coagulation factor V/VIII homology domain) of neuropilin-2 (Nrp-2) that acts as a coreceptor for VEGF-R2 and -R3 (Favier *et al.* 2006). The N-terminal propeptide enhances this binding, meaning that the partially processed ΔC-VEGF-C binds stronger to Nrp-2 than the fully processed ΔNΔC-VEGF-C (Karpanen *et al.* 2006).

VEGF-C is highly conserved across different species. Within the VHD, murine and rat VEGF-C are identical to the human sequence in 114 out of 116 amino acids (98%) (Fig. 2.6).

```
murine ΔNΔC-VEGF-C      AHYNTEILKSIDNEWRKTQCMPREVCIDVGKEFGAATNTFFKPPCVSVYRCGGCCNSEGL 60
rat ΔNΔC-VEGF-C         AHYNTEILKSIDNEWRKTQCMPREVCIDVGKEFGAATNTFFKPPCVSVYRCGGCCNSEGL 60
human ΔNΔC-VEGF-C       AHYNTEILKSIDNEWRKTQCMPREVCIDVGKEFGVATNTFFKPPCVSVYRCGGCCNSEGL 60
                        ********************************.************************

murine ΔNΔC-VEGF-C      QCMNTSTGYLSKTLFEITVPLSQGPKPVTISFANHTSCRCMSKLDVYRQVHSIIRR 116
rat ΔNΔC-VEGF-C         QCMNTSTGYLSKTLFEITVPLSQGPKPVTISFANHTSCRCMSKLDVYRQVHSIIRR 116
human ΔNΔC-VEGF-C       QCMNTSTSYLSKTLFEITVPLSQGPKPVTISFANHTSCRCMSKLDVYRQVHSIIRR 116
                        *******.*********************************************
```

Figure 2.6. Alignment of ΔNΔC-VEGF-C sequences from different species. Murine (Uniprot P97953, A108-R223), rat (Uniprot O35757, A108-R223) and human ΔNΔC-VEGF-C (Uniprot P49767, A112-R227) aa sequences were aligned using ClustalW. "*" denotes 100% identical residues in all sequences, "." denotes residues with semiconservative substitutions (as given per ClustalW, http://www.ebi.ac.uk/2can/tutorials/protein/clustalw2.html)

The homologous portions of human VEGF-C (the VHD) are ~60% identical to human VEGF-D (Achen *et al.* 1998), ~33% to human VEGF-A_{165} (Leung *et al.* 1989), ~28% to human VEGF-B_{167} (Olofsson *et al.* 1996), ~25% to Orf virus VEGF-E (Ogawa *et al.* 1998), ~24% to human PlGF1 (Maglione *et al.* 1991), ~24% to *T. flavoviridis* snake venom VEGF (Takahashi *et al.* 2004) and ~17-22% to human PDGF-A and PDGF-B (Betsholtz *et al.* 1986) (Fig. 2.7)

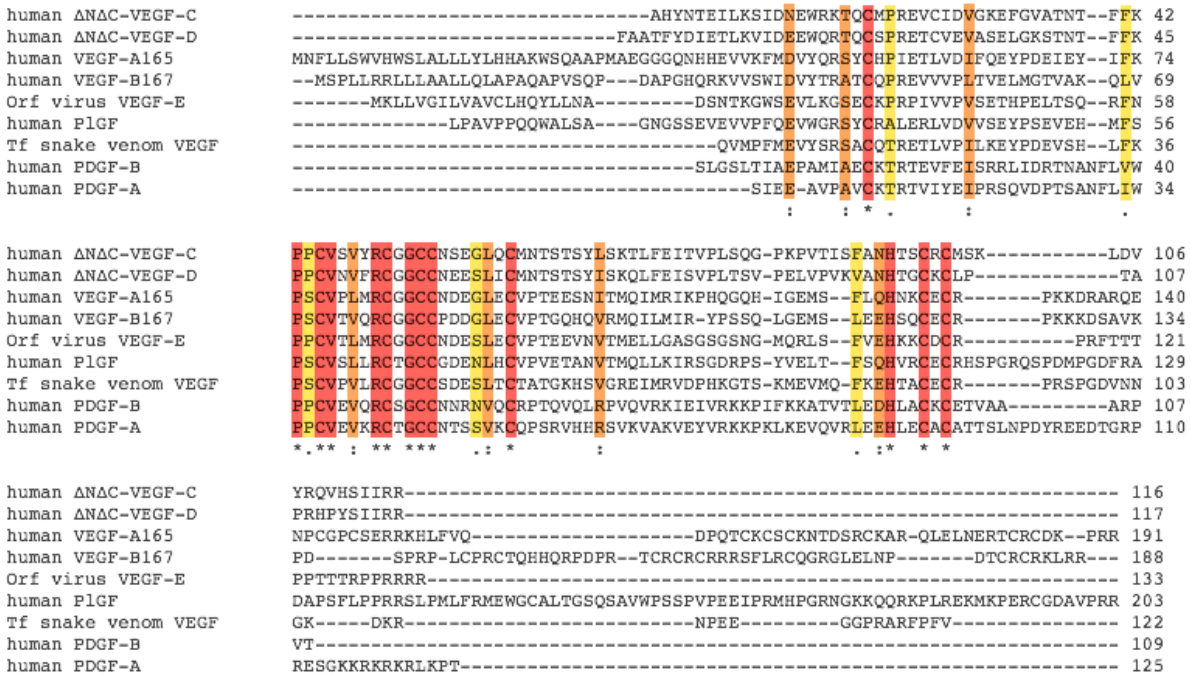

Figure 2.7. Alignment of aa sequences of the VEGF family members. VEGF family members are aligned in order of their degree of identity with ΔNΔC-VEGF-C (A112-R227) (Uniprot P49767). Shown sequences are human ΔNΔC-VEGF-D (F89-R205) (Uniprot O43915), human VEGF-A165 (Uniprot P15692-4), human VEGF-B167 (Uniprot P49765-2), Orf virus VEGF-E (Uniprot Q2F842), human PlGF (L19-R221) (Uniprot P49763), *T. flavoviridis* snake venom VEGF (Q25-V146) (Uniprot P67862), human PDGF-B (S82-T190) (Uniprot P01127) and human PDGF-A (S87-T211) (Uniprot P04085).
"*" denotes 100% identical residues in all sequences (red), ":" denotes residues with conservative substitutions (orange), "." denotes residues with semiconservative substitutions (yellow) (as given per ClustalW, http://www.ebi.ac.uk/2can/tutorials/protein/clustalw2.html).

The binding affinities of fully processed VEGF-C to its main receptors are reported as 410 pM for VEGF-R2 and 135 pM for VEGF-R3 as measured by surface plasmon resonance (Joukov *et al.* 1997).

VEGF-C, together with its sister protein VEGF-D, forms an own subfamily within the VEGF family of proteins. VEGF-D shares a very similar processing scheme (McColl *et al.* 2003; McColl *et al.* 2007) and virtually overlapping receptor specificities (Achen *et al.* 1998) with VEGF-C and is therefore often investigated in parallel to VEGF-C.

2.2.3. Molecular signaling by VEGF-C and its receptors

VEGF-C can bind to Nrp-2, VEGF-R3 and, when fully processed, to VEGF-R2. Through its antiparallel dimeric appearance, the VEGF-C dimer contains two full VEGF-R binding sites (on both opposite ends of the dimer). Binding to VEGF-Rs therefore leads to the physical approximation of two VEGF-Rs, which in turn autophosphorylate themselves through their intracellular tyrosine kinase moiety and are thereby activated. Phosphorylated receptors recruit interacting proteins and induce the activation of signaling pathways that involve an array of second messengers, as described below (Fig. 2.8).

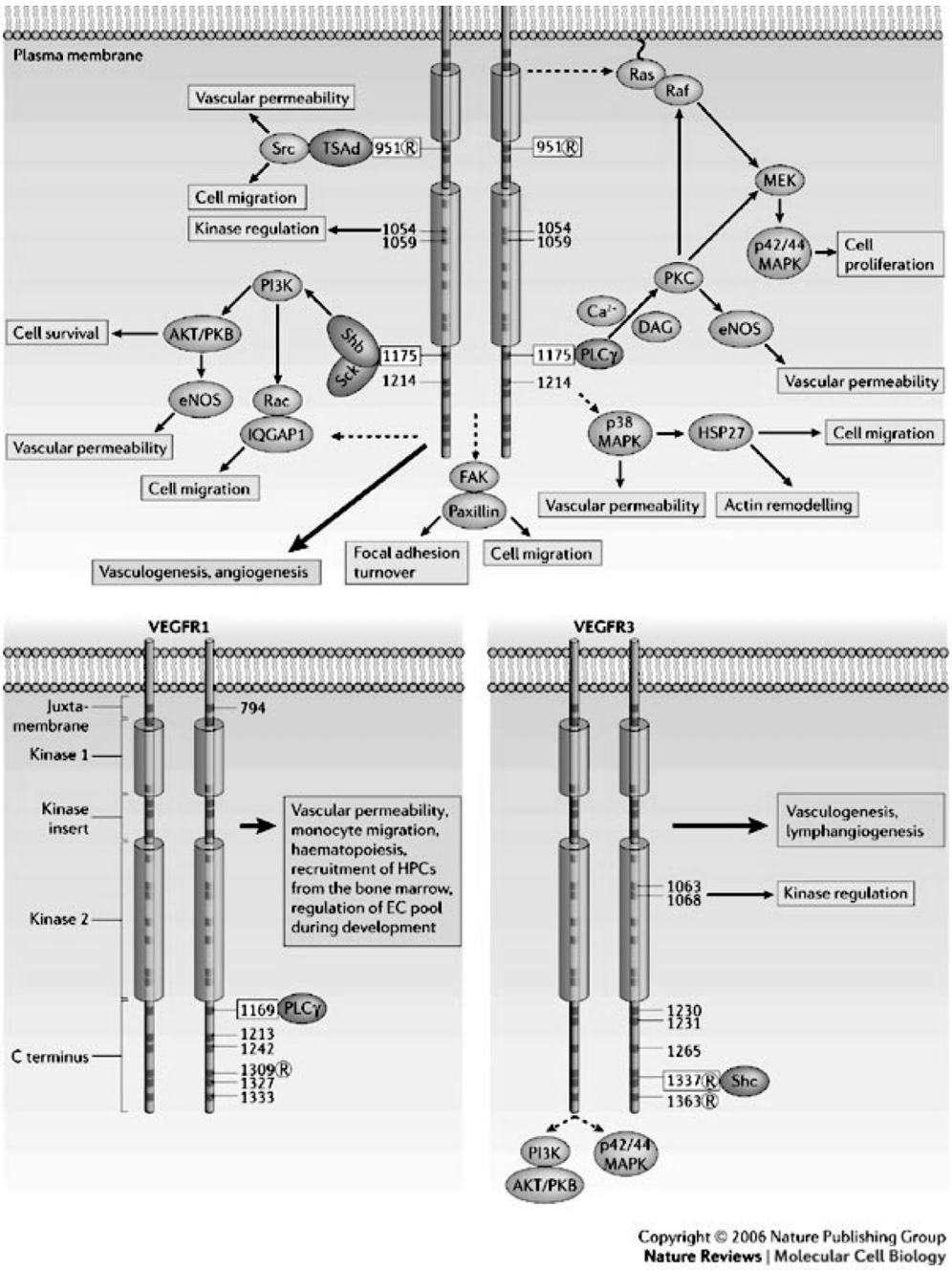

Figure 2.8. Phosphorylation sites and signaling pathways of VEGF-receptors. Reprinted from Olsson *et al.* 2006.

Activation of VEGF-R2 is achieved by autophosphorylation at Tyr1175, to which phospholipase C-gamma (PLC-gamma) binds and subsequently mediates the activation of the mitogen-activated protein kinase (MAPK)/extracellular-signal-regulated kinase-1/2 (ERK1/2) cascade and proliferation of endothelial cells (Takahashi *et al.* 2001). Besides PLC-gamma, the adaptor protein Shb also binds to

P-Tyr1175 and allows activation of PI3K, which in turn activates the serine/threonine kinase AKT/PKB downstream of phosphoinositide 3-kinase (PI3K), which mediates survival of the endothelial cells (Fujio *et al.* 1999). Phosphorylated Tyr951 is a binding site for the signaling adaptor TSAd (T-cell-specific adaptor; also known as VEGF receptor-associated protein (VRAP)) (Matsumoto *et al.* 2005). The phosphorylated Tyr951/TSAd pathway has been shown to regulate endothelial-cell migration. Phosphorylation sites at Tyr1054 and Tyr1059 are mainly thought to autoregulate VEGF-R2 kinase activity (Dougher *et al.* 1999). Other phosphorylation sites and signaling pathways exist as well and are extensively covered elsewhere (Olsson *et al.* 2006).

Autophosphorylation of VEGF-R3 leads to the association of the adaptor proteins Shc and Grb2 via the VEGF-R3 tyrosine 1337 (Pajusola *et al.* 1994; Fournier *et al.* 1995), promotes the protein kinase C-dependent activation of extracellular signal-regulated kinases (ERK)-1 and -2, involved in cell proliferation, and the PI3K regulated activation of protein kinase B/AKT (PKB/AKT) (Makinen *et al.* 2001), implicated in cell survival. These downstream signaling pathways are identical in VEGF-R2 and -R3. The role of other phosphorylation sites (Tyr1230, Tyr1231, Tyr1265, Tyr1337 and Tyr1363) in signal transduction downstream of VEGF-R3 remains to be identified. The kinase activity of VEGF-R3 is probably regulated by phosphorylation of conserved residues in the kinase domain (Tyr1063 and Tyr1068) (Olsson *et al.* 2006).

The existence of VEGF-R2 and -R3 heterodimers has also been reported, but the significance of this observation remains unclear (Dixelius *et al.* 2003).

VEGF-R2 is expressed on blood and lymphatic endothelial cells and activation of VEGF-R2 leads to promotion of survival, proliferation and migration of blood vascular and lymphatic endothelial cells.

In adults, VEGF-R3, also known as Flt-4, is specifically expressed by lymphatic, but not blood vascular endothelium in most normal tissues (Kaipainen *et al.* 1995; Partanen *et al.* 2000). However, there have been observations that VEGF-R3 becomes re-expressed by activated blood vascular endothelial cells associated with tumor growth and tissue repair (Partanen *et al.* 1999; Valtola *et al.* 1999; Kubo *et al.* 2000; Paavonen *et al.* 2000). Activation of VEGF-R3 activates principally the same signaling pathways as VEGF-R2, but is more restricted to the lymphatic endothelium, and hence promotes survival, proliferation and migration of lymphatic endothelial cells, which leads to lymphangiogenesis and in pathological situations to angiogenesis. Expression of VEGF-R3 might also occur on tumor cells, where it is thought to mediate autocrine or paracrine stimulation by tumor or stromal cell derived VEGF-C and -D (Kodama *et al.* 2008; Matsuura *et al.* 2009).

2.2.4. Mouse models used to investigate the role of VEGF-C/D

Knockout mice strains

In *Vefg-c*$^{-/-}$ mice, endothelial cells commit to the lymphatic lineage but they do not sprout to form lymphatic vessels. These homozygous knockout mice die prenatally due to fluid accumulation in the tissue caused by a non-functional lymphatic network. Heterozygous *Vegf-c*$^{+/-}$ mice are born but develop cutaneous lymphatic hypoplasia and lymphedema, demonstrating that both *Vegf-c* alleles are required for normal lymphatic development (Karkkainen *et al.* 2004).

Contrary to this, *Vegf-d* deficient mice are viable and do not show any phenotype, the lymphatic vessels develop normally and are functional. Thus, in mice, it seems that VEGF-D is dispensable for the development of a normal lymphatic vasculature (Baldwin *et al.* 2005). However, when *Vegf-d*^{null} mice were subjected to an orthotopically implanted metastatic tumor model of pancreatic adenocarcinoma, *Vegf-d*^{null} mice had a significantly decreased number of metastases to the draining lymph node, while primary tumor growth was not affected (Koch *et al.* 2009).

The insights into the role of VEGF-C and VEGF-D gained from mouse models may however not directly apply to the human situation, since murine VEGF-D, unlike human VEGF-D, does not bind to VEGF-R2 but only to VEGF-R3 (Baldwin *et al.* 2001). In contrast, murine VEGF-C is reported to possess the same receptor specificity as in humans and thus binds to VEGF-R2 and -R3.

VEGF-R3 deficient mice die at embryonic day 9 because of defective remodeling and maturation of the blood vascular network, even before lymphatic vessels emerge from the veins (Dumont *et al.* 1998). Chy mice, which possess a mutation in the *Vegf-r3* gene leading to inactivation of the tyrosine-kinase function of VEGF-R3, develop lymphedema (Karkkainen *et al.* 2001) and can be used as a model for hereditary lymphedema as seen in human patients with Milroy disease (Karkkainen *et al.* 2000).

The effects of VEGF-C and -D on lymphatic endothelium are in part also mediated by the coreceptor neuropilin-2 that may promote signaling via VEGF-R3 (Karpanen *et al.* 2006) – neuropilin-2 deficient mice are characterized by impaired patterning of the lymphatic vasculature; small lymphatic vessels and capillaries are severely reduced while larger, collecting lymphatic vessels develop normally (Yuan *et al.* 2002).

Targeted overexpression in mice

The K14 mouse model was developed to allow targeted overexpression of VEGFs in the epidermis of transgenic mice. In this model, an expression cassette encompassing the keratin-14 promoter (K14, a promoter specifically active only in epidermal keratinocytes (Vassar *et al.* 1989)) and the gene of interest was introduced in an oocyte. The oocytes are subsequently screened for random integration of the expression cassette into the genome. Targeted overexpression of VEGF-A, -C and -D has been achieved with this method.

VEGF-C overexpression in the epidermis of FVB/NIH mice results in hyperplasia of the lymphatic vessels in the skin (Jeltsch *et al.* 1997). Overexpression of human VEGF-D or human VEGF-C C156S (a mutant of VEGF-C that only binds to VEGF-R3) in the same model also resulted in hyperplasia of lymphatic vessels in the skin, while blood vessels were not affected (Veikkola *et al.* 2001). This shows that exclusive VEGF-R3 activation is sufficient to promote lymphangiogenesis. However, VEGF-R2 might also be involved in lymphangiogenesis, as proteolytically processed human VEGF-C and -D can also activate VEGF-R2 that is expressed both on lymphatic and on blood vascular endothelium (Kriehuber *et al.* 2001; Hirakawa *et al.* 2003; Hong *et al.* 2004; Hirakawa *et al.* 2005). A role of VEGF-R2 in lymphangiogenesis is further supported by recent findings that K14-driven epidermal expression of VEGF-A_{164} – which does not bind to VEGF-R3 – increases lymphangiogenesis and lymph node metastasis in a mouse model of squamous cell carcinoma (Hirakawa *et al.* 2005) and promotes lymphangiogenesis in mouse models of wound healing (Hong *et al.* 2004) and psoriasis (Kunstfeld *et al.* 2004). Furthermore, adenoviral expression of murine VEGF-A_{164} induces strong lymphangiogenesis (besides angiogenesis) in adult immunodeficient mice (Nagy *et*

al. 2002). Some part of the VEGF-A induced lymphangiogenesis might also be due to a secondary effect mediated by increased vascular permeability and recruitment of inflammatory cells that produce VEGF-C or -D (Cursiefen *et al.* 2004; Baluk *et al.* 2005).

Mouse cornea models

Transparency of the cornea, the window of the eye, is an essential prerequisite for clear vision. To sustain this transparency, the cornea is one of the few tissues that completely lack blood and lymphatic vessels. Delivery of molecules to the cornea has been used to identify both pro- and anti(lymph)angiogenic factors. VEGF-A is a strong inducer of corneal angiogenesis and corneal avascularity is usually retained by expression of soluble VEGF-R1, which traps VEGF-A and thereby prevents vascularization of the cornea (Ambati *et al.* 2006). Recently, it was reported that the VEGF-R3 specific ligands VEGF-C C156S and murine VEGF-D can also induce strong angiogenesis (besides lymphangiogenesis) in the mouse cornea model, and that the newly induced blood vessels express VEGF-R3. However, the angiogenic effect was at least in part mediated by the recruitment of VEGF-A secreting macrophages by VEGF-C C156S and murine VEGF-D (Chung *et al.* 2009).

2.2.5. Lymph node and distant metastasis induced by VEGFs

Tumor metastasis represents the hallmark of malignancy in cancer. For several decades, lymphatic metastasis was considered a rather passive process, where tissue-invading cancer cells encounter preexisting lymphatic vessels and are then taken up and drained to lymph nodes. However, the recent progress in the

identification of lymphatic vessel-specific markers, as well as the identification of lymphatic growth factors, has enabled experimental studies in rodents that have provided compelling evidence for an active role of tumor-induced lymphangiogenesis in the promotion of lymph node metastasis. Overexpression of VEGF-C or VEGF-D by cancer cells significantly promoted tumor lymphangiogenesis and lymph node metastasis in mice (Karpanen *et al.* 2001; Mandriota *et al.* 2001; Skobe *et al.* 2001; Stacker *et al.* 2002; Von Marschall *et al.* 2005). In a chemically induced, multistep skin cancer model, transgenic overexpression of VEGF-A or VEGF-C by epidermal keratinocytes enhanced both tumor-associated lymphatic vessel growth and metastasis to sentinel lymph nodes (Hirakawa *et al.* 2005; Hirakawa *et al.* 2007).

Recently, it was demonstrated that increased lymphangiogenesis in sentinel lymph nodes occurs even before the first metastatic cancer cell arrives (Hirakawa *et al.* 2005; Harrell *et al.* 2007; Hirakawa *et al.* 2007). Lymphangiogenic growth factors are drained from the primary tumor via its peritumoral (and maybe also intratumoral) lymphatic vessels and arrive in the sentinel lymph node, were they induce lymphangiogenesis and prepare the “soil” for future metastasizing tumor cells.

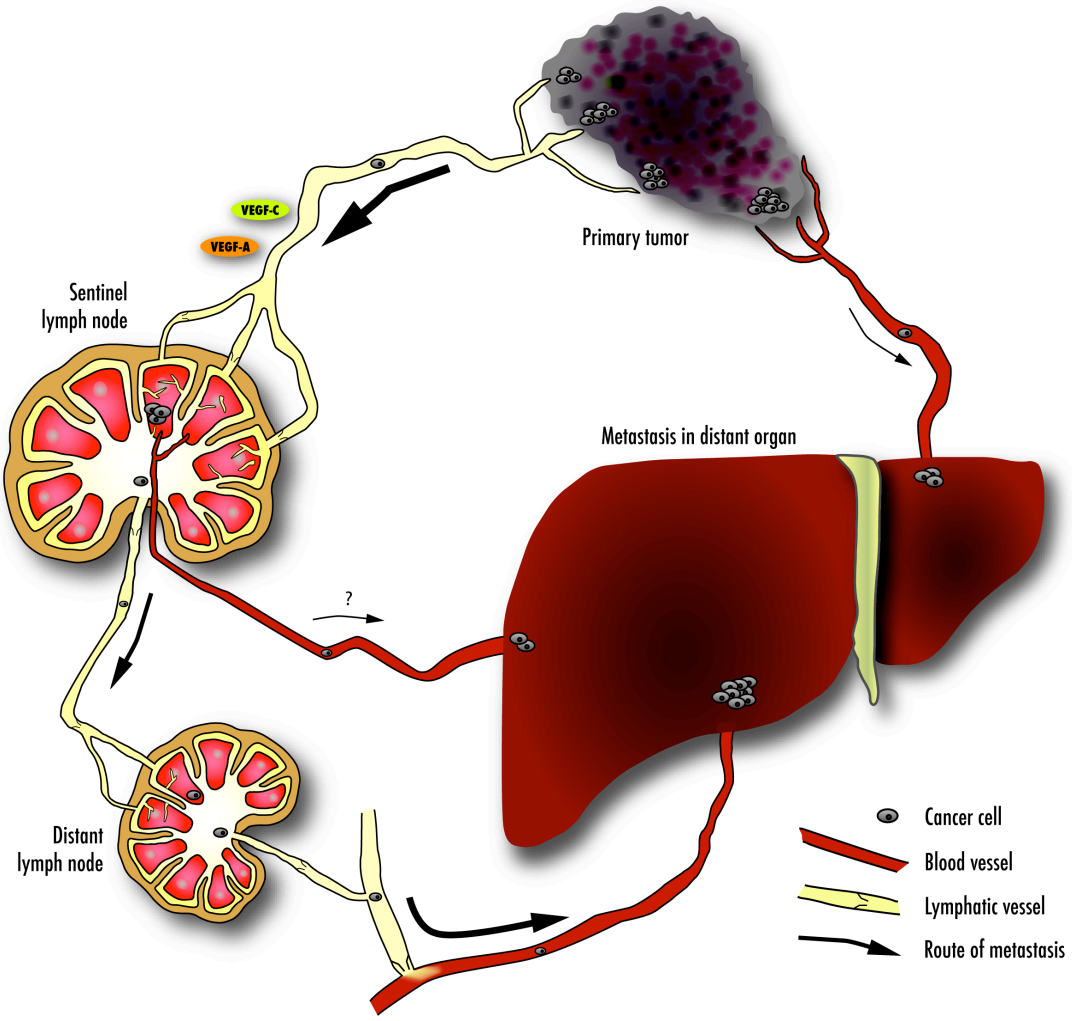

Figure 2.9. Tumor-induced lymphangiogenesis and its impact on lymphatic and distant metastasis. VEGF-A and/or -C secreted from the primary tumor and/or tumor-associated macrophages induces peritumoral lymphangiogenesis. Via the newly formed peritumoral lymphatic vessels, the lymphangiogenic growth factors are drained to the sentinel lymph node where they mediate lymph node lymphangiogenesis. These premetastatic niches are subsequently colonized by metastatic cancer cells from the primary tumor, which in turn secrete lymphangiogenic growth factors and spread further to non-sentinel lymph nodes and eventually distant organs. Original artwork.

These insights gained from mouse models have been confirmed in human cancers as well. In many human tumors, the expression of high levels of VEGF-C

(and to a lesser extent VEGF-D) has also been correlated with lymphatic vessel invasion, the emergence of sentinel and distant lymph node metastasis and overall poor prognosis (Table 2.1 and Rinderknecht *et al.* 2009). The strongest correlations have been found in melanoma and breast cancer (Dadras *et al.* 2003; Dadras *et al.* 2005; Van den Eynden *et al.* 2007).

As a conclusion, therapies that aim to block lymphangiogenesis induced by the primary tumor and reduce the metastatic risk appear promising. The main lymphangiogenic factors VEGF-C and -D are therefore attractive targets for cancer therapy, and agents that are capable of blocking VEGF-C/D and reducing cancer aggressiveness and metastatic dissemination are highly needed to prevent disease progression.

Table 2.1. Publications on correlation of lymphatic vessel density (LVD), lymphatic vessel invasion (LVI), lymph node metastasis (LNM), poor prognosis and VEGF-A/C/D expression.

		Correlation of marker expression with				
Marker	**Detection method**	**LVD**	**LVI**	**LNM**	**Poor prognosis**	**Ref**
Malignant melanoma						
VEGF-C	IHC	+	nd	+	nd	(Dadras *et al.* 2005)
	IHC	nd	nd	+	nd	(Schietroma *et al.* 2003)
	ELISA, serum	nd	nd	+	nd	(Vihinen *et al.* 2007)
VEGF-D	IHC	nd	nd	-	nd	(Dadras *et al.* 2005)
	IHC	nd	nd	-	nd	(Schietroma *et al.* 2003)
Breast cancer						
VEGF-A	IHC	+	+	+	+	(Mohammed *et al.* 2007)
VEGF-C	IHC	+	+	+	+	(Zhang *et al.* 2008b)
	IHC	+	-	+	+	(Mohammed *et al.* 2007)
	IHC	nd	+	-	+	(Kinoshita *et al.* 2001)
	IHC	nd	-	-	nd	(Hoar *et al.* 2003)
	IHC	nd	nd	+	+ uv (- mv)	(Nakamura *et al.* 2003b)
	ELISA, intratum.	nd	nd	-	Inverse corr (uv/mv)	(Bando *et al.* 2006)
	qRT-PCR	+	nd	+	nd	(Nakamura *et al.* 2005)
	qRT-PCR	nd	-	- (+[a])	nd	(Koyama *et al.* 2003)
	RPA	nd	nd	-	nd	(Gunningham *et al.* 2000)
VEGF-D	IHC	nd	nd	+	+ (uv/mv)	(Nakamura *et al.* 2003a)
	IHC	-	-	-	-	(Mohammed *et al.* 2007)
	IHC	nd	nd	-	-	(Currie *et al.* 2004)
	qRT-PCR	nd	Inv. correl.	-	nd	(Koyama *et al.* 2003)
Colorectal carcinoma						
VEGF-A	ELISA / RT-PCR	nd / nd	nd / nd	+ / +	nd / nd	(George *et al.* 2001)
	RPA	nd	nd	-	nd	(Hanrahan *et al.* 2003)
VEGF-C	IHC	+	+	+	+ uv (- mv)	(Soumaoro *et al.* 2006)
	IHC	+	+	+	nd	(Fukunaga *et al.* 2006)
	IHC, invasive edge & surface	nd	+ (inv. edge) - (surface)	+ (uv/mv) (inv. edge)	+ (uv/mv)	(Onogawa *et al.* 2004)
	IHC	nd	nd	+	nd	(Jia *et al.* 2004)
	IHC	nd	nd	+	nd	(Maeda *et al.* 2003)
	IHC	nd	+	+	+ (mv)	(Furudoi *et al.* 2002)

		Correlation of marker expression with				
Marker	**Detection method**	**LVD**	**LVI**	**LNM**	**Poor prognosis**	**Ref**
VEGF-C	IHC / qRT-PCR	nd / nd	+ / + (uv)	+ / +	nd / nd	(Kawakami *et al.* 2003)
	RT-PCR	nd	nd	-	nd	(George *et al.* 2001)
	qRT-PCR	nd	nd	-	nd	(Takeuchi *et al.* 2003)
	RPA	nd	nd	-	nd	(Hanrahan *et al.* 2003)
VEGF-D	IHC, invasive edge & surf.	nd	- (inv. edge & surface)	+ uv, - mv (inv. edge)	+ uv (- mv)	(Onogawa *et al.* 2004)
	IHC	nd	-	+ (uv/mv)	-	(Funaki *et al.* 2003)
	IHC	nd	nd	+	+	(White *et al.* 2002)
	RT-PCR	nd	nd	-	nd	(George *et al.* 2001)
	RPA	nd	nd	-	nd	(Hanrahan *et al.* 2003)
Gastric cancer						
VEGF-A	IHC	nd	-	-	nd	(Kabashima *et al.* 2001)
VEGF-A/C	IHC	nd	- / - / +[b]	- / - / +[b]	nd	(Kondo *et al.* 2007)
VEGF-C	IHC	+	+	-	+	(Da *et al.* 2008)
	IHC	nd	+	+ (uv/mv)	nd	(Amioka *et al.* 2002)
	IHC	nd	nd	+	nd	(Zhang *et al.* 2005)
	IHC	nd	+	+	nd	(Onogawa *et al.* 2005)
	IHC	nd	+	+	nd	(Yan *et al.* 2004a)
	IHC	nd	-	+	-	(Juttner *et al.* 2006)
	IHC	nd	+	+	nd	(Yan *et al.* 2004b)
	IHC	nd	+	-	nd	(Kabashima *et al.* 2001)
	IHC	nd	+	+ / -[c]	nd	(Ishikawa *et al.* 2003)
	IHC	nd	+	+ uv (- mv)	+	(Takahashi *et al.* 2002)
	IHC / RT-PCR	nd / nd	+ / nd	+ / +	+ (uv/mv) / nd	(Yonemura *et al.* 1999)
	RT-PCR	nd	+	+	-	(Shida *et al.* 2006)
	RT-PCR	nd	nd	+	nd	(Kitadai *et al.* 2005)
	RT-PCR	nd	nd	+	nd	(Liu *et al.* 2004)
	qRT-PCR	nd	nd	+	nd	(Yuanming *et al.* 2007)
VEGF-D	IHC	nd	-	-	nd	(Onogawa *et al.* 2005)
	IHC	nd	+	+ / -[c]	nd	(Ishikawa *et al.* 2003)
	IHC,	nd	+	+	+	(Juttner *et al.* 2006)
	RT-PCR	nd	nd	-	nd	(Kitadai *et al.* 2005)
	RT-PCR	nd	+	-	-	(Shida *et al.* 2006)
	qRT-PCR	-	nd	-	nd	(Yuanming *et al.* 2007)
Bladder transitional cell carcinoma						
VEGF-C	IHC	nd	+	+	+	(Suzuki *et al.* 2005)
	IHC	nd	nd	+	+	(Zu *et al.* 2006)
Cervical cancer						
VEGF-A	ELISA, serum	nd	nd	-	-	(Mitsuhashi *et al.* 2005)
VEGF-C	IHC	+	+	+	+ uv (- mv)	(Gombos *et al.* 2005)
	IHC	nd	-	-	nd	(Van Trappen *et al.* 2003)
	IHC	nd	nd	+	+	(Ueda *et al.* 2002)
	ELISA, serum	nd	nd	-	+	(Mitsuhashi *et al.* 2005)
VEGF-D	IHC	nd	-	-	nd	(Van Trappen *et al.* 2003)
Endometrial cancer						
VEGF-A	IHC	nd	+	-	+ uv (- mv)	(Hirai *et al.* 2001)
VEGF-C	IHC	nd	+	+	+ (uv/mv)	(Hirai *et al.* 2001)
VEGF-D	IHC, tumor & stroma cells	nd	+[d] (vessel invasion)	+[d]	+ uv / - mv (tumor) + uv/mv, stroma	(Yokoyama *et al.* 2003)
Esophageal cancer						
VEGF-A	ELISA, serum	nd	nd	-	nd	(Krzystek-Korpacka *et al.* 2007)
	qRT-PCR	nd	nd	-	nd	(Loges *et al.* 2007)
VEGF-C	IHC	nd	+[d]	+[d]	nd	(Kitadai *et al.* 2001)
	IHC,	nd	nd	+	nd	(Byeon *et al.* 2004)
	ELISA, serum	nd	nd	+	nd	(Krzystek-Korpacka *et al.* 2007)
	qRT-PCR	nd	nd	+	nd	(Loges *et al.* 2007)
VEGF-D	qRT-PCR	nd	nd	-	nd	(Loges *et al.* 2007)
Laryngopharyngeal squamous cell carcinoma						
VEGF-C	IHC	- (it)	nd	+	+	(Hinojar-Gutierrez *et al.* 2007)
Lung adenocarcinoma						
VEGF-A	qRT-PCR	nd	-	+[e]	nd	(Niki *et al.* 2000)
VEGF-C	qRT-PCR	nd	+[f]	+[f]	nd	(Niki *et al.* 2000)
VEGF-D	qRT-PCR	nd	Inv.correl.	-	nd	(Niki *et al.* 2000)
Neck squamous cell carcinoma						
VEGF-A	RT-PCR	nd	nd	+ (uv/mv)	nd	(O-charoenrat *et al.* 2001)
VEGF-C	RT-PCR	nd	nd	+ (uv/mv)	nd	(O-charoenrat *et al.* 2001)
VEGF-D	RT-PCR	nd	nd	-	nd	(O-charoenrat *et al.* 2001)

		Correlation of marker expression with				
Marker	**Detection method**	**LVD**	**LVI**	**LNM**	**Poor prognosis**	**Ref**
Neuroblastoma						
VEGF-A	qRT-PCR	nd	nd	-	nd	(Komuro *et al.* 2001)
VEGF-C	qRT-PCR	nd	nd	-	nd	(Komuro *et al.* 2001)
Non-small cell lung cancer						
VEGF-A	ELISA, serum	nd	+	+	nd	(Tamura *et al.* 2003)
VEGF-C	IHC	nd	nd	-	+ uv (- mv)	(Arinaga *et al.* 2003)
	IHC	+	+	+	+	(Li *et al.* 2003)
	ELISA, serum	nd	+	+	nd	(Tamura *et al.* 2003)
Oral squamous cell carcinoma						
VEGF-A	IHC	nd	nd	-	nd	(Shintani *et al.* 2004)
VEGF-C	IHC	nd	nd	+	nd	(Shintani *et al.* 2004)
	IHC	nd	-	+ T1/2, - T3/4	+ uv (- mv)	(Kishimoto *et al.* 2003)
VEGF-D	IHC	nd	nd	+	nd	(Shintani *et al.* 2004)
Ovarian cancer						
VEGF-A	IHC	nd	nd	-	-	(Nishida *et al.* 2004)
VEGF-C	IHC	nd	nd	+	+ uv	(Nishida *et al.* 2004)
	IHC	+ (it)	nd	+	+	(Ueda *et al.* 2005)
Pancreatic adenocarcinoma						
VEGF-C	IHC	- (it/pt)	nd	-	-	(Sipos *et al.* 2005)
	IHC, tumor margin & center	nd	+ at margin - at center	+ at margin - at center	- +[g]	(Kurahara *et al.* 2004)
VEGF-D	qRT-PCR	-	nd	-	-	(Sipos *et al.* 2005)
	IHC, tumor margin & center	nd	- at margin & center	+ at margin - at center	- +[g]	(Kurahara *et al.* 2004)
Prostate cancer						
VEGF-A	qRT-PCR	nd	nd	tumor protein & mRNA: inv. correl. + plasma VEGF-A	nd	(Kaushal *et al.* 2005)
	WB					(Kaushal *et al.* 2005)
	ELISA, plasma					(Kaushal *et al.* 2005)
VEGF-C	IHC	nd	nd	+	nd	(Jennbacken *et al.* 2005)
	RPA	nd	nd	-	nd	(Stearns *et al.* 2004)
VEGF-D	qRT-PCR	nd	nd	- for mRNA	nd	(Kaushal *et al.* 2005)
	WB			+ for tumor and plasma VEGF-D		(Kaushal *et al.* 2005)
	ELISA, plasma					(Kaushal *et al.* 2005)
	RPA	nd	nd	+	nd	(Stearns *et al.* 2004)
Thyroid cancer						
VEGF-A	RT-PCR	nd	nd	-	nd	(Bunone *et al.* 1999)
VEGF-C	RT-PCR	nd	nd	+	nd	(Bunone *et al.* 1999)
	IHC	nd	+	+	nd	(Yu *et al.* 2005)
VEGF-D	IHC / qRT-PCR	+ (it/pt) / nd	nd / nd	+ / +	nd / nd	(Yasuoka *et al.* 2005)

[a] for VEGF-C/D ratio; [b] + for VEGF-A and -C combined, - for VEGF-A or -C alone; [c] + in undifferentiated tumors, - in differentiated tumors; [d] for VEGF-C or -D from tumor and stromal cells; [e] for VEGF-A/VEGF-D ratio; [f] for VEGF-C/VEGF-D ratio; [g] for VEGF-C and -D combined; it, intratumoral; LNM, lymph-node metastasis; LVD, lymphatic vessel density; LVI, lymphatic vessel invasion; mab, monoclonal antibody; mv, multivariate; nd, not determined; pab, polyclonal antibody; pt, peritumoral; RPA, RNase protection assay; uv, univariate; VA, VEGF-A; VC, VEGF-C; VD, VEGF-D; +, statistically significant correlation ($p \leq 0.05$); -, no significant correlation. Modified from Rinderknecht *et al.* 2009.

2.2.6. Therapeutic strategies to block lymph node metastasis

Blockade of the VEGF-C/D – VEGF-R2/R3 axis might be achieved by blocking of the individual growth factors or receptors by neutralizing antibodies. Another possibility is the concomitant neutralization of VEGF-C and -D by use of a soluble VEGF-R3 trap.

Interference with the VEGF-C/D – VEGF-R2/3 system has shown promising results in reducing tumor metastasis and/or primary tumor growth in a number of models. Notably, blocking of VEGF-D by a mouse monoclonal anti-human-VEGF-D antibody (Achen *et al.* 2000; Stacker *et al.* 2001) was effective in halting primary tumor growth and suppressing local tumor metastasis in a mouse xenograft tumor model. Similarly, neutralizing antibodies against VEGF-R3 inhibited lymph node metastasis (Shimizu *et al.* 2004; Roberts *et al.* 2006; Burton *et al.* 2008) and soluble VEGF-R3, that traps both VEGF-C and VEGF-D, blocked lymphangiogenesis and lymph node metastasis in several models (He *et al.* 2002; Lin *et al.* 2005).

Blocking of VEGF-C by antibodies has been reported in only a few studies (Shin *et al.* 2002; Tomanek *et al.* 2002; Timoshenko *et al.* 2007; Albuquerque *et al.* 2009), none of which involved tumor studies. Furthermore, none of these antibodies are of human origin, which hampers their use in human therapy due to immunogenicity.

Compared to other inhibitors of the VEGF-C – VEGF-R2/3 axis, an anti-VEGF-C antibody would have the main benefit of specifically blocking the action of VEGF-C. This is important since the VEGF / VEGF receptor interaction network is highly redundant (Fig. 2.10). Anti-VEGF receptor antibodies, for instance, only block the action of a VEGF ligand on the specific targeted receptor, but not on other VEGF receptors activated by the ligand (Fig. 2.11). At the same time, they block all

interaction with the targeted receptor, indiscriminate of the VEGF ligand. Soluble VEGF-receptors (VEGF-traps), on the other hand, block all ligands that bind to them. This broad-spectrum inhibition (which might be advantageous in cancer therapy) may have impacts on other tissues, where VEGF ligand and receptor expression also occurs. For instance, VEGF-D is also expressed in the osteoblast, where it regulates bone regeneration in an autocrine manner via VEGF-R3 (Orlandini *et al.* 2006). Interference with the VEGF-D / VEGF-R3 axis poses therefore the risk of inhibition of bone regeneration.

The complex nature of the VEGF / VEGF receptor network makes it also difficult to determine direct and secondary effects of ligand or receptor blockage. By inhibiting one ligand from binding to a certain receptor, this actually makes the receptor more available for binding of other ligands, which in turn reduces activation of a second receptor. Thus, the blocking of one molecule may shift equilibriums in the whole delicate VEGF system. For instance, the development of a neutralizing anti-PlGF antibody was reported recently (Fischer *et al.* 2007). By blocking PlGF from binding to its receptors VEGF-R1 and soluble VEGF-R1 (sVEGF-R1), (s)VEGF-R1 becomes more available for binding of VEGF-A, and since the affinity of VEGF-A to (s)VEGF-R1 is higher than to VEGF-R2, VEGF-A may bind more to the decoy receptor sVEGF-R1. This would decrease the receptor occupancy on VEGF-R2 and therefore the activation level of the pro-angiogenic receptor and reduces angiogenic signaling. At the same time, the now non-occupied VEGF-R2 molecules might bind higher levels of processed VEGF-C or -D and thereby lower the receptor occupancy on VEGF-R3.

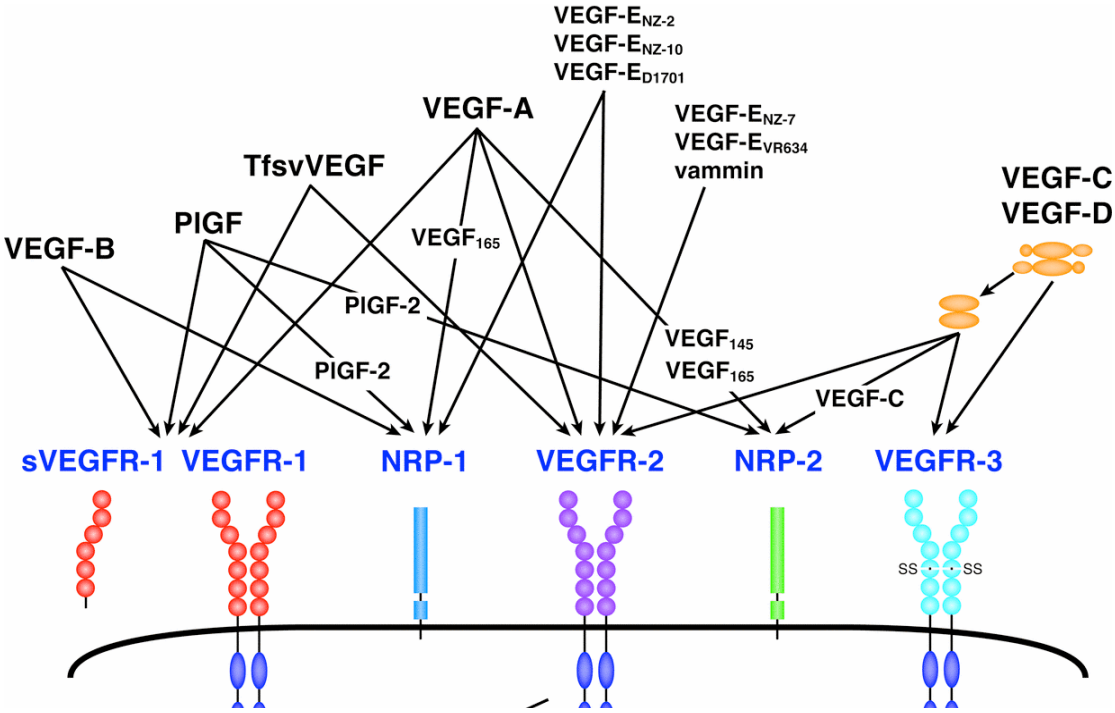

Figure 2.10. Overview of the VEGF / VEGF-receptor system. The VEGF system is characterized by a high complexity of signaling pathways. VEGFs usually bind to more than one receptor and receptors usually can bind more than one ligand. Reprinted from Takahashi *et al.* 2005.

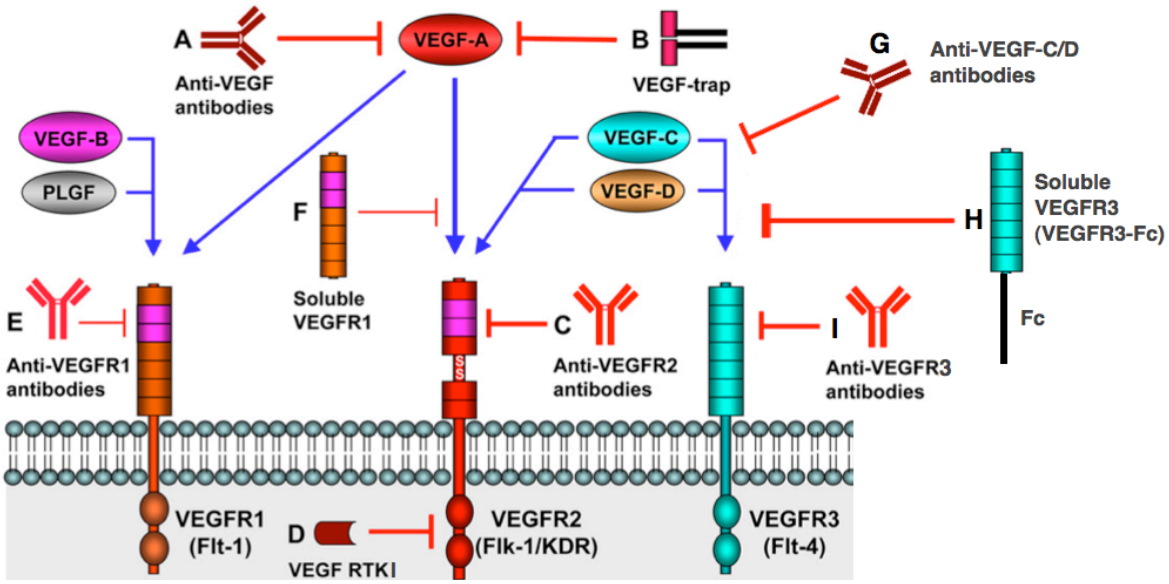

Figure 2.11. Scheme of different VEGF network inhibitors. In the VEGF network, different targets can be used for blockage of signaling. Neutralizing antibodies against the growth factors (A, G) block binding of the ligands to all their receptors. VEGF-trap (B) and other soluble VEGF receptor

constructs (F, H) act as receptor decoys and prevent binding of multiple ligands to their membrane-bound receptors. Blocking antibodies against the VEGF receptors (C, E, I) inhibit multiple ligands from binding to one of their receptors. Finally, small molecules (receptor tyrosin kinase inhibitors, RTKIs) against the intracellular tyrosine kinase function of VEGF receptors are usually somewhat unspecific and block all VEGF-Rs (and possibly other RTKs) at once. Modified from Li *et al.* 2009.

In contrast to the expression of VEGF-D in osteoblasts, VEGF-C is expressed in osteoclasts, where it enhances bone resorption in an autocrine manner via VEGF-R3 (Zhang *et al.* 2008a). It seems that in the bone, VEGF-C and VEGF-D are counterplayers and blocking VEGF-C could potentially reduce bone degradation.

VEGF-C undergoes excessive processing by proprotein convertases before and after secretion; this processing trims the full length VEGF-C by an N-terminal and C-terminal propeptide and generates ultimately the fully processed, mature ΔNΔC-VEGF-C (Siegfried *et al.* 2003). This middle third domain contains the VEGF homology domain (VHD), the region of highest homology between VEGF family members, and is the most active form of VEGF-C with highest affinity to VEGF-R3 and the only form of VEGF-C that also binds VEGF-R2 (Joukov *et al.* 1997).

As a general conclusion, ΔNΔC-VEGF-C represents probably the most important lymphangiogenic VEGF variant to block.

2.2.7. Other possible applications of VEGF-C blockage

VEGF-C dependent tumors

Next to its role in metastasis as outlined above, VEGF-C and -D might also directly activate VEGF-R3 expressed on tumor cells (Kodama *et al.* 2008; Matsuura *et al.* 2009), which might lead to autocrine activation of cancer cells, primary cancer growth and a more aggressive cancer phenotype. Blockage of the VEGF-C/D –

VEGF-R3 axis in tumors has been performed with a neutralizing anti-VEGF-R3, and this blockage resulted in reduced growth of the primary tumor in several different experimental mouse tumor models (Laakkonen *et al.* 2007). Blocking of VEGF-C could also be advantageous in a number of cancers of endothelial cells that directly rely on VEGF-C signaling. For example, Kaposi's sarcoma (KS) is characterized by the presence of a core of spindle-shaped cells that possess characteristics of lymphatic endothelium. VEGF-C potently induces proliferation of these cells *in vitro* (Skobe *et al.* 1999) and may play a critical role in controlling KS cell growth, migration, or invasion (Marchio *et al.* 1999). If this is the case, inhibition of VEGF-C signaling may be useful for inhibiting KS progression by acting on tumor cells directly. This may also be true for lymphangiomas (Huang *et al.* 2001) and other lymphatic neoplasms (Mentzel *et al.* 2002). Furthermore, VEGF-C was found to induce proliferation, survival and resistance of acute myeloid leukemia (AML) and acute lymphocytic leukemia (ALL) blast cells *in vitro*, by autocrine interaction with VEGF-R3 (Dias *et al.* 2002).

(Auto)inflammatory diseases

VEGF-C might also play a role in diseases and immune reactions where (lymphatic) vascular remodelling takes place, such as the autoinflammatory diseases rheumatoid arthritis (Paavonen *et al.* 2002) and psoriasis (Kunstfeld *et al.* 2004; Schonthaler *et al.* 2009). Mechanistically, VEGF-C is upregulated by the inflammatory enzyme cyclo-oxygenase 2 (COX-2) through the EP_1/Src/HER-2/Neu signaling pathway (Su *et al.* 2004); also, the *Vegf-c* gene gets activated in inflammatory conditions by NF-kappaB, for which binding sites in the *Vegf-c* promoter have been found (Ristimaki *et al.* 1998). However, blockade of VEGF-C might not always be beneficial in inflammatory conditions, for instance, in a mouse

model of chronic airway inflammation, blockade of lymphangiogenesis by soluble VEGF-R3 aggravated bronchial edema (Baluk *et al.* 2005).

Bone degeneration

As reported recently, osteoclasts were directly stimulated by VEGF-C to induce RANKL-mediated bone resorption, which was reduced by the VEGF-C scavanger VEGF-R3-Fc. Osteoclasts express VEGF-R3, and VEGF-C stimulated Src phosphorylation in osteoclasts (Zhang *et al.* 2008a). An anti-VEGF-C antibody could therefore be used in the treatment of osteoporosis and cancer-induced bone degeneration (e.g. in multiple myeloma and breast carcinoma). The specific inhibition of VEGF-C could be advantageous because use of a VEGF-R3-Fc protein also scavanges VEGF-D, which is an activator of osteocalcin expression in osteoblasts and thereby promotes bone growth (in contrast to VEGF-C).

Anti-VEGF-A refractory tumors

Treatment with anti-VEGF antibodies in glioma lead to a phenotypic change with upregulation of VEGF-D and increased reactivity to VEGF-C and -D accompanied by intracellular changes in signal transduction. This may represent an escape mechanism of the tumor to therapies targeting the VEGF-A/VEGFR-2 system with a secondary activation of the VEGF-C/D-VEGFR3 system (Grau *et al.* 2007).

Age-related macular degeneration

The “wet” form of age-related macular degeneration (AMD) is marked by the neovascularisation of the subretinal space, originating from choroidal blood vessels that introduce hemorrhage and thereby cause irreversible damage to the photoreceptors and rapid vision loss. AMD is currently treated with the anti-VEGF-A

monoclonal antibodies bevacizumab and ranibizumab. However, the involvement of VEGF-C in the ingrowth of blood and lymphatic vessels into the subretinal space has also been discussed. For instance, it has been shown that human retinal pigment epithelial cells express VEGF-C and VEGF-R3 (Ikeda *et al.* 2006; Zhao *et al.* 2006) and that VEGF-C promotes survival of retinal vascular endothelial cells through VEGF-R2 (Zhao *et al.* 2007).

Organ rejection

Rejection of human kidney transplants is often accompanied by inflammatory lymphangiogenesis, mediated by infiltrating macrophages that express VEGF-C, VEGF-D and VEGF-R3 (Kerjaschki *et al.* 2004). The corneal avascularity prevents traffic of antigen-presenting cells into the lymph nodes and the induction of an immune response, and so it prevents graft rejection when corneas are transplanted (Liu *et al.* 2002). Soluble VEGF-R2 (sVEGF-R2) normally prevents growth of lymphatic vessels in the cornea, and administration of exogenous sVEGF-R2 inhibited lymphatic vessel formation and doubled corneal transplant survival rate (Albuquerque *et al.* 2009). Further insight into the role of lymphatic growth factors in corneal graft rejection was gained by the discovery that cells in the stroma of the cornea upon inflammation upregulate VEGF-R3 and that blockage of VEGF-R3 significantly increases corneal transplant survival (Chen *et al.* 2004).

2.3. Antibody therapy

2.3.1. Definition of an antibody, properties

The term antibody was first used in the late 19th century, when the German scientist Paul Ehrlich, working on antitoxins to ricin and abrin, wrote *"if two substances give rise to two different "Antikörper" (antibodies), then they themselves must be different"* (Ehrlich 1891). The development of the term is extensively covered elsewhere (Lindenmann 1984). Even prior to Paul Ehrlich, antibody activity against diptheria and tetanus toxins was already described by Emil von Behring and Shibasaburo Kitasato in 1890 (Behring 1890). The proteinaceous origin of antibodies was only discovered in 1929 by Michael Heidelberger (Heidelberger *et al.* 1929) and the antibody structure was finally described in the late 1960s by Rodney Porter (Porter 1967) and Gerald Edelman (Edelman *et al.* 1969), for which they jointly received the Nobel Prize for Physiology or Medicine in 1972.

Antibodies are constituents of the humoral immune response and are produced by specialized leukocytes, the plasma B-cells. Antibodies are capable of binding to a specific structure, the antigen, and are used to identify and neutralize foreign pathogens, such as bacteria and viruses. The basic structure of an antibody consists of two identical light chains of 25 kDa each and two identical heavy chains of 50 kDa each. Each light chain is covalently linked to a heavy chain and both heavy chains are linked to each other by virtue of disulfide bridges. The spatial structure resembles a "Y" (Fig. 2.12). Heavy and light chain both contain N-terminal variable aa sequences (V_H and V_L, respectively) and C-terminal constant sequences (C_{H1-3} and C_L, respectively).

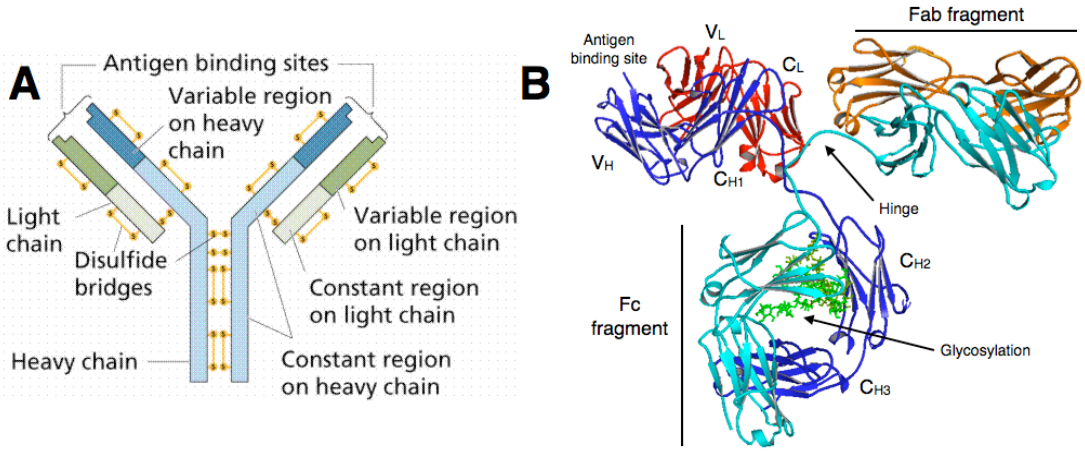

Figure 2.12. Structure and features of an antibody. A: Conceptual representation of an antibody. Reprinted from Purves *et al.*, Life: The Science of Biology, 4th Edition, by Sinauer Associates (www.sinauer.com) and WH Freeman (www.whfreeman.com); B: Three-dimensional structure of a murine IgG2a anti-canine lymphoma antibody, heavy chains are in blue and cyan, light chains in red and orange, sugar residues added to C_{H2} by glycosylation are represented in green (pdb code 1IGT, modeled with MacPyMOL, original artwork).

Antigen binding and specificity is mediated by the variable sequences of both heavy and light chains; within these regions, three clusters of hypervariable loops or "complementarity determining regions" (CDR) make the actual contacts with the antigen. The immune system is thought to be able to express several billion (about 10^{11}) different antibody sequences, but the encoding of these aa sequences is accomplished by only three different multigene families, one for each lambda light chain, kappa light chain and heavy chain. In the germline DNA, each multigene family consists of multiple variable (V), diversity (D) and joining (J) gene segments, arranged consecutively. The diversity in antibody specificity is achieved by combinatorial assembly of V, D and J segments in a process called V(D)J recombination. The transcript encoding the variable domain of heavy chains is created from the assembly of a V, D and J segment; further downstream on the transcript, the constant domain gene is also included. The light chain transcript is

assembled from a V and a J segment, they lack the D segment; either the lambda or kappa constant domain is then added.

CDRs 1 and 2 of heavy and light chains are encoded by the V genes, while light chain CDR3 (LCDR3) is encoded by V and J segments and heavy chain CDR3 (HCDR3) by V, D and J segments. Random removal or addition (e.g. N-nucleotide addition) of nucleotides between the different V, D and J segments provides additional variability, called junctional diversity, and explains why LCDR3 and especially HCDR3 show the greatest variability among the CDRs (Fig. 2.13).

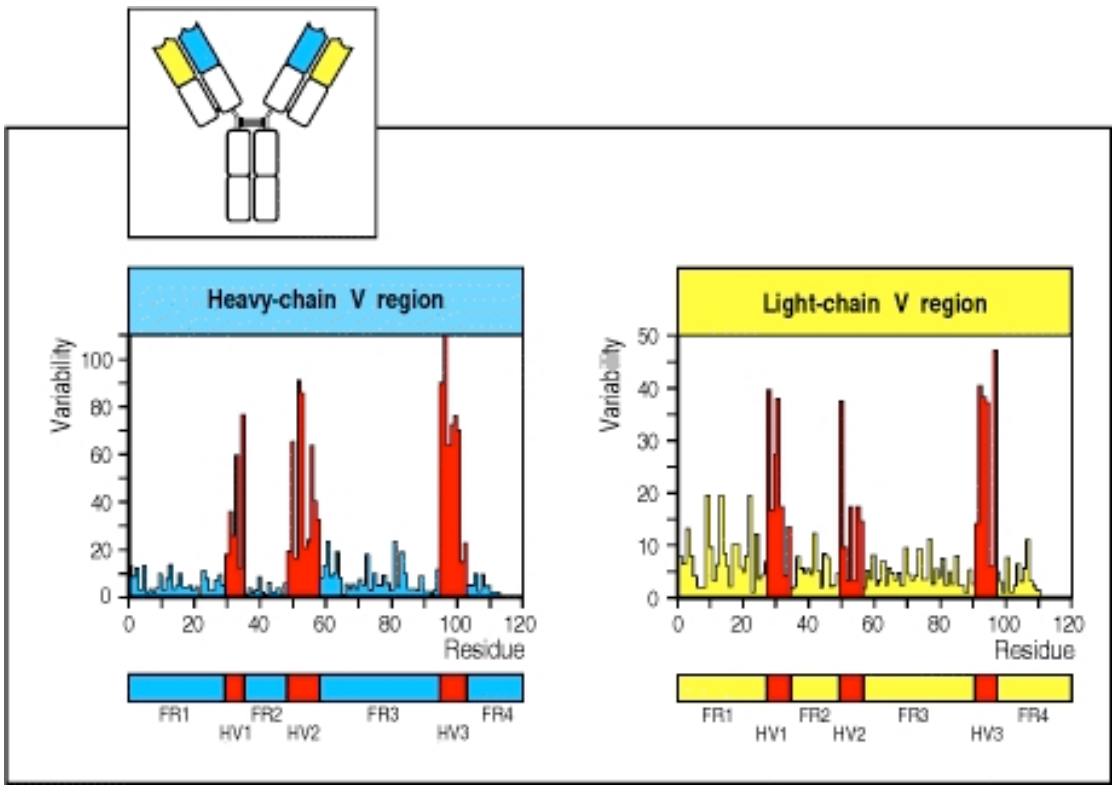

Figure 2.13. Discrete regions of hypervariability in V domains. A variability plot derived from comparison of the aa sequences of several dozen heavy-chain and light-chain V domains. At each amino acid position the degree of variability is the ratio of the number of different amino acids seen in all of the sequences together to the frequency of the most common aa. Three hypervariable regions (HV1, HV2, and HV3) are indicated in red and are also known as the complementarity-determining regions, CDR1, CDR2, and CDR3. They are flanked by less variable framework regions (FR1, FR2,

FR3, and FR4, shown in blue or yellow). Reprinted from “Immunobiology: the immune system in health and disease” 5th edition. Janeway C., Travers P. Walport M. and Shlomchik M. Edited by Garland Science.

Furthermore, LCDR3 and particularly HCDR3 establish most of the contact to the antigen and are the most important determinants of antigen binding (Dixelius *et al.* 2003) (Fig. 2.14).

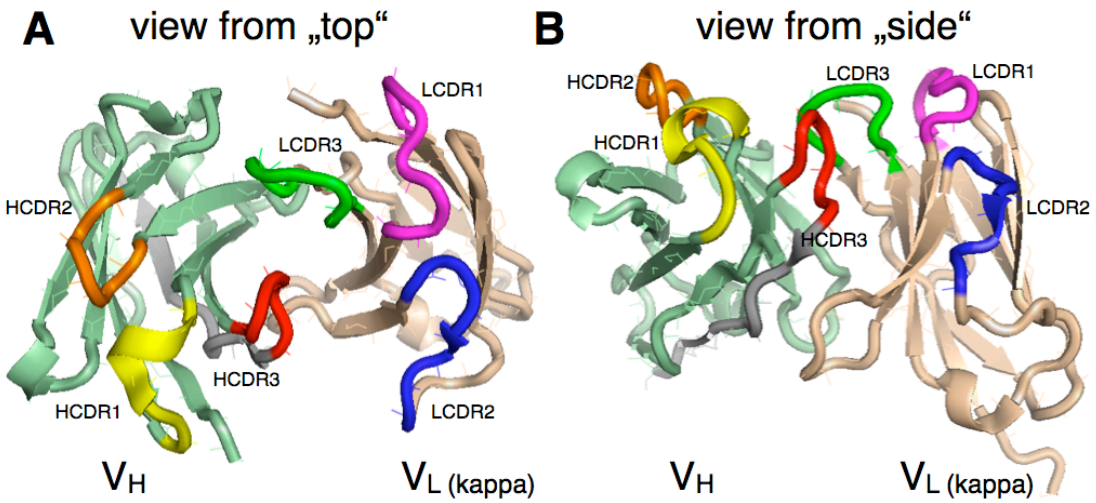

Figure 2.14. Complementarity determining regions (CDRs) on variable domains. Three-dimensional representation of the CDRs on V_H and $V_{L\text{-kappa}}$ in the human anti-polyhydroxybutyrate antibody Fv (pdb code 2D7T, modeled with MacPyMOL). A: view from “top”, where the antigen would be binding; B: view from “side”. Original artwork.

Different classes of antibodies exist, defined by their heavy chains. Heavy chains alpha, delta, epsilon, gamma and mu give rise to immunoglobulins (Ig) A, D, E, G and M, respectively. Every class has a specific function (Fig. 2.15) and class switching (isotype switching) from one class to another class can also happen. Thereby, the light chains of an antibody with given specificity remain constant and the C gene of the heavy chain is exchanged while keeping the V_H domain.

Functional activity	IgM	IgD	IgG1	IgG2	IgG3	IgG4	IgA	IgE
Neutralization	+	–	++	++	++	++	++	–
Opsonization	–	–	+++	*	++	+	+	–
Sensitization for killing by NK cells	–	–	++	–	++	–	–	–
Sensitization of mast cells	–	–	+	–	+	–	–	+++
Activates complement system	+++	–	++	+	+++	–	+	–

Figure 2.15. Different effector functions of human immunoglobulins. Reprinted from "Immunobiology: the immune system in health and disease" 5th edition. Janeway C., Travers P. Walport M. and Shlomchik M. Edited by Garland Science.

2.3.2. Mode of action

The different antibody functions are mediated by different structures of the antibody molecule. For antibody therapy, targeting, neutralization, antibody-dependent cell-mediated cytotoxicity (ADCC) and complement activation are the most important mechanisms.

The selective binding of antibodies to their target structure is used in the concept of targeted delivery of cytotoxic payloads, e.g. the anti-CD20 antibody ibritumomab (Zevalin®), which is functionalized with radioactive yttrium-90 or indium-111 via the chelator tiuxetan, used against non-Hodgkin lymphoma. Highly selective accumulation at the site of action allows selective irradiation of the target cell. Phage-derived fully human antibodies are also used for this application. The anti-EDB antibody L19, engineered by the Laboratory of Prof. Neri at ETH Zurich, targets the extra domain B of fibronectin, a marker of tumor-induced neovascularization. It has been modified with more than 30 effector molecules, e.g. TNF-alpha, IL12,

truncated tissue factor, IL2 or liposomes containing cytotoxic drugs (Menrad *et al.* 2005). By linkage to L19, IL-2 can be delivered with high specificity to the tumor site, were it activates immune cells to combat the tumor. This has been shown in B-cell non-Hodgkin lymphoma, where a combination of rituximab and L19-IL2 completely eradicated the tumor (Schliemann *et al.* 2009).

Neutralization of toxins, viruses or bacteria is mediated by simple binding of the antibody to a biologically active target structure on the toxin or pathogen, thereby sterically blocking the binding of the toxin or pathogen to enzymes or cells. For therapy, antibodies are engineered to neutralize or inhibit a specific target protein, e.g. VEGF-A in the case of the antibody bevacizumab (Avastin®), used against several cancers including colon cancer.

ADCC is dependent on interactions between cellular Fc receptors (FcR) on immune accessory cells and the antibody Fc domains (Steplewski *et al.* 1983). The binding of Fc domain-containing IgG1 or IgG3 molecules to target cells creates opportunities for the IgG Fc domains to interact with Fc receptors expressed mainly by natural killer (NK) cells, but also by neutrophils, mononuclear phagocytes and dendritic cells (Nimmerjahn *et al.* 2006). Such binding crosslinks FcR on these cells and they become activated as a result. Activation of these cells has several consequences; for example, activated NK cells bound via their low affinity Fc receptor (the FcgammaRIIIA or CD16A) initiate lysis of the antibody coated cell by secretion of perforin and granzymes (Smyth *et al.* 2005). They also release cytokines and chemokines that can inhibit cell proliferation and tumor-related angiogenesis, and increase tumor immunogenicity through increased cell surface expression of major histocompatibility complex (MHC) antigens (Iannello *et al.* 2005). The anti-CD-

20 antibody rituximab (MabThera®), used in therapy of lymphoma, works partly like this (Weng *et al.* 2003).

IgM, IgG1 or IgG3 antibodies bound to cells or other structures can also activate the complement system via its classical pathway. Thereby, the plasma complement protein C1 binds to the Fc-tail of antigen-complexed antibodies and initiates the complement cascade which results in the generation of an enzyme complex that first cleaves the complement protein C3 into the products C3a and C3b, and then, upon addition of C3b to the complex, cleaves C5 into C5a and C5b and finally allows the assembly of the “membrane attack complex” (MAC) together with C6, C7, C8 and C9. The MAC induces pores in the plasma membrane of the antibody-coated cell (similar to the action of perforin from NK cells) and leads to osmotic swelling and finally rupture of the target cell (Tschopp *et al.* 1986). This occurs e.g. with the anti-CD52 antibody alemtuzumab (MabCampath®) *in vivo* (Osterborg *et al.* 1997). Other antibody mediated host defense mechanisms are opsonization and activation of mast cells.

2.3.3. Bevacizumab (Avastin®)

Genentech’s blockbuster drug Avastin® (bevacizumab), is a humanized monoclonal antibody against human VEGF-A (Presta *et al.* 1997), raised originally in mice (Kim *et al.* 1992). In many solid tumors, when the tumor size reaches a certain limit, the tumor center becomes hypoxic due to limited oxygen supply from the surrounding normal blood vessels in the tissue. The VEGF-A gene is regulated by the hypoxia-induced factor 1-alpha (HIF-1alpha), a transcription factor that drives VEGF-A transcription and expression in the case of hypoxia (Forsythe *et al.* 1996). Through increased expression of the blood vascular growth factor VEGF-A, new

blood vessels from preexisting ones are formed around and within the tumor (angiogenesis), and oxygen as well as nutrient supply and metabolic waste disposal are reconstituted for the tumor. This so-called angiogenic switch allows further expansion of the tumor and typically enhances tumor aggressiveness. Bevacizumab was designed to counteract this angiogenic switch and is based on the original principle of anti-angiogenic therapies proposed already in 1971 by Judah Folkman (Folkman 1971). When bevacizumab is administered parentally to cancer patients, it binds to VEGF-A in the blood and near the tumor site and prevents the binding of VEGF-A to its receptors, VEGF-R2 and VEGF-R1 as well as neuropilin-1 and -2 (Nrp-1/2). Activation of VEGF-R2 is thereby inhibited and angiogenesis at the tumor site is reduced, which should lead to decreased metabolic supply to the tumor and to reduced tumor growth – at least in theory. Bevacizumab has been FDA-approved for use as a single agent in recurrent glioblastoma multiforme (brain cancer) (Cohen *et al.* 2009) and for concomitant use with chemotherapeutic drugs in metastatic colorectal cancer (Hurwitz *et al.* 2004; Willett *et al.* 2004), non-small cell lung cancer (Hurwitz *et al.* 2004; Willett *et al.* 2004), metastatic renal cell carcinoma (Summers *et al.*) and HER2-negative metastatic breast cancer (Miller *et al.* 2007). Furthermore, bevacizumab has been used off-label for treatment of neovascular age-related macular degeneration (AMD) (Ciulla *et al.* 2009), an eye illness caused by unwanted growth of blood vessels on the macula. Ranibizumab (Lucentis®), an affinity-matured Fab-fragment of bevacizumab was further developed to be used in AMD and has FDA-approval (Ciulla *et al.* 2009).

Recently, it has been suggested, that bevacizumab might not completely block angiogenesis at the tumor site, but might rather mediate the normalization and functional enhancement of abnormal blood vessels within and around the tumor.

This might then allow the jointly administered chemotherapeutic agents to better reach the tumor and to work more effectively (Jain 2005; Yang *et al.* 2005). Adjuvant treatment with bevacizumab prolongs median overall survival and progression-free survival of colon carcinoma patients by 4 to 5 months (Hurwitz *et al.* 2004).

A comprehensive review on other possible mechanisms of VEGF-A-targeted therapies can be found elsewhere (Ellis *et al.* 2008). By switching to other angiogenic signaling pathways, the tumor can become resistant to anti-VEGF-A treatment with bevacizumab and resumes growth and aggressiveness (Casanovas *et al.* 2005).

2.3.4. Immune responses against therapeutic antibodies and proteins

The main advantage of phage-derived monoclonal antibodies is their fully human sequence repertoire. In the early times of immunotherapy with monoclonal antibodies derived from mouse B-cell hybridomas, the field was almost killed by the severe side-effects that the administration of non-human antibodies elicited (Reichert 2001). Recognition of the murine antibodies by the human immune system lead to the production of human anti-mouse antibodies (HAMA), that neutralized the murine antibodies and lead to the development of serum sickness (Tjandra *et al.* 1990). The development of techniques to humanize rodent-derived monoclonal antibodies was therefore seen as an enormous progress in the field of antibody therapy (Riechmann *et al.* 1988). However, also humanized or even fully human antibodies can be immunogenic; the following paragraph discusses an example based on anti-TNF-alpha biologics.

Adalimumab (Humira®) is the first fully human monoclonal antibody that was approved by the FDA. Cambridge Antibody Technologies originally developed the

antibody; today, it is sold by Abbott, Inc. It was selected by phage-display to bind and neutralize tumor necrosis factor alpha (TNF-alpha) and is used against different forms of arthritis, Morbus Crohn, ankylosing spondylitis and psoriasis. Similar biologics that inhibit TNF-alpha are the recently introduced fully human monoclonal antibody golimumab (Simponi®), the mouse-human chimeric monoclonal antibody infliximab (Remicade®) and the TNF-receptor-2-Fc fusion protein etanercept (Enbrel®). Since infliximab is a murine-human chimeric antibody, it elicits human anti-chimeric antibodies (HACAs) in 15% to 50% percent of treated patients (Hanauer *et al.* 2002; Baert *et al.* 2003). When they occur, HACAs are linked to a higher rate of infusion reactions and decreased efficacy of therapy (Baert *et al.* 2003). Contrary to the chimeric antibody infliximab, the fully human monoclonal antibodies adalimumab and golimumab as well as the soluble receptor etanercept should not elicit neutralizing antibodies. However, in studies on adalimumab use in rheumatoid arthritis, about 20% of the treated patients still developed human anti-human anti-adalimumab antibodies (Bartelds *et al.* 2010) and clinical responsiveness towards the drug was correlated with the emergence of anti-adalimumab antibodies (Bartelds *et al.* 2007; Radstake *et al.* 2009). Neutralizing antibodies against the soluble receptor etanercept were observed in less than 10% of the patients and have not been observed to lead to decreased efficacy (Bartelds *et al.* 2007; Radstake *et al.* 2009).

2.3.5. Hybridoma vs. antibody library

Classically, monoclonal antibodies are generated with the hybridoma method introduced by Köhler and Milstein in 1975 (Kohler *et al.* 1975). It is based on immunizing animals (often mice) with the target protein or a peptide from the target protein together with a carrier protein like keyhole limpet hemocyanine (KLH) or

ovalbumin. Over the course of several weeks, an initial injection as well as two to three booster injections are necessary to induce maturation of B-cells and production of antibodies against the injected protein. The peripheral plasma B-cells from the animal's spleen or lymph nodes are then harvested and fused with immortal myeloma cells to form a "hybridoma". By limiting dilution or FACS, single hybridoma clones are produced and analyzed for secretion of the antibody of interest. Clones of interest are expanded and form an immortalized antibody-producing cell line that produces monoclonal antibodies.

Monoclonal antibodies produced in this process are antibodies from murine or other non-human origin. Such non-human antibodies are usually immunogenic when injected into humans. Upon repeated injection, neutralizing antibodies against the foreign protein are generated by the immune system (as in any other challenge with a non-self protein). For murine antibodies, human anti-mouse antibodies are raised, which inhibit their action and lead to treatment side effects, as discussed above.

The antigen-binding of an antibody is conferred by small and well-localized regions (the CDRs) in the V_H and V_L domains. The other domains of an antibody can be thought of as a "framework". By exchanging the framework parts of the foreign antibody with human aa sequences, the antibody can be made less immunogenic. Dependent upon the degree of substitution with human sequences, such originally foreign antibodies are called chimeric or humanized (Fig. 2.16) (Riechmann *et al.* 1988).

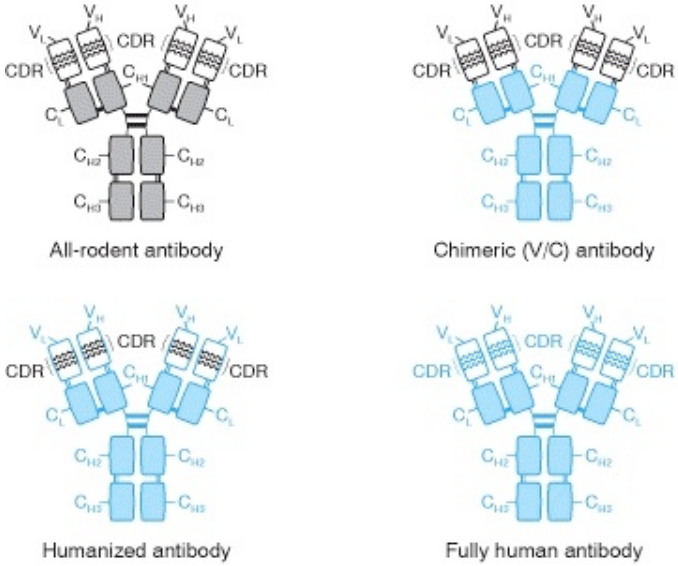

Figure 2.16. Humanization of rodent antibodies. Early versions contained the variable domains of a rodent antibody attached to the constant domains of a human antibody, a so-called chimeric antibody. The immunogenicity of the rodent mAb is reduced, while allowing the effector functions to be selected for the therapeutic application. A further stage of humanizing antibodies is possible. The essential antigen-binding site is a subset of the variable region characterized by hypervariable sequences, the complementarity-determining regions (CDRs). Accordingly, second generation humanized antibodies were CDR-grafted antibodies: the hypervariable antigen-binding loops of the rodent antibody were built into a human antibody, creating a humanized antibody. Reprinted from "Human molecular genetics" 2nd edition, Strachan T. and Read A., Garland Science.

Recently, the development of a "Xenomouse" made it possible to directly obtain fully human antibodies from immunized mice. In the Xenomouse, the murine immunoglobulin gene loci have been replaced with their human counterparts (Green 1999).

Next to the problem of immunogenicity, the generation of antibodies in living organisms must deal with the problem of immunogenic tolerance. Due to the mechanism of B-cell tolerance, B-cell clones that recognize self-antigens are deleted from the animal's immune system (Sinclair 2004). This means that antigens that are highly conserved between species are only poorly immunogenic and finding an

antibody against such antigens might be difficult. As an example, from more than 10 hybridoma monoclonal antibodies raised in mice against human VEGF-A (sharing 85% identity to murine VEGF-A), none was able to bind murine VEGF-A (Liang *et al.* 2006). To produce animal-derived monoclonal antibodies against highly conserved self-antigens, more sophisticated methods like the use of B-cell tolerance defective mice are necessary (Zhou *et al.* 2009).

Genetic engineering of antibody libraries is a more recent and alternative way to generate antibodies. Billions of natural or synthetic antibody sequences are expressed ("displayed") on the surface of e.g. a phage (Marks *et al.* 1991), and the respective antibody is found by selection and amplification of desired binders. Through the unique physical linkage of phenotype (antibody specificity on the surface of e.g. the phage) and genotype (DNA sequence in the phage virion coding for the displayed antibody) by the phage hull, a once found antibody is easily amplified by transduction of phage-susceptible bacterial strains with the isolated phage virion. Determination of the antibody aa sequence by looking at the DNA sequence is also accomplished readily. Other antibody and DNA carriers (yeast and ribosomes) have also been described (Hoogenboom 2005).

Antibody phage-display offers the great advantage of shortcutting the animal's immune system and allows the selection of antibodies against virtually any antigen, including self-antigens, which are normally non-immunogenic. By using antibody frameworks based on human germline V-gene segments, binders with human amino-acid sequences can be obtained and easily be reformatted into fully human IgG or other formats. This offers the advantage of significantly reduced immunogenicity compared to non-human, chimeric or humanized antibodies, when used in human therapy.

2.4. Antibody Phage-Display

2.4.1. Library types and construction

Antibody phage-display libraries exist in two main classes: either based on the natural antibody sequence repertoire encoded by germline DNA extracted from B-cells (natural libraries) or based on engineered randomization of antibody CDRs within an identical framework (synthetic libraries). Natural libraries can be constructed from B-cells of naïve (non-immune, healthy) individuals or from immunized individuals.

Libraries constructed from pre-immunized donors are antigen-biased, meaning the antibody sequences are directed against pathological antigens (e.g. tumor or autoimmune antigens) in the diseased patient or against the antigen used for immunization of the animal. Immune libraries often lead to identification of high-affinity binders, since the host's B-cells may already have undergone maturation by the immune system. As a drawback, antibody phage libraries from immunized donors must be constructed anew for each antigen and the isolation of binders against self-antigens is not possible since the immune system deletes B-cells displaying self-reactive antibodies.

Naïve natural libraries on the other hand are not antigen biased and they can be used to select antibodies against virtually any antigen, since the range of antibody sequences isolated from B-cells has not been limited by prior immunization.

Synthetic libraries have the same advantages as natural naïve antibody libraries, with the added bonus of dealing with DNA sequences that are engineered and therefore precisely known. This greatly facilitates subsequent affinity maturation with degenerate PCR and reformatting to other antibody formats.

2.4.2. ETH-2 Gold library

The ETH-2 Gold antibody phage-display library is a fully synthetic library in the single-chain Fv (scFv) format, cloned in the laboratory of Prof. Neri by Dr. Michela Silacci and others in 2005 (Silacci *et al.* 2005). It contains more than 3 x 10^9 individual clones. The library is based on three human germline V-gene segments, one heavy chain segment (DP47) which pairs with one of the two light chain segments, lambda (DPL16) or kappa (DPK22). Antigen recognition is largely driven by the CDR3 loops, which make the most contact with the antigen. Therefore, library diversity was introduced into the CDR3 regions of both heavy and light chains, by means of PCR using partially degenerate primers. The CDR3 of the heavy chain DP47 segment was engineered to contain four to six completely randomized amino acids. The CDR3 of the lambda light chain DPL16 segment contains a six aa randomized sequence with at least one proline residue, and the CDR3 of the kappa light chain DPK22 segment contains also six aa residues with a glycine residue at the second or third position and a proline residue at the fifth position (Fig. 2.17). The two variable fragments are joined together by a flexible linker consisting of $Gly_4SerGly_4SerGly_4$ in the order of N_{term}-V_H-linker-V_L-C_{term}.

Figure 2.17. Overview of the scFv sequence and the randomization strategy. The aa sequences are oriented from the N- to the C-terminus. “Amber” denotes the amber stop codon TAG, which can be read either as a stop (by non-suppressor *E.coli* strains) or as a glutamine residue (by suppressor strains). “pIII” stands for the phage coat protein pIII, to which the scFv is fused. “X” denotes any aa residue. Modified from Silacci *et al.* 2005.

The DNA constructs were then inserted in a phagemid vector (pHEN1) that harbors an upstream bacterial periplasmic secretion signal (*pelB*), a downstream myc-tag that will be fused to the N-terminus of the scFv, an amber stop codon and the phage coat protein gene pIII (Fig. 2.18). In *E.coli* amber suppressor strains containing the *supE* mutation (such as the XL1-blue strain, or the semisupressor strain TG1), the amber stop codon will be read as a glutamine codon, the scFv sequence will be fused with the phage coat protein pIII and displayed on the tip of the phage. As the pHEN1 vector is a phagemid vector, formation of phage particles from bacteria containing the pHEN1 phagemid requires superinfection with a helper phage (e.g. VCSM13 or M13KO7) that provides all the other necessary phage proteins required for phage particle assembly. The phage carrying the antibody is the

filamentous phage M13, which infects bacterial strains expressing a F-pilus, encoded on the F-episome. The minor coat protein pIII is expressed at one end of the phage particle, in three to five copies, to some of which the scFv is fused and thereby displayed.

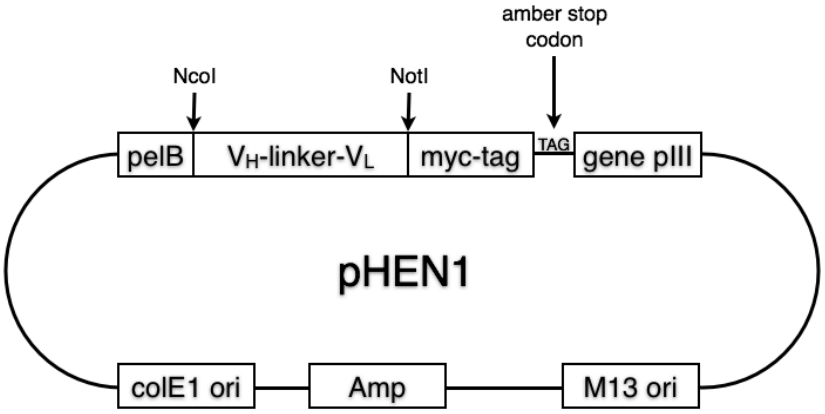

Figure 2.18. Map of the features on the pHEN1 plasmid. The phagemid pHEN1 is used to drive expression of scFv fragments, either as soluble scFv when using an amber-suppressor *E.coli* strain or as pIII fusions when expressed on phage (requires coinfection of the bacteria with a helper phage). *PelB*, bacterial periplasmic secretion signal; colE1 ori, pUC based high copy number origin of replication; M13 ori, M13 phage origin of replication that drives singled stranded DNA replication, needed for phage packaging. Modified from Silacci *et al.* 2005.

For secretion of soluble scFv molecules, non-suppressor *E.coli* strains are infected with the antibody carrying phages. The scFv gene is then translated up to the amber stop codon and a soluble scFv will be secreted to the periplasmic space, due to the *pelB* leader sequence. Some of the scFv will eventually leak out from the periplasmic space to the culture medium. In practice, the versatile TG1 semi-suppressor strain can be used for both production of phage particles bearing pIII-fused scFv by amber-suppression and superinfection with a helper phage and secretion of soluble scFv by incomplete suppression of the amber stop codon. For facilitated detection of the scFv, a myc-tag (EKQLISEEDL) has been fused to the C-

terminus of the scFv, just prior to the amber stop codon. Since the DP47 human heavy chain IgG germline segment belongs to the VH3 family (Tomlinson *et al.* 1994), protein A binds to the framework 1 (FR1) and CDR2 / FR3 region of the heavy chain (Hillson *et al.* 1993; Potter *et al.* 1997) and can be used to purify the scFv from bacterial supernatant via affinity chromatography.

2.4.3. Panning strategies

Two main strategies are usually employed when phage-display libraries are panned for binders against antigens. The technique must allow specific retention of the binding scFv-displaying phage. This is achieved by use of a matrix that allows capturing of the antigen and the associated scFv and phage. Often, the antigen is coated on a plastic surface modified to allow specific adsorption of proteins (e.g. Nunc Maxisorp surfaces). Immunotubes or 8-well strips are useful varieties of such supports. The phage library is then added and phages displaying scFv that bind to the coated antigen are allowed to bind. Non-binding phages are then washed away and remaining binding phages are eluted specifically from the support with a low or high pH buffer that destabilizes the antigen-scFv complex (Fig. 2.19).

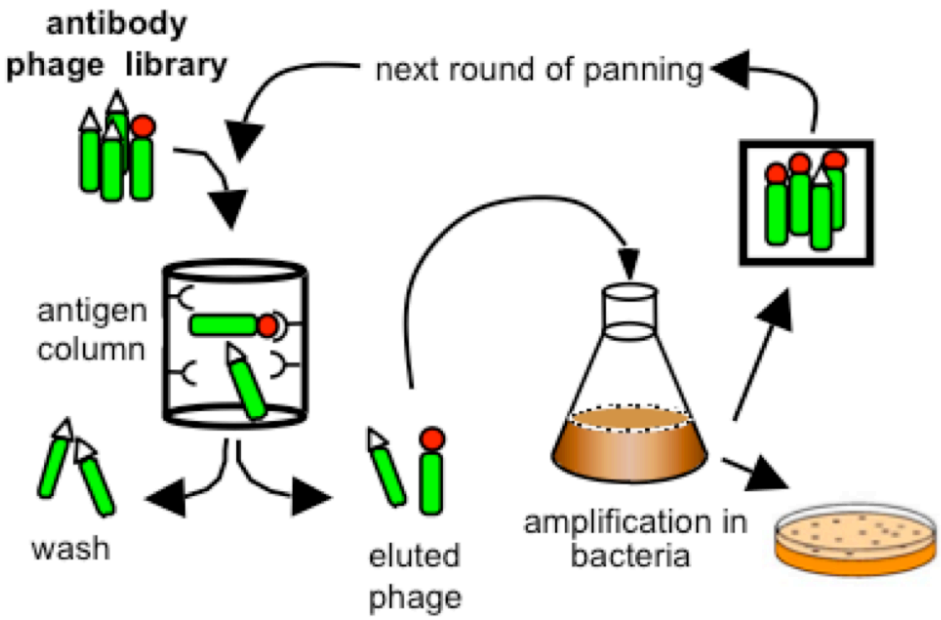

Figure 2.19. Principle of the phage panning process. An antibody phage library is added to a support coated with an antigen. Phages that do not bind to the antigen (white triangular tip) are subsequently washed away while binding phages (red round tip) are specifically eluted. The eluted phages (now enriched in binders) are used to infect *E.coli* and get amplified in the bacteria (with the help of a helper phage). A second round pool of phages is then prepared that is enriched for the antigen-binding phages and used to repeat the process, further enriching antigen-binding phage clones.

The main advantage of this direct coating approach is that the antigen can be used as is, without further modifications. However, adsorption of the protein antigen on the plastic surface can lead to denaturation of the antigen, thereby changing the structure of the protein and leading to selection of binders directed against the incorrectly folded antigen structure. Also, passive adsorption may result in “islets” of locally highly concentrated antigen, which may promote selection of phages that display more than one scFv and profit from avidity rather than affinity when binding to multiple antigen copies.

To overcome the possible problems encountered by panning using the direct coating method, panning using a biotinylated antigen (“biopanning”) was introduced. Here, a small biotin molecule is covalently attached to free primary amines on the antigen (lysines residues or the N-terminus) via amine-reactive chemistry using *N*-hydroxysulfosuccinimide (NHS). The panning itself is carried out in solution, meaning antibody carrying phages and the biotin-modified antigen are mixed in a buffer and the formation of a complex of antigen and antigen-specific phages is allowed before the complex is captured to a support. The capturing can be performed with streptavidin-coated maxisorp 8-well strips or paramagnetic beads (dynabeads) together with a magnet. Washing and elution are performed as described above.

Due to the solution phase binding procedure, a homogenous density of antigen is achieved and selection of binders is driven by affinity rather than avidity. Also, adsorption-induced denaturation of the antigen is prevented. Nevertheless, through the covalent modification of the antigen with a linker and the biotin moiety, the antigen structure might also be affected and binding to key determinants on the antigen may be obstructed. This is especially problematic when searching for neutralizing binders against bioactive epitopes or enzymatic clefts that are known to contain lysine residues.

2.5. Aim and working strategy of this thesis

Based upon the findings that tumor-induced lymphangiogenesis enhances metastasis of many solid tumors and that this lymphangiogenesis is mainly driven by VEGF-C, we intended to engineer an inhibitor that interferes with this pathway. Since blocking of VEGF-D, VEGF-R2 or VEGF-R3 has certain disadvantages as outlined above, we have decided to use fully processed, mature ΔNΔC-VEGF-C as our target molecule. Furthermore, no tumor studies with a function-blocking anti-VEGF-C antibody have been reported so far. Since ΔNΔC-VEGF-C is highly conserved between species and since we wanted to generate a human antibody fragment, we used the fully human synthetic ETH-2 Gold antibody phage-display library to generate a lead binder against VEGF-C.

3. Results

3.1. Analysis of *Pichia pastoris*-derived ΔNΔC-VEGF-C

The ΔNΔC-VEGF-C, kindly provided by Prof. Ballmer-Hofer, Paul-Scherrer-Institute, Villigen, Switzerland, was subjected to analysis to determine its purity and identity. SDS-PAGE analysis revealed a doublet band at about 21 kDa under reducing conditions and a doublet band at about 33 kDa as well as weaker bands of higher molecular mass under non-reducing conditions, which is in good agreement to previous reports (Cao *et al.* 1998). No major contaminating proteins could be observed (Fig. 3.1 A). The relatively small size of the dimer (as compared to the calculated 42 kDa) could be explained by the influence of the heavy glycosylation of ΔNΔC-VEGF-C on the electophoretic mobility and / or tight packing of the VEGF-C dimer.

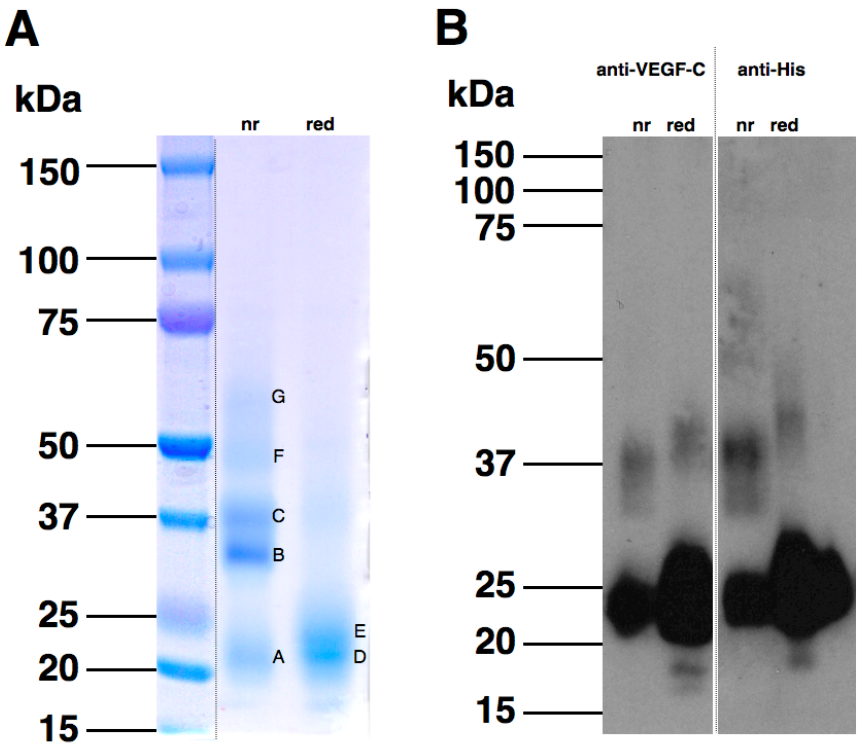

Figure 3.1. SDS-PAGE and immunoblot analysis of *P. pastoris*-derived human ΔNΔC-VEGF-C. (A) 8 µg of ΔNΔC-VEGF-C were separated on a 4-12% precast SDS-PAGE gel under non-reducing (nr) and reducing (red) conditions and stained with Coomassie-blue. Indicated bands were excised,

destained, the proteins were reduced, alkylated, digested with trypsin and eluted. Tryptic peptides were subjected to MALDI-MS/MS. (B) 500 ng of ΔNΔC-VEGF-C were separated on a 10% precast SDS-PAGE gel under non-reducing (nr) and reducing (red) conditions, transferred to a nitrocellulose membrane and immunoblotted using a polyclonal rabbit anti-human VEGF-C antibody (IBL) or a mouse anti-His antibody (Qiagen), followed by detection with HRP-labeled anti-rabbit or anti-mouse antibodies, respectively.

Matrix-assisted laser desorption/ionization (MALDI) tandem mass-spectroscopy of bands A to G observed in the Coomassie-staining of SDS-PAGE-resolved ΔNΔC-VEGF-C as well as a non-electrophoresed sample of ΔNΔC-VEGF-C identified only the recombinant ΔNΔC-VEGF-C in all samples (except band A), with no other contaminating proteins, neither human nor host-derived. The higher molecular weight bands are thus probably higher oligomers of ΔNΔC-VEGF-C. The observed doublet bands likely are the result of differential glycosylation. The 129 aa sequence translated to a protein size of 14.7 kDa, about 7 kDa are added by glycosylation at two possible N-glycosylation sites (Uniprot P49767). Western blotting with anti-VEGF-C (IBL) and anti-His antibodies revealed the same bands as seen in the SDS-PAGE analysis, with fractions of dimers in the reduced sample and fractions of monomers in the non-reduced sample (Fig. 3.1 B). Size-exclusion gel-filtration on a Superdex 75 column revealed a major peak at about 10 ml, eluting between the 52 kDa homodimer glutathione-S-transferase and the 27 kDa monomeric scFv peak (Fig. 3.2). This indicated that *P. pastoris*-derived ΔNΔC-VEGF-C exists as a dimer in physiological buffer conditions.

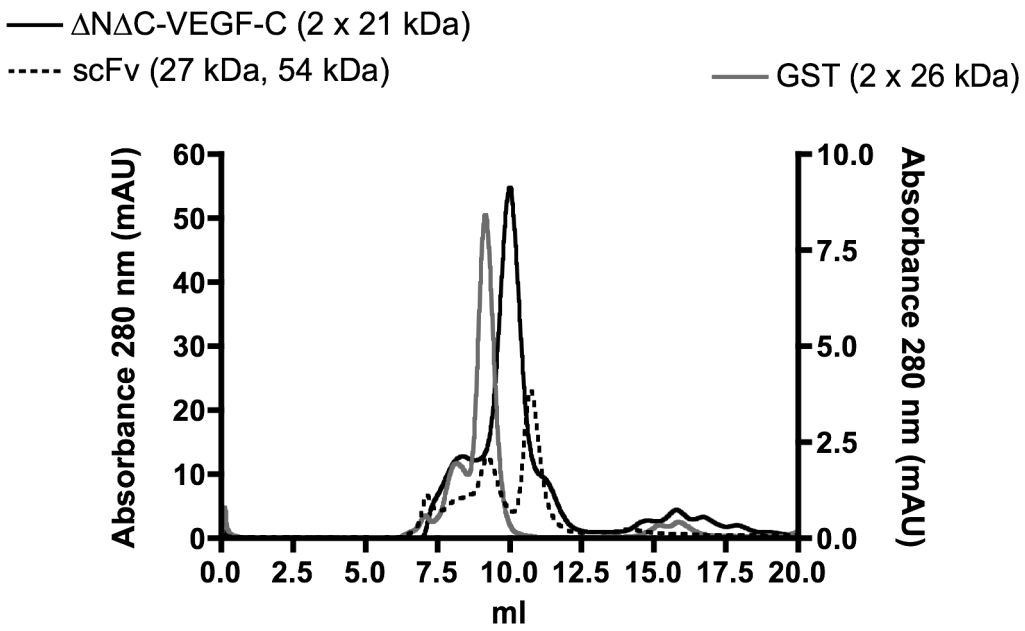

Figure 3.2. Size-exclusion gel-filtration profile of *P. pastoris*-derived ΔNΔC-VEGF-C. 100 µg of ΔNΔC-VEGF-C in 100 µl PBS were injected on a Superdex 75 10/300 GL column and eluted using PBS at 0.5 ml/min.

3.2. Selection of anti-VEGF-C scFv

We employed the human fully synthetic ETH-2 Gold antibody phage-display library (Silacci *et al.* 2005) to select for binders against *P. pastoris*-derived human ΔNΔC-VEGF-C. During the course of the selection against VEGF-C, a 974-fold increase in the ratio of output vs. input phage titers, expressed as the enrichment factor, was observed from round 2 to round 3, while the mock selection with uncoated immunotubes yielded a more than 30 times less strong enrichment (Table 3.1).

Antigen	Round	Input (tu)	Output (tu)	Ratio (out / in)	Enrichment (ratio n / ratio n-1)
VEGF-C	1	5.0×10^{12}	1.2×10^{6}	2.4×10^{-7}	n/a
VEGF-C	2	5.4×10^{13}	1.2×10^{4}	2.2×10^{-10}	0.00093
VEGF-C	3	6.7×10^{13}	1.5×10^{7}	2.2×10^{-7}	974
mock	1	5.0×10^{12}	5.0×10^{5}	4.0×10^{-8}	n/a
mock	2	6.3×10^{13}	4.0×10^{4}	6.3×10^{-10}	0.016
mock	3	4.0×10^{13}	8.0×10^{5}	2.0×10^{-8}	32

Table 3.1. Enrichment factors during panning. Transducing units (tu) before and after panning rounds were determined using titration of transduced colonies. Ratio of output vs. input in the same round and enrichment, i.e. the factor by which the ratio of rescued phages differed from round n-1 to round n were calculated. “Mock” refers to selections with uncoated immunotubes.

In the subsequent ELISA screening, 23 of 64 randomly picked clones from round 3 reacted against ΔNΔC-VEGF-C, while none of the randomly picked clones from the 2nd round of selection were positive (Fig. 3.3).

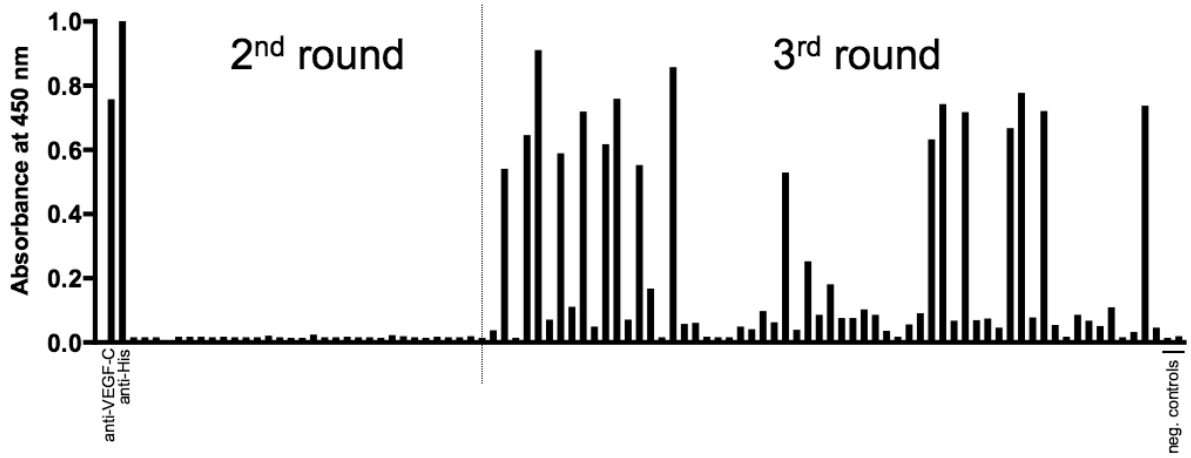

Figure 3.3. ELISA screening of random clones obtained after 2 or 3 rounds of panning against ΔNΔC-VEGF-C. After two rounds of panning none of 28 randomly picked clones were reactive against VEGF-C. In contrast, 23 of 64 randomly picked clones (36%) after the third round of panning bound to VEGF-C.

Out of these 23 clones, 4 clones possessing unique aa sequences were identified by sequencing. All 4 unique clones beared lambda light chains, 3 of these 4 clones (VC1, VC2 and VC3) showed 3 identical aa in the randomized CDR3 (1 identical aa out of 6 in CDR-L3, 2 identical aa out of 4 in CDR-H3), while the fourth clone (VC4) had a completely unrelated sequence (Table 3.2).

	CDR-H3						CDR-L3						
Clone	95	96	97	98	99	100	91	92	93	94	95	96	Frequency of recovery
VC1	**E**	**S**	**S**	**M**	-	-	**P**	**I**	**R**	**W**	**A**	**P**	17/64
VC2	**E**	**S**	**L**	**P**	-	-	**P**	**R**	**F**	**Y**	**P**	**V**	3/64
VC3	**E**	**S**	**L**	**P**	-	-	**P**	**G**	**S**	**E**	**R**	**P**	1/64
VC4	**W**	**P**	**A**	**T**	**G**	-	**V**	**D**	**A**	**W**	**P**	**G**	2/64

Table 3.2. Amino-acid sequences in the randomized CDR3s of anti-VEGF-C scFvs. Numbering according to Chothia *et al.* 1989.

As the isoelectric point (pI) of *P. pastoris*-derived ΔNΔC-VEGF-C is 8.3 (as deduced from the aa sequence, although glycosylation also affects the pI), we decided to use 100 mM glycine-HCl pH 2.2 for elution as we speculated that acidic elution is better suited for destabilizing the VEGF-C / phage complex. Interestingly, a parallel panning with 100 mM TEA, pH 12, as the elution agent did not yield any binders after 4 rounds of panning.

Since the aa sequence of *P. pastoris*-derived ΔNΔC-VEGF-C and mammalian cell-derived ΔNΔC-VEGF-C differs at the C- and N-terminal ends, all 4 clones were tested on both antigens. The 3 clones with partial identity (VC1, VC2 and VC3) bound to an epitope present on both ΔNΔC-VEGF-C derived from *P. pastoris* and mammalian cells while the fourth, unrelated clone (VC4), bound only to *P. pastoris*-derived ΔNΔC-VEGF-C but not to mammalian cell-derived ΔNΔC-VEGF-C (Fig. 3.4 A), indicating that the epitope for the scFvs VC1, VC2 and VC3 are different from the epitope recognized by scFv VC4.

After cleavage of the C- and N-terminal propeptides, both VEGF-C and VEGF-D exist as the fully processed, mature ΔNΔC protein. This central VEGF homology domain (VHD) in VEGF-C and VEGF-D is highly homologous (more than 50% identity and more than 70% homology). Clone VC2, howeverm did not bind to

mammalian cell-derived ΔNΔC-VEGF-D, confirming the specificity for VEGF-C (Fig. 3.4 B).

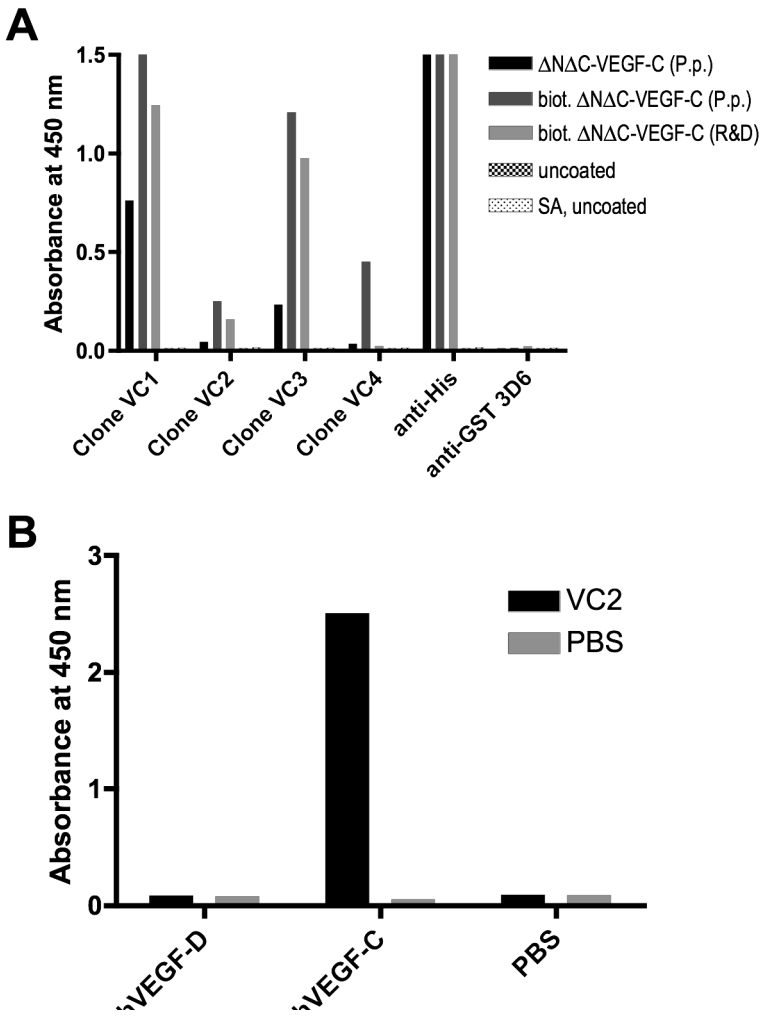

Figure 3.4. Binding specificities of the anti-VEGF-C scFv clones. (A) ELISA analysis of representative anti-VEGF-C scFv clones for the 4 different aa sequences obtained. Maxisorp or streptavidin (SA) precoated plates were coated with His-tagged human ΔNΔC-VEGF-C derived from *P. pastoris* (P.p.) or biotinylated His-tagged human ΔNΔC-VEGF-C from mammalian cells or *P. pastoris*, respectively. Control surfaces were left untreated. Antibody fragments and control antibodies were subsequently added and the ELISA was developed. (B) Cross-reactivity as tested by ELISA. Human ΔNΔC-VEGF-C or ΔNΔC-VEGF-D (both from mammalian cells) were coated on a maxisorp plate. Anti-VEGF-C scFv clone VC2 was added and the ELISA was developed.

All 4 clones were then expressed on a 1 liter scale and scFvs were purified from the supernatants via protein-A based affinity chromatography, with yields of 4 to 8 mg scFv per liter. An SDS-PAGE (Fig. 3.5 A) and anti-myc immunoblot (Fig. 3.5 B) analysis is shown below. The major band was the 27 kDa monomer band with higher bands containing a myc-tag and two lower bands not containing a myc-tag.

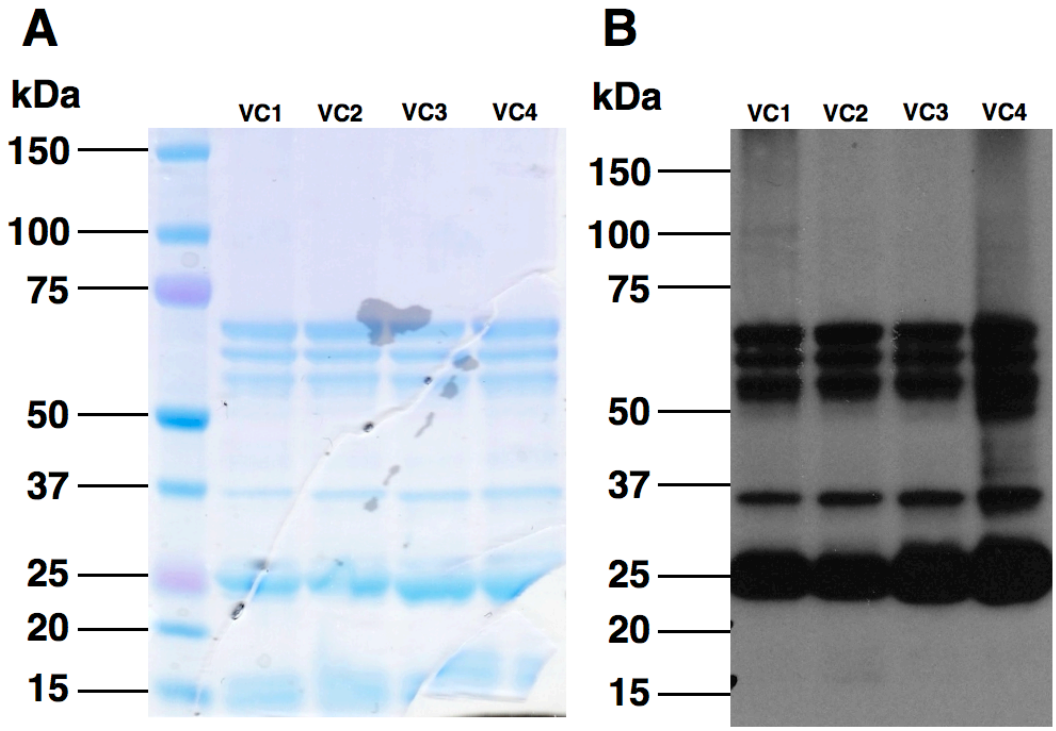

Figure 3.5. SDS-PAGE and anti-myc immunoblot analysis of anti-VEGF-C scFv. Protein-A purified scFv were resolved on a 4-12% acrylamide gel and (A) Coomassie-blue stained or (B) transferred to a nitrocellulose membrane and immunoblotted with anti-myc and secondary antibodies.

The 4 clones were next analyzed with surface plasmon resonance (SPR) on a streptavidin-coated BIAcore chip to which biotinylated *P. pastoris* or mammalian cell-derived ΔNΔC VEGF-C were immobilized. This analysis revealed different binding profiles. Clone VC2 was chosen for affinity maturation since it displayed the best apparent binding affinity for VEGF-C (Fig. 3.6 A,B).

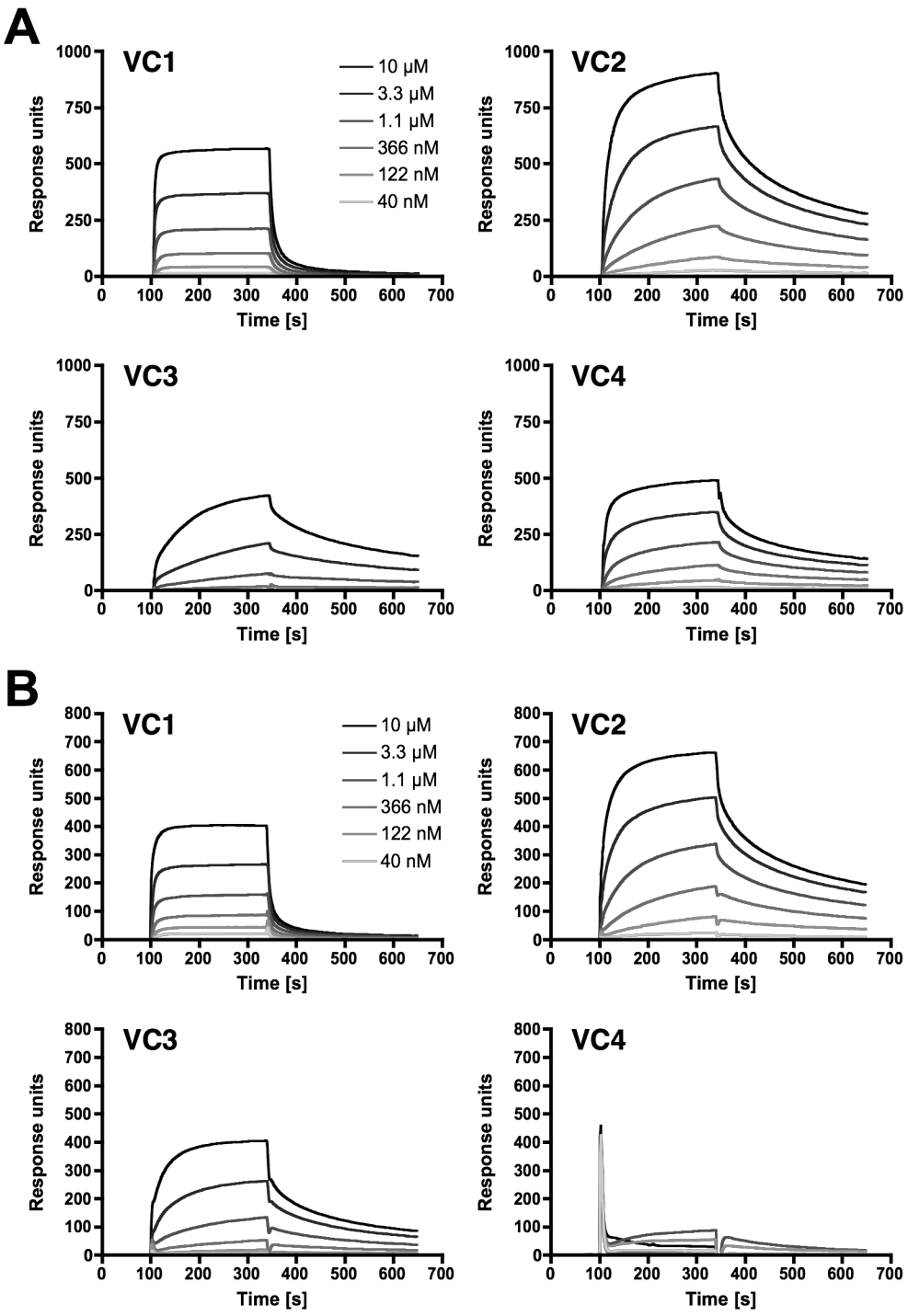

Figure 3.6. BIAcore profiles of the four different anti-VEGF-C scFv clones. 40 nM to 10 µM of Protein-A purified scFv were injected on a streptavidin-BIAcore chip coated with appr. 2'000 RU biotinylated (A) *P. pastoris*-derived or (B) mammalian cell-derived ΔNΔC-VEGF-C.

3.3. Affinity maturation

Antibody phage libraries to be used in affinity maturation selections were constructed essentially as described (Villa *et al.* 2008), based on the aa sequence of clone VC2. Randomizations were engineered in CDR1 of both heavy and light chains. The obtained library consisted of 3.3 x 10^6 clones, of which 14 randomly picked clones all contained the scFv insert as assessed by colony PCR analysis (Fig. 3.7 A). More than 90% of 96 randomly picked clones were capable of expressing a soluble scFv antibody fragment, as assessed by Dot Blot analysis (Fig. 3.7 B). Sequencing of 6 random clones revealed completely randomized aa sequences in the desired CDR-H1 and CDR-L1, while the VC2 parental aa sequence was retained in all other residues (Fig. 3.7 C).

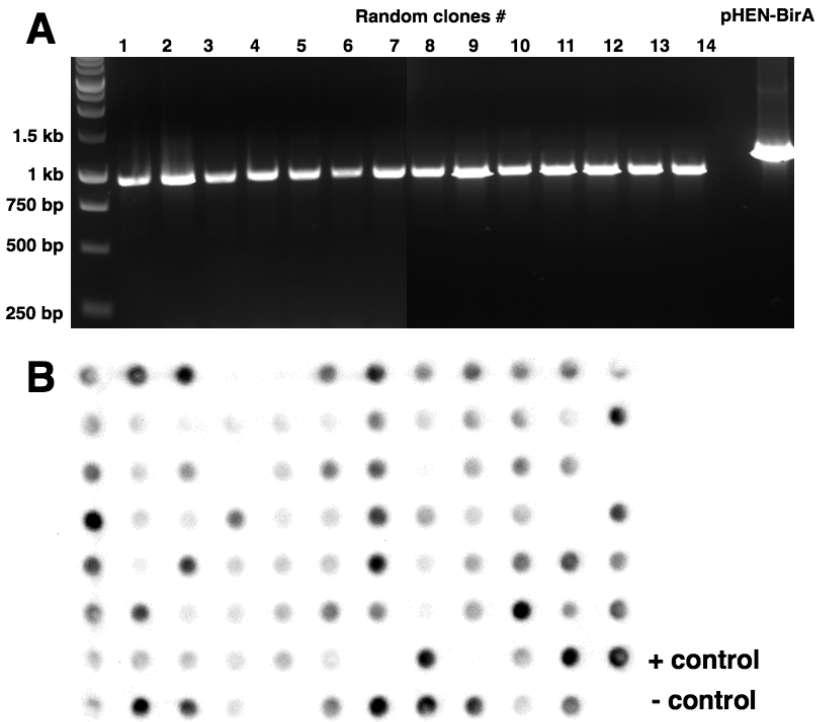

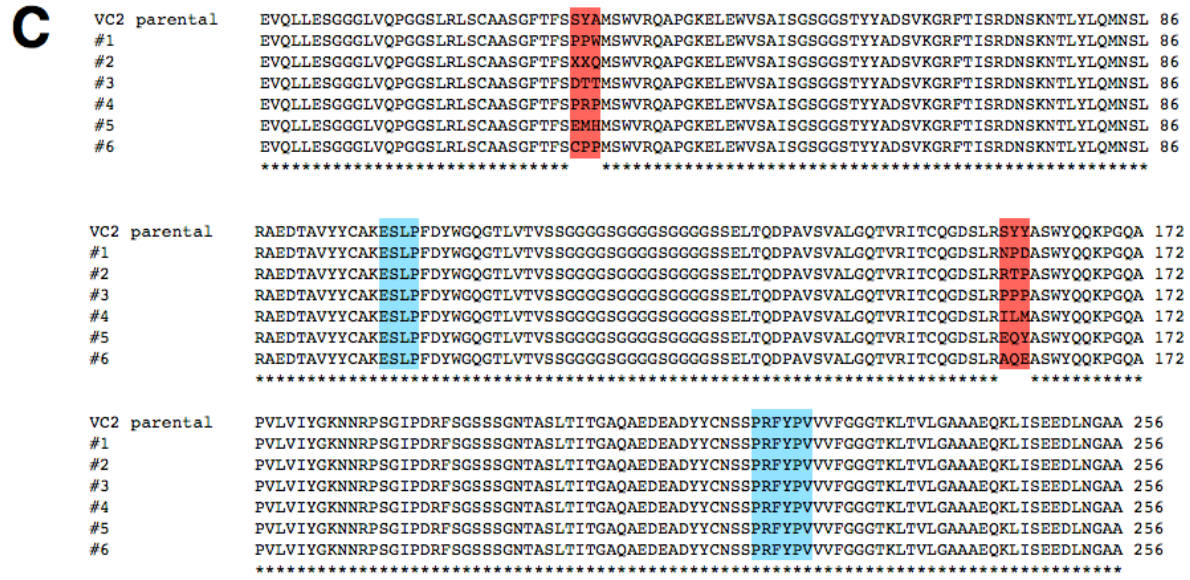

Figure 3.7. Quality analysis of the affinity maturation library. (A) Colony-PCR analysis of 14 randomly picked clones from the affinity maturation library, performed using primers LMB3long and fdseqlong on randomly picked scFv bearing pHEN1 plasmids. Control is the BirA bearing pHEN1 plasmid. Expected sizes: scFv, 959 bp; BirA, ca. 1.25 kb. (B) Dot-Blot analysis of 94 randomly picked affinity maturation library clones. 80 µl of bacterial supernatant were dot-blotted on a nitrocellulose membrane and detected using anti-myc and anti-mouse horseradish-peroxidase. 86 from 94 (91%) randomly picked clones express scFv. (C) Alignment of 6 randomly picked clones from the affinity maturation library. The sequences of the randomly picked clones show introduced diversity in the randomized CDR1 of heavy and light chain shown in red, while the CDR3 loops (shown in blue) selected in the first panning and the rest of the scFv sequence are retained.

After 1 to 3 rounds of panning of this affinity maturation library on varying concentrations of biotinylated *P. pastoris* and mammalian cell-derived ΔNΔC-VEGF-C, random clones from several selections were analyzed by ELISA. This analysis showed that more selection rounds and higher antigen concentration increased the percentage and signal intensity of binders identified (Fig. 3.8 A,B).

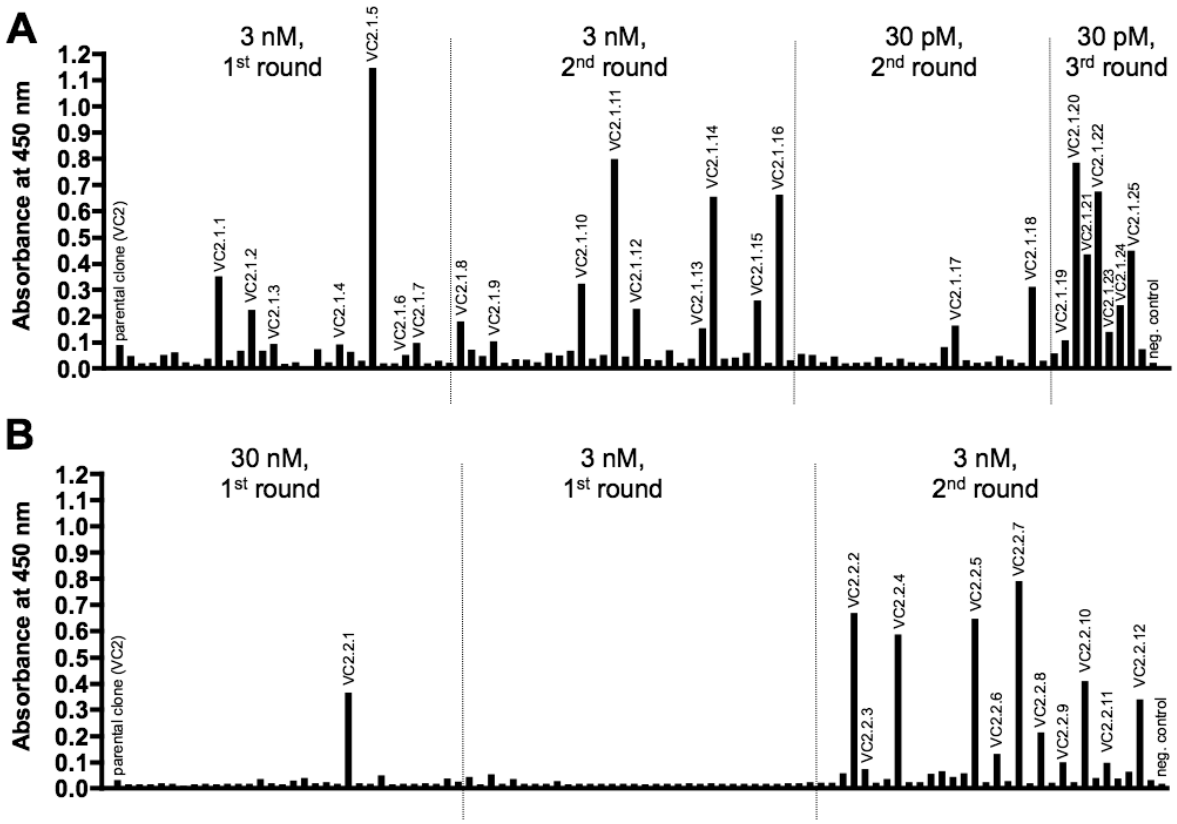

Figure 3.8. ELISA analysis of affinity matured clones. ELISA analysis of bacterial supernatants from randomly picked affinity matured clones after 1 to 3 rounds of selection on biotinylated (A) *P. pastoris*-derived or (B) mammalian cell-derived ΔNΔC-VEGF-C.

Sequencing of 10 positive clones that showed some of the highest ELISA signals and of 2 negative controls was subsequently performed. One clone (VC2.1.6) was identified to be identical to the parental scFv VC2, and clones VC2.2.5 and VC2.1.11 were identical to each other. The positive clones showed a converging selection of CDR-H1 (Table 3.3).

	CDR-H1			CDR-H3						CDR-L1			CDR-L3						
Clone	31	32	33	95	96	97	98	99	100	31a	31b	32	91	92	93	94	95	96	Frequency of recovery
Library	S	Y	A	X	X	X	X	(X)	(X)	S	Y	Y	X	X	X	X	X	X	NA
VC1	S	Y	A	**E**	**S**	**S**	**M**	-	-	S	Y	Y	**P**	**I**	**R**	**W**	**A**	**P**	17/64
VC2	S	Y	A	**E**	**S**	**L**	**P**	-	-	S	Y	Y	**P**	**R**	**F**	**Y**	**P**	**V**	3/64
VC3	S	Y	A	**E**	**S**	**L**	**P**	-	-	S	Y	Y	**P**	**G**	**S**	**E**	**R**	**P**	1/64
VC4	S	Y	A	**W**	**P**	**A**	**T**	**G**	-	S	Y	Y	**V**	**D**	**A**	**W**	**P**	**G**	2/64
VC2.2.2	*Q*	*N*	*Y*	E	S	L	P	-	-	*E*	*N*	*W*	P	R	F	Y	P	V	NA
VC2.2.5	*Q*	*N*	*Y*	E	S	L	P	-	-	*H*	*S*	*Q*	P	R	F	Y	P	V	NA
VC2.1.5	*K*	*N*	*Y*	E	S	L	P	-	-	*K*	*G*	*W*	P	R	F	Y	P	V	NA
VC2.1.20	*Q*	*N*	*Y*	E	S	L	P	-	-	*K*	*N*	*N*	P	R	F	Y	P	V	NA
VC2.2.4	*Q*	*N*	*Y*	E	S	L	P	-	-	*S*	*G*	*N*	P	R	F	Y	P	V	NA
VC2.2.1	*K*	*N*	*A*	E	S	L	P	-	-	*N*	*D*	*Y*	P	R	F	Y	P	V	NA
VC2.2.7	*G*	*N*	*Y*	E	S	L	P	-	-	*K*	*G*	*Y*	P	R	F	Y	P	V	NA
VC2.2.3	*N*	*N*	*Y*	E	S	L	P	-	-	*Q*	*N*	*T*	P	R	F	Y	P	V	NA
VC2.1.6	*S*	*Y*	*A*	E	S	L	P	-	-	*S*	*Y*	*Y*	P	R	F	Y	P	V	NA
VC2.1.26	*N*	*K*	*Y*	E	S	L	P	-	-	*A*	*H*	*M*	P	R	F	Y	P	V	NA
VC2.2.13	*Q*	*S*	*L*	E	S	L	P	-	-	*Q*	*W*	*K*	P	R	F	Y	P	V	NA

Table 3.3. Amino acid sequences of parental and affinity matured anti-VEGF-C scFv. Numbering according to Chothia *et al.* 1989. VC1 to VC4: first generation anti-VEGF-C scFv; VC2.2.2 to VC2.1.6: positive anti-VEGF-C scFv clones from affinity maturation; VC2.1.26, VC2.2.13: negative scFv clones from affinity maturation. X denotes amino acids that are randomized in the library.

In CDR-H1 sequences, X-Asn-Tyr (X-N-Y) was selected in 7 of 8 cases, while X was always a hydrophilic residue (Asp, Glu, Asn, Gln, His, Lys, Arg; D, E, N, Q, H, K, R) or a glycine. In CDR-L1, sequences were more heterogeneous. CDR1s of negative controls exhibited an even more diverse pattern. An amber stop codon (TAG, coding for Stop or Gln) was found in the CDR-H1 of 4 out of 8 positive clones and in the CDR-L1 of 1 out of 8 positive clones and was corrected to CAG (coding only for Gln) by PCR. Three clones (VC2.2.2, VC2.2.5 and VC2.1.5) were chosen for further characterization, since they showed the strongest ELISA signal. Protein-A purified fractions were further purified by size-exclusion chromatography (Fig. 3.9).

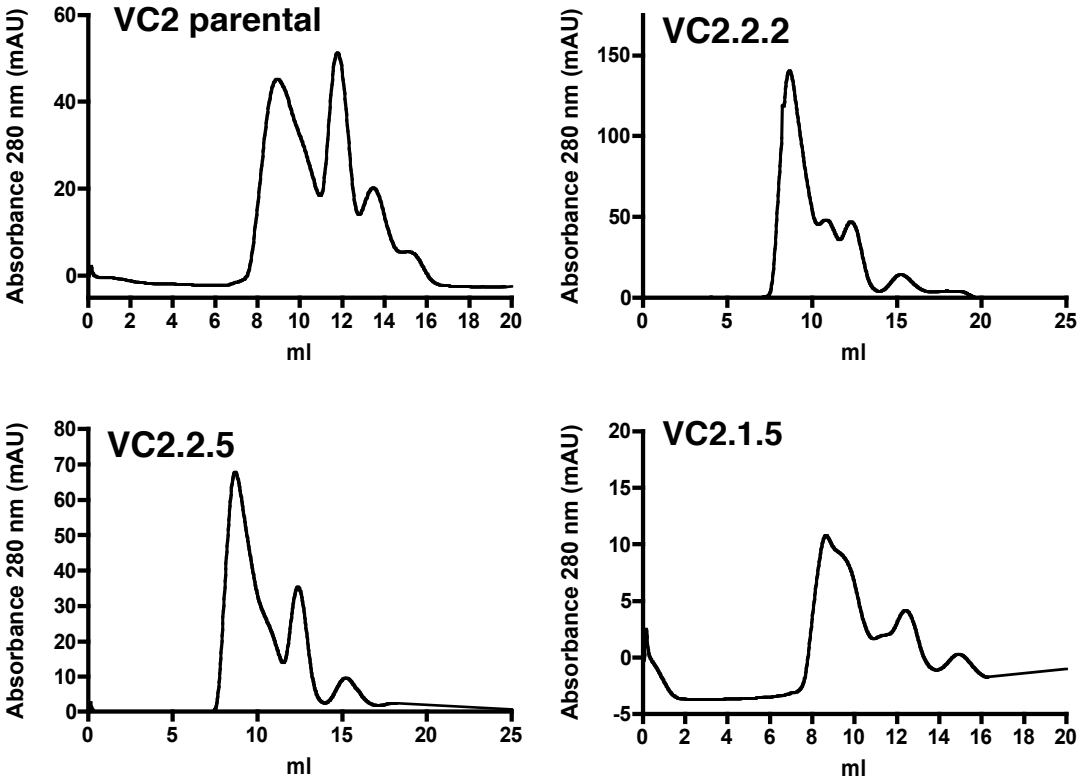

Figure 3.9. Size-exclusion gel-filtration of anti-VEGF-C scFv preparations. The parental scFv VC2 as well as 3 daughter clones were injected on a Superdex 75 column. Monomeric fractions at about 12 ml were collected and used for determination of the affinity constant in BIAcore experiments.

The size exclusion chromatography (SEC) analysis showed a major peak at about 9 ml, corresponding to putative non-covalently linked scFv:scFv' homodimers (54 kDa), and another peak at about 12 ml, corresponding to putative scFv monomers (27 kDa) (Holliger *et al.* 1993). The formation of monomers is normally facilitated by the presence of the flexible polypeptide linker ($Gly_4SerGly_4SerGly_4$) between the V_H and V_L domains (Huston *et al.* 1988). However, the SEC profiles of the anti-VEGF-C scFv clones revealed a markedly reduced amount of monomers vs. oligomers. The monomeric fractions were collected and used for further BIAcore analysis for determination of kinetic constants.

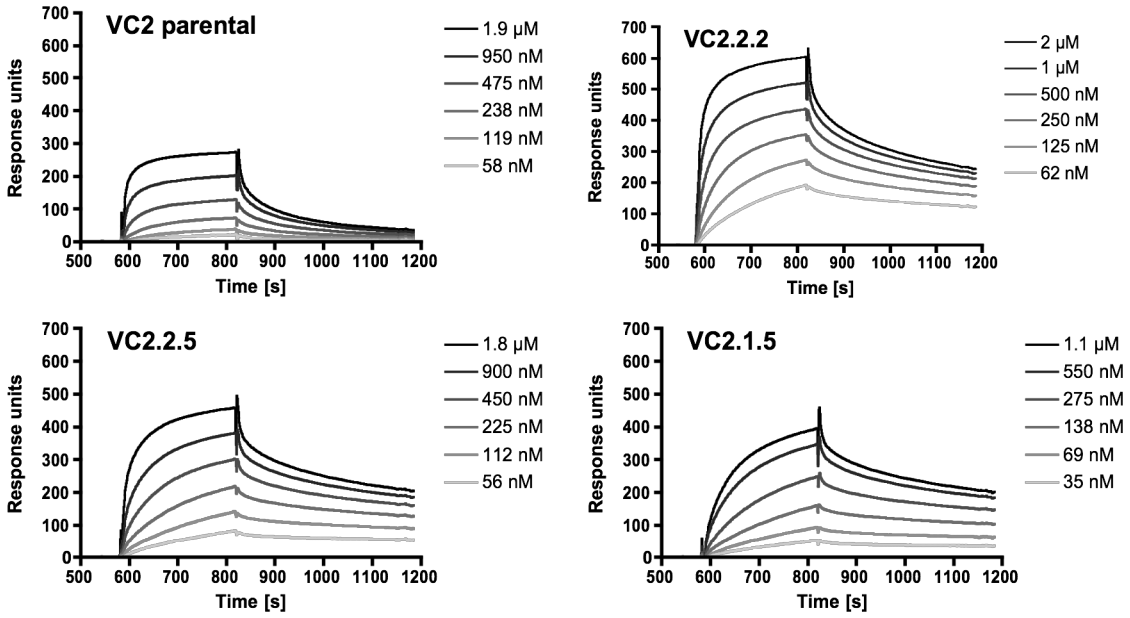

Figure 3.10. BIAcore profiles of monomeric affinity matured anti-VEGF-C scFv. The monomeric fractions prepared by SEC were injected at different concentrations on a streptavidin BIAcore chip coated with biotinylated mammalian cell-derived ΔNΔC-VEGF-C. Kinetic constants were subsequently derived from these dilution sensorgrams using BIAevaluation 3.1 software.

Kinetic analysis using BIAevaluation3.1 software revealed dissociation constants of 22, 35 and 43 nM for VC2.2.2, VC2.2.5 and VC2.1.5, respectively, an improvement of almost 4-fold compared to the parental scFv VC2 (81 nM) (Fig. 3.10 and Table 3.4). VC2.2.2, which exhibited the lowest K_d, was subsequently used for further analysis of blocking capacity.

scFv	k_{on} (1/Ms)	k_{off} (1/s)	K_d (nM)	K_d improvement
VC2	4.45×10^4	3.58×10^{-3}	81	-
VC2.1.5	2.39×10^4	1.02×10^{-3}	43	1.9
VC2.2.2	5.65×10^4	1.22×10^{-3}	22	3.7
VC2.2.5	2.85×10^4	1.00×10^{-3}	35	2.3
VC2.2.2 dimer	7.43×10^4	1.38×10^{-3}	19	4.2

Table 3.4. Comparison of the kinetic constants of the affinity matured anti-VEGF-C scFvs. The kinetic constants were fitted from dilution series of monomeric scFv preparations with BIAevaluation3.1 software using a 1:1 Langmuir binding model.

The peak in the VC2.2.2 sample at 9 ml, corresponding to putative dimeric scFv, was also collected and injected on the same BIAcore chip as the monomers. Observed kinetic constants of the monomeric and dimeric fractions were similar and the apparent affinity of dimeric VC2.2.2 did not seem to profit significantly from the bivalency (Fig. 3.11 and Table 3.4).

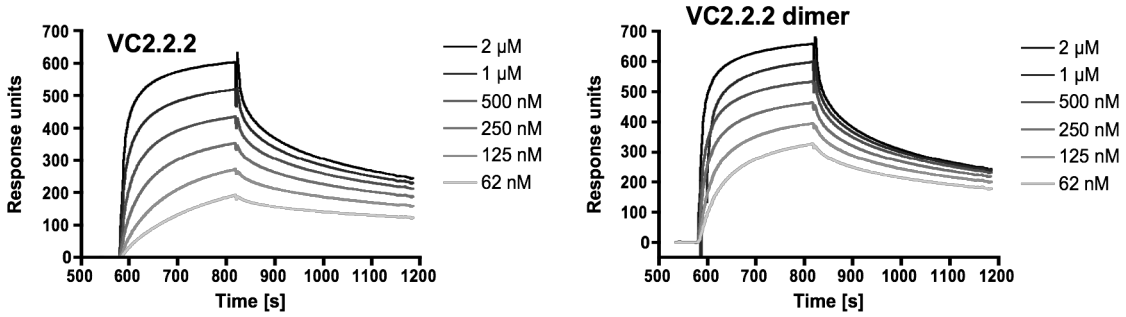

Figure 3.11. BIAcore profiles of monomeric and dimeric VC2.2.2 preparations. SEC fractions corresponding to putatively dimeric at 9 ml and monomeric scFv at 12 ml were collected and injected on a streptavidin BIAcore chip coated with biotinylated mammalian cell-derived ΔNΔC-VEGF-C.

3.4. VC2.2.2 anti-VEGF-C scFv blocks binding of VEGF-C to VEGF-R2 and VEGF-R3

3.4.1. BIAcore assay

Fully processed human VEGF-C (ΔNΔC-VEGF-C) exerts its action via binding to VEGF-R2 and VEGF-R3 and binds the two receptors with affinities of 410 and 135 pM, respectively (Joukov *et al.* 1997). VEGF-R2-Fc or VEGF-R3-Fc were bound to an anti-Fc coated BIAcore chip to generate a homogeneous receptor surface. ΔNΔC-VEGF-C was then injected over the receptor surface and binding occurred. In both cases, the receptor surface was able to bind almost equimolar amounts of VEGF-C, demonstrating the biological activity of the immobilized receptor. To assess the neutralizing capacity of VC2.2.2-scFv, ΔNΔC-VEGF-C was preincubated with

different concentrations of VC2.2.2-scFv to allow for the formation of the scFv-antigen complex, and this complex was then injected on the receptor surface (Fig. 3.12).

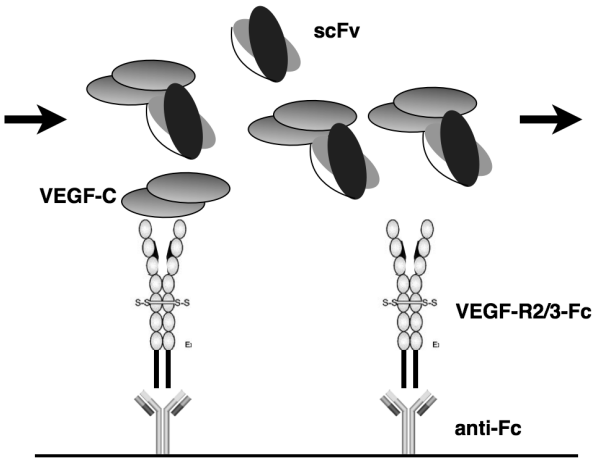

Figure 3.12. Schematic representation of the competitive BIAcore experiment. VEGF-R2-Fc or VEGF-R3-Fc are bound to an anti-Fc coated sensorchip. ΔNΔC-VEGF-C preincubated with scFv is then injected on the chip and binding of VEGF-C to the receptor is measured.

The binding of ΔNΔC-VEGF-C to immobilized VEGF-R3 was dose-dependently inhibited by anti-VEGF-C scFv VC2.2.2 (Fig. 3.13 A), but not by the irrelevant anti-GST control scFv (Fig. 3.13 B). With 900-fold molar excess of VC2.2.2-scFv, an 86% reduction of response was achieved.

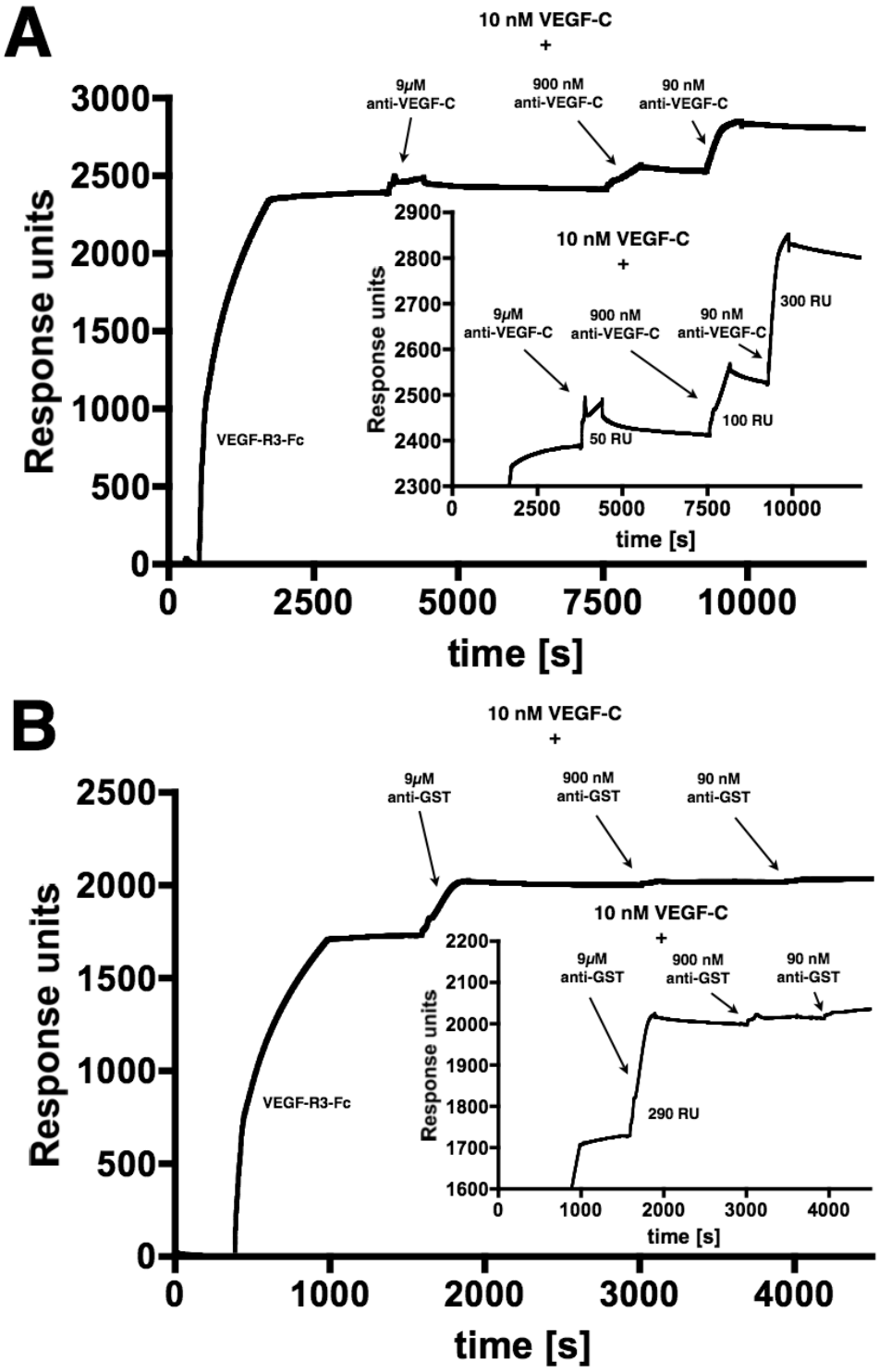

Figure 3.13. Blocking of VEGF-C binding to VEGF-R3 as measured per BIAcore. VEGF-R3-Fc was bound to a CM5-sensorchip coated with anti-human IgG antibody. 10 nM ΔNΔC-VEGF-C were then preincubated with a 9 to 900 times molar excess of (A) anti-VEGF-C scFv or (B) anti-GST control scFv and injected on the VEGF-R3-Fc surface. The amount of binding of ΔNΔC-VEGF-C was measured by SPR.

On the VEGF-R2 surface, binding of ΔNΔC-VEGF-C was also dose-dependently inhibited by injection of a mixture of ΔNΔC-VEGF-C preincubated for 30 minutes with anti-VEGF-C scFv VC2.2.2 (Fig. 3.14). With 900-fold molar excess of VC2.2.2-scFv, an 81% reduction of response was achieved.

Binding of 10 nM VEGF-A to VEGF-R2 resulted in a response comparable to the binding of 10 nM ΔNΔC-VEGF-C but was not blocked by a 900-fold molar excess of anti-VEGF-C scFv VC2.2.2, demonstrating the specificity of the anti-VEGF-C scFv (Fig. 3.14).

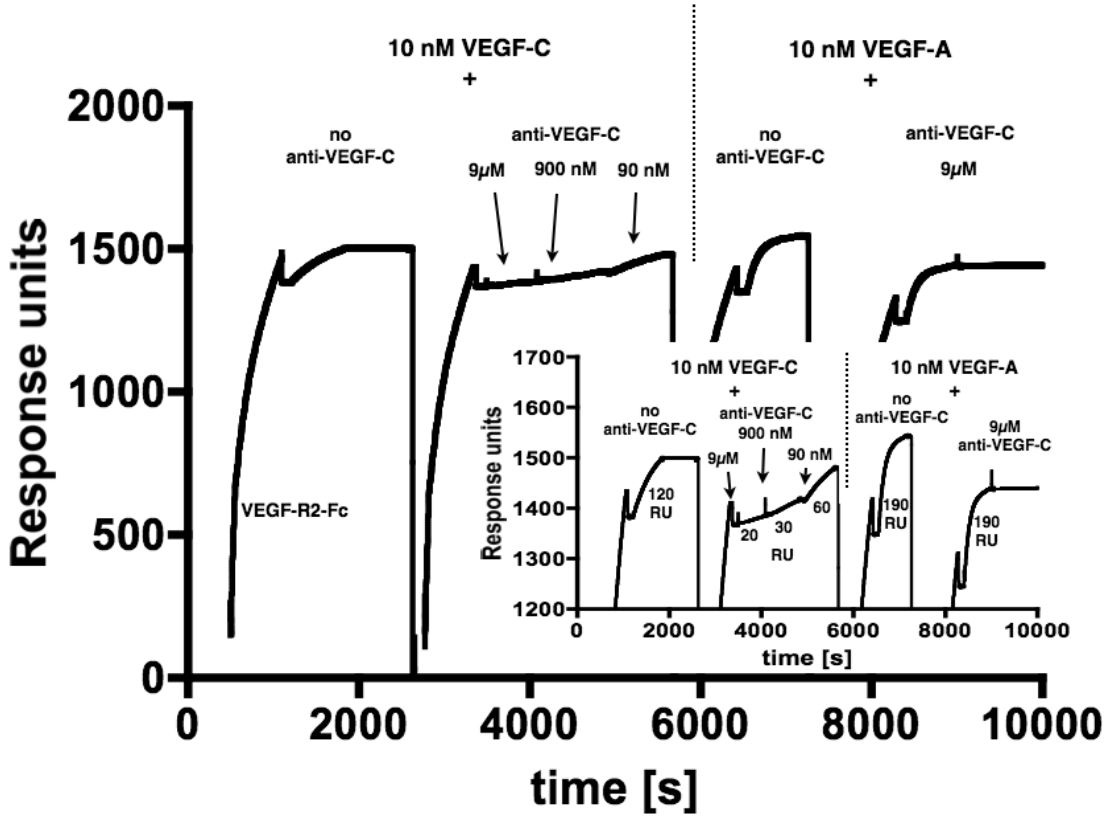

Figure 3.14. Blocking of VEGF-C binding to VEGF-R2 as measured per BIAcore. VEGF-R2-Fc was bound to a CM5 sensorchip coated with anti-human IgG antibody. 10 nM of ΔNΔC-VEGF-C or VEGF-A with or without preincubation together with anti-VEGF-C scFv were then injected on the VEGF-R2 surface and bound VEGF-A or VEGF-C was measured by SPR.

3.4.2. Competitive ELISA

The flow-based BIAcore VEGF-C neutralization assay measures the neutralizing potency of the VC2.2.2 anti-VEGF-C scFv only during a short time span, since the scFv-bound VEGF-C had only a short lasting possibility (the passage through the flow-cell requires seconds) to dissociate from the scFv and to bind to the immobilized VEGF-R on the chip. The equilibrium between dissociation from the scFv and association to the VEGF-R might not be reached during the passage through the flow cell. Therefore, we next used competitive ELISA to characterize the neutralization potency of the anti-VEGF-C scFv over a longer time span.

We found that VC2.2.2 anti-VEGF-C scFv dose-dependently blocked the binding of biotinylated ΔNΔC-VEGF-C to immobilized VEGF-R, while the anti-GST control scFv did not block this binding (Fig. 3.15). Blocking of VEGF-R2 binding was more efficient than blockage of VEGF-R3 binding, in agreement with the findings in the BIAcore assay and the reported finding that the affinity of ΔNΔC-VEGF-C to VEGF-R3 is higher than to VEGF-R2 (Joukov *et al.* 1997).

With a 900-fold molar excess of VC2.2.2 anti-VEGF-C scFv, binding of biotinylated ΔNΔC-VEGF-C to VEGF-R2 was inhibited by 95% ± 1.0%, while the binding to VEGF-R3 was blocked by 74% ± 3.5%. Blocking reached a significance level of $p<0.05$ (Student's *t*-test) vs. irrelevant control antibody for VC2.2.2 anti-VEGF-C scFv concentrations ≥ 200 nM or 100-fold molar excess over biotinylated VEGF-C.

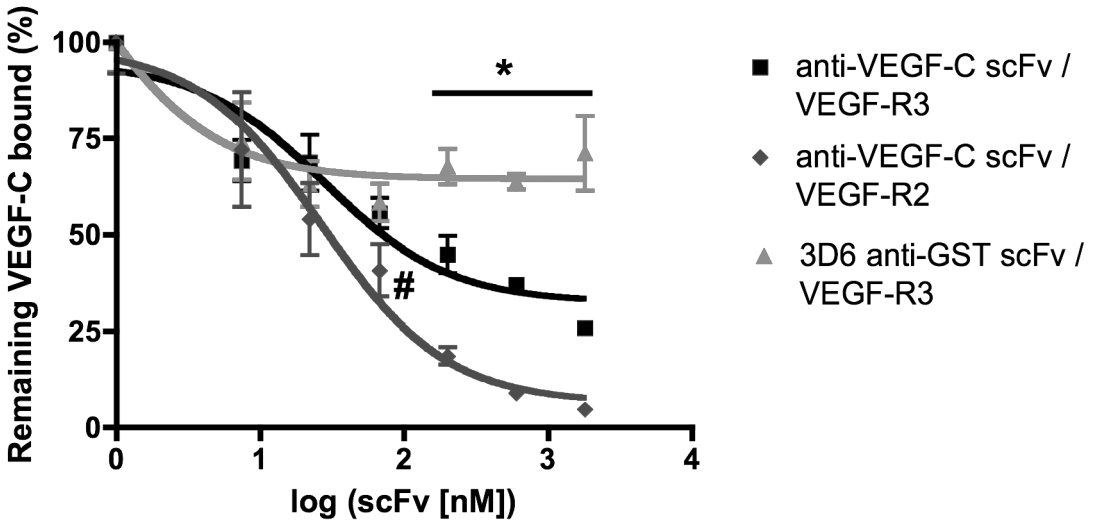

Figure 3.15. Blocking of VEGF-C-binding to VEGF-R2 and -R3 as measured by competitive ELISA. 2 nM biotinylated ΔNΔC-VEGF-C were preincubated with varying amounts of anti-VEGF-C scFv or control scFv and added on a VEGF-R2 or VEGF-R3 coated microtiter plate. Plotted datapoints represent means of 4 replicates ± SEM. The datapoints were fitted to a sigmoidal dose-response curve model using GraphPad Prism 4. Inhibition of VEGF-C binding by anti-VEGF-C scFv reached significance vs. the control scFv (*; $p<0.05$, Student's *t*-test) at a molar excess of 100x more anti-VEGF-C scFv vs. VEGF-C. #: $p=0.067$ for anti-VEGF-C / VEGF-R2 vs. control at molar excess of 33x more anti-VEGF-C than VEGF-C.

3.5. VC2.2.2 anti-VEGF-C scFv binds to an epitope implicated in VEGF receptor binding

To locate the epitope on ΔNΔC-VEGF-C to which VC2.2.2 anti-VEGF-C scFv binds, a peptide microarray consisting of overlapping 15-mer peptides, spanning the whole ΔNΔC-VEGF-C aa sequence, was used. Cy3-labelled VC2.2.2-scFv and Cy5-labelled anti-GST scFv were allowed to competitively bind to the peptide array. Upon scanning, the ratio of median signals from Cy3 vs Cy5 channels were used to generate a list of peptides bound by the respective scFvs.

P. pastoris-derived ΔNΔC-VEGF-C, the positive control protein, emerged as the top-hit from this scan, being bound more than 100 times stronger by the anti-VEGF-C scFv than by the irrelevant scFv (Table 3.5). This validates the usefulness of the peptide-array. Other peptides more strongly bound by the VC2.2.2 anti-VEGF-C scFv vs. the irrelevant anti-GST scFv were peptides containing the sequence FFKPPCVSVYRC (more than 22 times stronger) as well as the C-terminal sequence spanning SCRCMS to RQVHSIIRRHHHHHH (more than 4 times stronger).

Peptide / Protein	**log2 ratio**	Stdev	**aVEGF-C Signal**	Stdev	**aVEGF-C SNR**	Stdev	**aGST Signal**	Stdev	**aGST SNR**	Stdev
ΔNΔC-VEGF-C	**6.26**	0.19	**8346**	5844	**11.4**	5.0	**202**	79	**2.9**	1.1
ΔNΔC-VEGF-C	**6.18**	0.12	**8531**	5797	**25.8**	30.0	**213**	78	**3.5**	2.1
TNTFFKPPCVSVYRC	**5.98**	0.03	**51361**	1256	**112.7**	9.5	**917**	48	**16.9**	5.5
FFKPPCVSVYRCGGC	**4.50**	0.12	**45671**	391	**120.2**	89.2	**2114**	184	**46.4**	17.6
SCRCMSKLDVYRQVH	**4.29**	0.17	**34911**	1322	**332.6**	215.7	**1872**	142	**49.4**	12.4
RQVHSIIRRHHHHHH	**4.22**	0.17	**22414**	1071	**166.6**	43.8	**1302**	86	**34.8**	6.4
VYRQVHSIIRRHHHH	**3.69**	0.03	**32602**	1576	**63.8**	29.1	**2615**	189	**26.4**	3.1
KLDVYRQVHSIIRRH	**2.67**	0.07	**25280**	2821	**123.0**	68.9	**4041**	269	**64.3**	14.5
PPCVSVYRCGGCCNS	**2.13**	0.05	**1555**	65	**25.0**	2.4	**415**	37	**9.0**	2.1
SFANHTSCRCMSKLD	**1.58**	0.12	**1248**	54	**16.1**	4.5	**459**	9	**6.8**	3.8
NHTSCRCMSKLDVYR	**1.53**	0.24	**7390**	1362	**170.9**	95.4	**2577**	126	**58.3**	26.9
VTISFANHTSCRCMS	**1.24**	0.11	**2945**	165	**65.6**	24.5	**1272**	18	**31.9**	3.7
human IgG	**0.07**	0.01	**9348**	531	**41.3**	7.5	**8917**	583	**31.3**	4.8
human IgG	**0.03**	0.06	**9071**	491	**34.0**	15.0	**8833**	423	**27.3**	9.3
mouse IgG	**-0.05**	0.04	**4873**	474	**24.4**	11.2	**4969**	363	**27.1**	8.6
mouse IgG	**-0.05**	0.01	**4885**	268	**43.0**	6.9	**4994**	310	**32.1**	5.5
CMSKLDVYRQVHSII	**-0.36**	0.13	**401**	43	**7.0**	1.1	**388**	32	**4.5**	3.0
QCMNTSTSYLSKTLF	**-0.96**	0.16	**1183**	81	**15.8**	5.8	**2065**	121	**10.4**	1.2

Table 3.5. Peptides specifically bound by VC2.2.2. Epitope mapping was carried out using a peptide microarray and fluorescently labeled antibodies competitively binding to the peptides. Values are arithmetic means and standard deviations from 3 subarrays. SNR: signal to noise ratio, log2 ratio are log2 (VC2.2.2 anti-VEGF-C / 3D6 anti-GST). All peptides that generated data with errors, SNRs <2 in both channels and signal intensities ≤100 in both channels were filtered out. Shown is a representative array from at least 3 replicates. Dye-swap arrays yielded similar results.

Importantly, ΔNΔC-VEGF-D, which is not bound by VC2.2.2-scFv, features two different residues in the FFKPPCVSVYRC region, which might be responsible

for the lack of cross-reactivity towards VEGF-D (Fig. 3.16). Interestingly, the FFKPPCVSVYRC sequence maps to the receptor-binding region on VEGF-C that contacts VEGF-R2 and VEGF-R3 (Fig. 3.17 A-G) (Jeltsch *et al.* 2006; Leppanen *et al.* 2010) and contains Cys156, the key-residue responsible for VEGF-R2 binding (Joukov *et al.* 1998).

```
rhVEGF-D (R&D)  ----------FAATFYDIETLKVIDEEWQRTQCSPRETCVEVASELGKSTNTFFKPPCVNVFRC 54
rhVEGF-C (R&D)  ----TEETIKFAAAHYNTEILKSIDNEWRKTQCMPREVCIDVGKEFGVATNTFFKPPCVSVYRC 60
rhVEGF-C (P.p)  EFHHHHHHLVPRGSHYNTEILKSIDNEWRKTQCMPREVCIDVGKEFGVATNTFFKPPCVSVYRC 64
                            .*: * ** **:**::*** ***.*::*..*:* :**********.*:**

rhVEGF-D (R&D)  GGCCNEESLICMNTSTSYISKQLFEISVPLTSVPELVPVKVANHTGCKCLP--TAPRHPY 112
rhVEGF-C (R&D)  GGCCNSEGLQCMNTSTSYLSKTLFEITVPLSQGPKPVTISFANHTSCRCMSKLDVYRQVH 120
rhVEGF-C (P.p)  GGCCNSEGLQCMNTSTSYLSKTLFEITVPLSQGPKPVTISFANHTSCRCMSKLDVYRQVH 124
                *****.*.* ********:** ****:***:. *: *.:..****.*:*:.   . *: :

rhVEGF-D (R&D)  S----HHHHHH---- 119
rhVEGF-C (R&D)  SIIRRHHHHHHHHHH 135
rhVEGF-C (P.p)  SIIRR---------- 129
                *
```

Figure 3.16. Alignment of recombinant human ΔNΔC-VEGF-C and ΔNΔC-VEGF-D. ΔNΔC-VEGF-C and ΔNΔC-VEGF-D, which were used to determine reactivity of anti-VEGF-C scFv, were aligned using ClustalW. Possible epitope regions found with the peptide microarray scan are colored in red (epitope A) and purple (epitope B). The amino acids in VEGF-D that are different from VEGF-C in epitope A are colored in orange. R&D, mammalian cell-derived ΔNΔC-VEGF-C/D; P.p, *P. pastoris*-derived ΔNΔC-VEGF-C.

The C-terminal sequence SCRCMS to RQVHSIIRRHHHHHH could also be part of the anti-VEGF-C epitope. This region lies in proximity to the loop 2 in the site 1 receptor-binding interface of VEGF-C (Fig. 3.17 A). Binding of anti-VEGF-C to this region could therefore also sterically hinder the binding of VEGF-C to its receptors. In recombinant human VEGF-D, this sequence is much less conserved than the FFKPPCVSVYRC sequence. This could explain why VEGF-D is not recognized by the anti-VEGF-C scFv (Fig. 3.16). The His-tag, however, can be excluded as being the actual anti-VEGF-C epitope or being part of the anti-VEGF-C epitope, since (i)

the C-terminal His-tag is present in both mammalian cell-derived recombinant VEGF-C and VEGF-D but rhVEGF-D is not bound and (ii) in the *P. pastoris*-derived ΔNΔC-VEGF-C (which was initially used for panning), the His-tag is present at the N-terminus and thus has different neighboring residues (Fig. 3.16)

Figure 3.17. (Figure on next page). Localization of putative epitopes on VEGF-C. The VEGF-C residues contacting VEGF-R2 as reported in Leppanen *et al.* 2010, are represented in yellow (N-terminal helix), red (loop 1), orange (loop 2) and brown (loop 3). The two epitope stretches identified in the peptide scan are colored in blue. From epitope B, only SCRCMSKL is shown, the C-terminal end is missing in the reported structure. Overlaps of epitope A and receptor-contacting residues in loop 1 are colored in purple (A). Residues in loop 1 found to affect VEGF-R2-binding (B) or VEGF-R3-binding (C) by mutational analysis (Jeltsch *et al.* 2006) are shown with the same colors. The localization of the epitopes within the VEGF-C dimer is shown in (D) and their interference with the boxed interface of VEGF-R2 (cyan) is shown in (E), with magnifications in “side” view (F) and “top view” (G). The pdb file 2X1X was used for the representation (www.pdb.org).

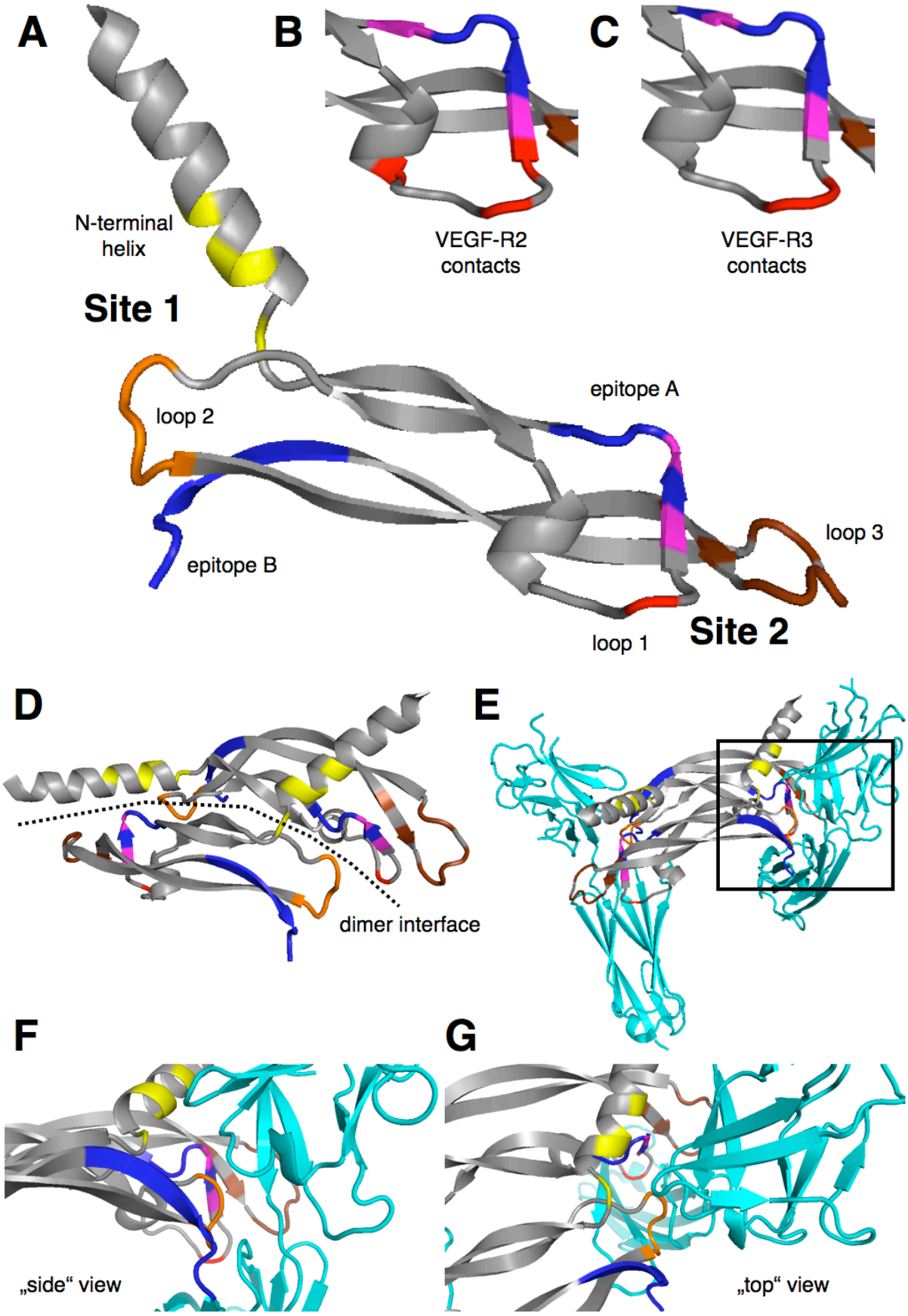
A
B
C
N-terminal
helix
VEGF-R2
contacts
VEGF-R3
contacts
Site 1
epitope A
loop 2
loop 3
epitope B
loop 1
Site 2
D
E
dimer interface
F
G
„side“ view
„top“ view

3.6. Reformatting of anti-VEGF-C scFv to IgG and Ig-like formats

3.6.1. Establishment of stable cell lines expressing anti-VEGF-C IgG

Since the scFv is a rather small molecule (27 kDa) and therefore is below the renal secretion limit of about 60 kDa, its half-life in blood when used *in vivo* would be short. In order to use the anti-VEGF-C antibody for *in vivo* blocking of VEGF-C, we therefore reformatted the scFv into a full IgG format. From a transient transfection of CHO-S cells with the IgG vectors, high reactivity of the supernatant against ΔNΔC-VEGF-C was observed, while supernatant from mock-transfected cells did not react against ΔNΔC-VEGF-C (Fig 3.18).

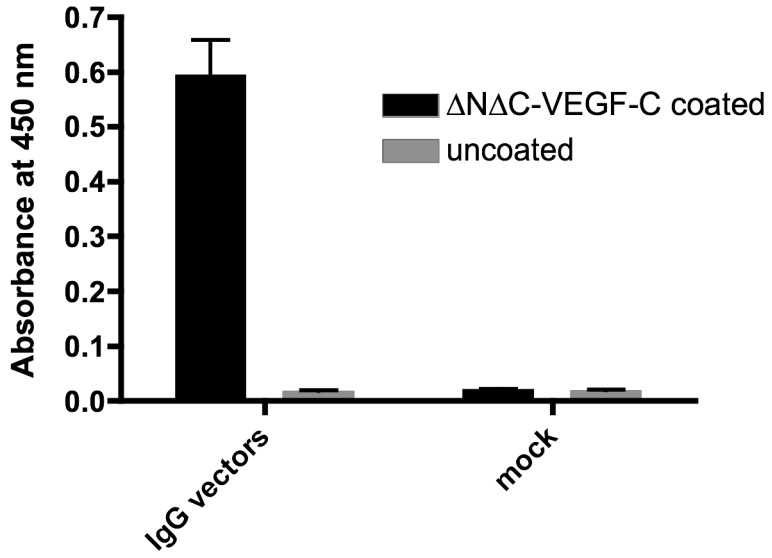

Figure 3.18. ELISA analysis of IgG-electroporated CHO-S cells. A polyclonal pool of CHO-S cells mock electroporated or co-electroporated with the VC-2.2.2-IgG heavy and light chain vectors was tested for binding to an ELISA plate coated or not with ΔNΔC-VEGF-C.

Co-electroporated, antibiotics-selected CHO-S cells were then sorted by FACS for high IgG expressers and individual clones in 96-well plates were screened by ELISA for reactivity of cell supernatants against VEGF-C. Six cell lines were

expanded and checked for IgG expression in a western blot. Out of the six cell lines, clones 1 and 6 showed complete lack of the 160 and 130 kDa bands, while the other 4 clones expressed weak 160 and 130 kDa bands and a stronger band at approx. 105 kDa (Fig. 3.19).

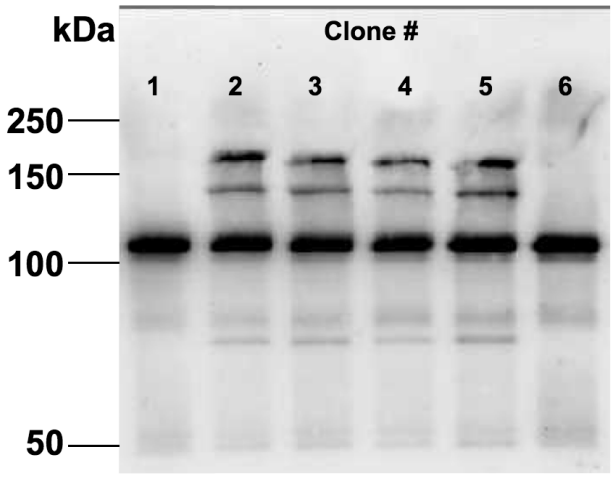

Figure 3.19. Anti-Fc immunoblot of supernatants from antibiotic-selected CHO-S VC2.2.2-IgG clones. Supernatants from sorted clones were collected and separated on an SDS-PAGE gel under non-reducing conditions. The proteins were subsequently transferred to a nitrocellulose membrane and immunoblotted, using an anti-human-Fc antibody coupled to HRP, and visualized using ECL-Plus.

Clone 3 was expanded and used to produce a larger amount of anti-VEGF-C IgG in roller bottles. The cleared cell culture supernatant was purified by Protein-A affinity chromatography. Western blotting of the supernatant with anti-Fc antibodies showed only a ca. 105 kDa band in the supernatant before purification. After purification, a strong band at 105 kDa as well as several weaker bands above 105 kDa were observed. Under reducing conditions, a 50 kDa band corresponding to the Ig heavy chain was observed (Fig 3.20 A).

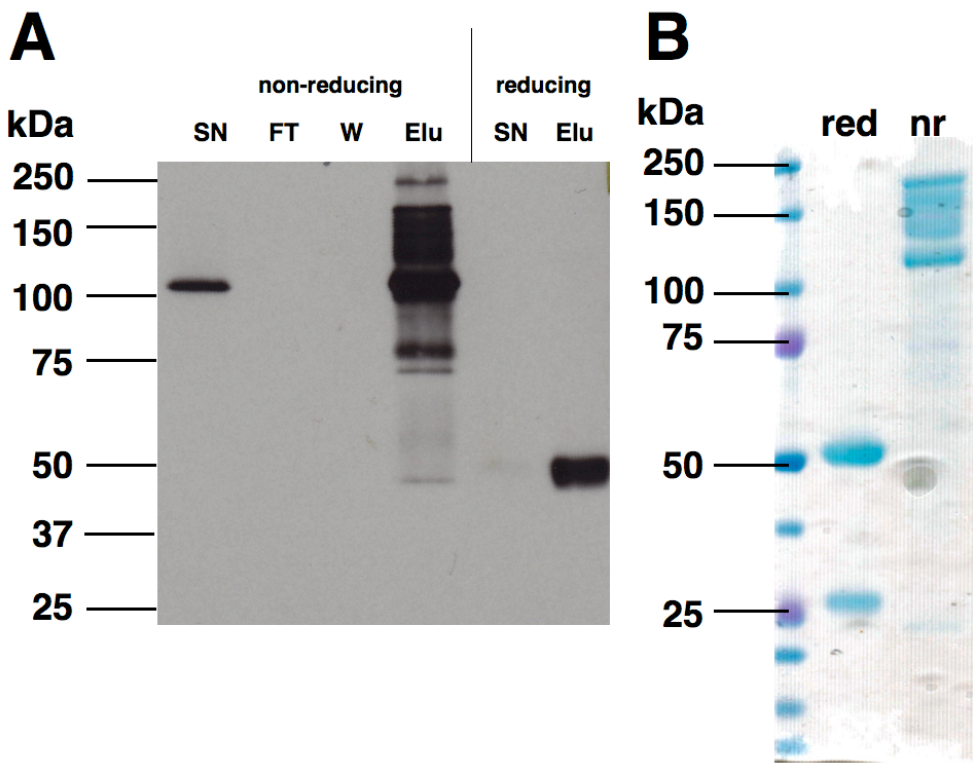

Figure 3.20. Immunoblot and SDS-PAGE analysis of the purified anti-VEGF-C IgG. (A) Anti-Fc immunoblot of supernatant (SN), flow-through (FT), wash (W) and eluate (Elu) from anti-VEGF-C IgG purification by protein-A affinity chromatography. (B) SDS-PAGE of protein-A purified anti-VEGF-C IgG. Red, reducing conditions; nr, non-reducing conditions.

The purified anti-VEGF-C IgG was then analyzed by SDS-PAGE. Under non-reducing conditions, the same bands were seen as in the western blot while under reducing conditions, two bands at 50 kDa, corresponding to the heavy chain, and 25 kDa, corresponding to the light chain, were observed (Fig. 3.20 B). These bands were cut out, proteins were digested in-gel and tryptic peptides were analyzed by MALDI-MS/MS. In the 25 kDa and 50 kDa band, several peptides corresponding to the tryptic digest of anti-VEGF-C light chain and heavy chain respectively were identified. However, in the 105 kDa, 130 kDa and 160 kDa bands, only peptides belonging to the anti-VEGF-C heavy chain could be identified. By SEC, the anti-VEGF-C IgG eluted as a homogeneous peak at the same volume as human IgG (Fig. 3.21).

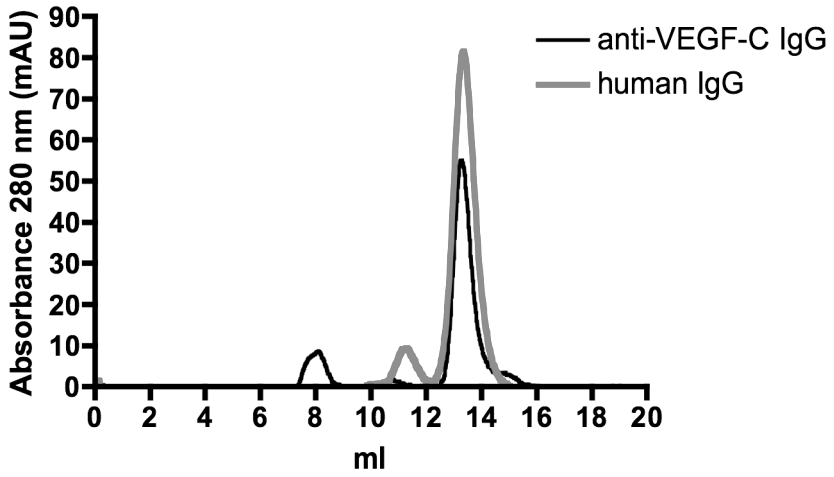

Figure 3.21. SEC profile of anti-VEGF-C IgG produced from stable clones. Protein-A purified samples were resolved on a Superdex 200 10/300 GL column with PBS as buffer at a flow rate of 0.5 ml/min.

3.6.2. Expression of anti-VEGF-C VC2.2.2-IgG by transient transfection

To approach the production of VC2.2.2-IgG via another route, we bulk-transfected CHO-S cells transiently using a polyethlyeneimine (PEI) based protocol. Transient gene expression (TGE) has been shown to produce high yields of up to several dozens of mg of IgG per liter of medium (Muller *et al.* 2007; Wulhfard *et al.* 2008). IgGs were produced and protein-A purified supernatant was analyzed by SDS-PAGE and immunoblot analysis, using an anti-Fc antibody. As opposed to IgGs produced by stably transfected CHO-S cells, three similarly strong bands with sizes of about 180 kDa, 140 kDa and 105 kDa could be observed (Fig. 3.22).

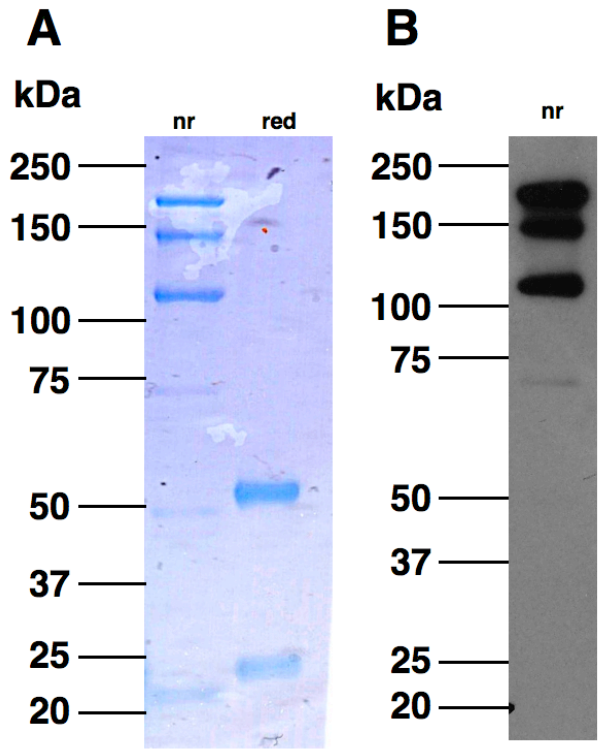

Figure 3.22. SDS-PAGE and immunoblot analysis of VC2.2.2-IgG produced from transiently-transfected CHO-S cells. Protein-A purified VC2.2.2-IgG was resolved on a 4-12% acrylamide gel and (A) Coomassie-stained or (B) transferred to a nitrocellulose membrane and detected using anti-Fc-HRP antibody.

The purified anti-VEGF-C IgG from TGE was then analyzed by SEC, where it showed an identical elution profile as a control human IgG (Fig. 3.23).

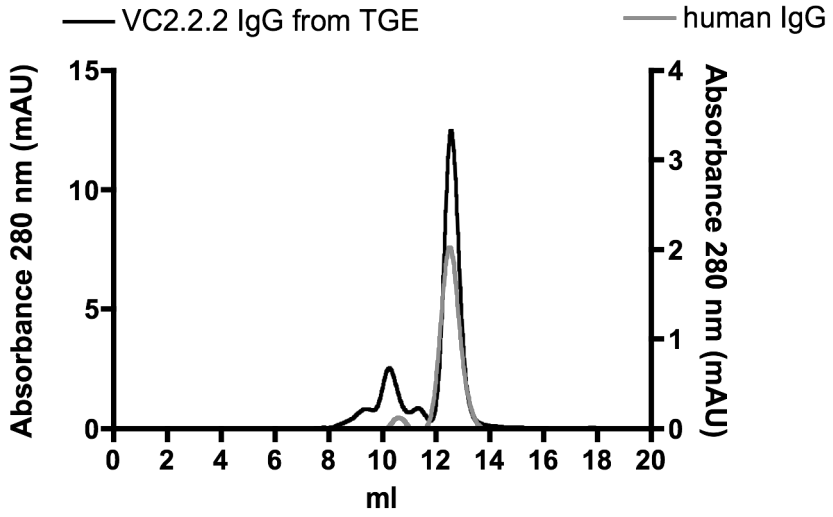

Figure 3.23. SEC profile of VC2.2.2-IgG from TGE. Protein-A purified samples were resolved on a Superdex 200 10/300 GL column with PBS as buffer at a flow rate of 0.5 ml/min.

Binding of the VC2.2.2-IgG produced by TGE to ΔNΔC-VEGF-C was completely abrogated as shown by ELISA (Fig. 3.24). This was in sharp contrast to the VC2.2.2-IgG produced from stably transfected CHO-S. As this was unexpected, the heavy and light chain vectors were resequenced and found to contain the correct VC2.2.2 sequences.

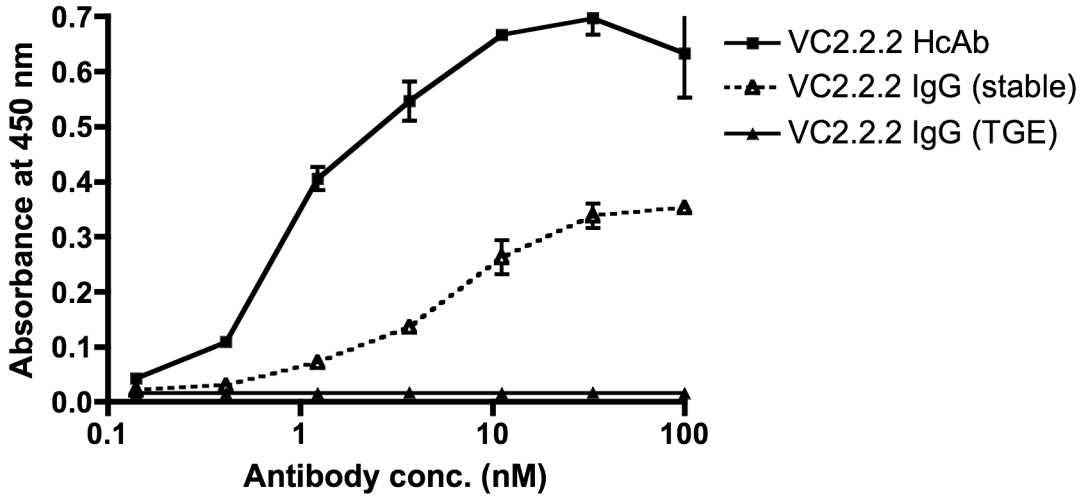

Figure 3.24. ELISA analysis of binding properties of VC2.2.2 heavy chain antibodies (HcAbs) and VC2.2.2-IgG secreted by stably and transiently transfected CHO-S cells. VC2.2.2 immunoproteins in different concentrations were incubated on an ELISA plate coated with 1 µg/ml *P. pastoris*-derived ΔNΔC-VEGF-C and detected using anti-human-Fc-HRP.

3.6.3. The anti-VEGF-C heavy chain is sufficient to bind VEGF-C

To check for loss of lambda light chain expression in stably selected CHO-S cells, a process described previously (Strutzenberger *et al.* 1999), we transiently co-transfected suspension CHO cells with the heavy and light chain vectors as well as heavy chain vectors only to identify the putative 105 kDa heavy chain dimer band. Western blotting with an anti-Fc antibody revealed the same three bands at 105 kDa, 130 kDa and 160 kDa as already seen from the stably and transiently transfected CHO clones for co-transfection of heavy and light chain vectors. When the heavy

chain vector was transfected alone, only a weak 105 kDa band was seen (Fig. 3.25). The weak expression of heavy chain is due to retention of the heavy chain by the immunoglobulin binding protein (BiP), an ER chaperone; heterodimerization with the light chain releases BiP and the full IgG can be secreted (Hendershot 1990).

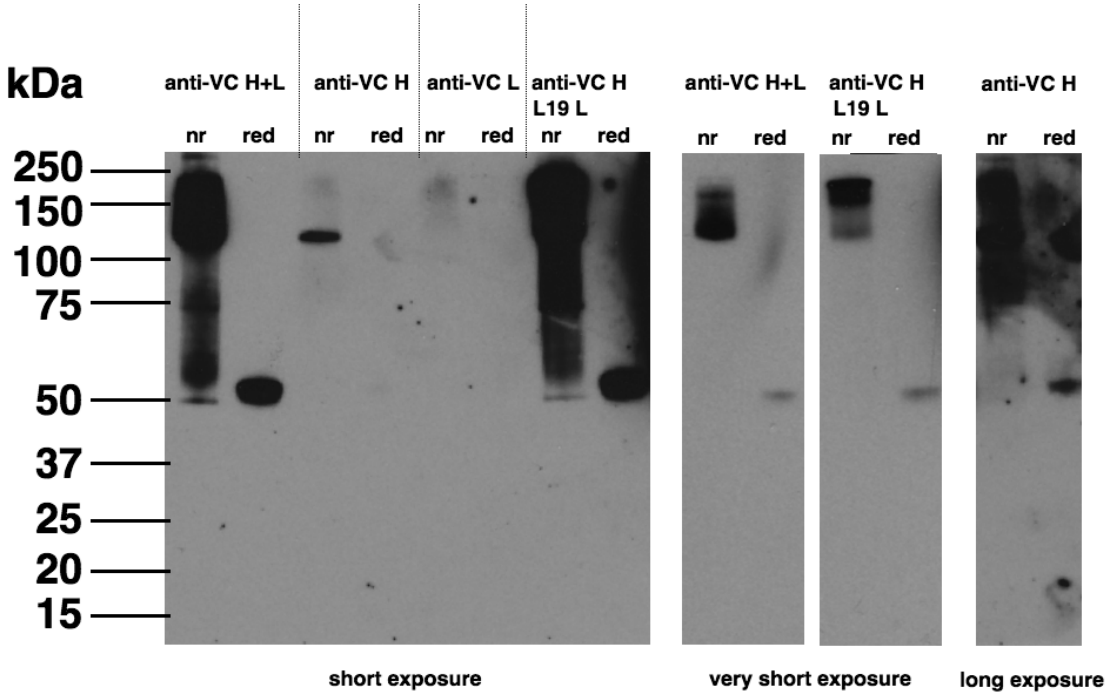

Figure 3.25. Secretion of different antibody species by transiently transfected CHO-S cells. Supernatants of CHO-S cells transiently transfected with the indicated vector combinations were separated on SDS-PAGE, transferred to a nitrocellulose membrane and immunoblotted with an anti-human-Fc antibody coupled to HRP. Nr, non-reducing; red, reducing; anti-VC, anti-VEGF-C vectors; L19, L19 anti-EDB vectors; H, heavy chain vector; L, light chain vector.

Reactivity against ΔNΔC-VEGF-C was tested by ELISA. Surprisingly, supernatant containing heavy chain only reacted much stronger with VEGF-C than full IgG (Fig. 3.24 and 3.26 A), although the concentration of heavy chain was much lower than the concentration of full IgG, for reasons discussed above. Unspecific stickiness of the heavy chain was not observed, as VEGF-A was not bound (Fig. 3.26 B).

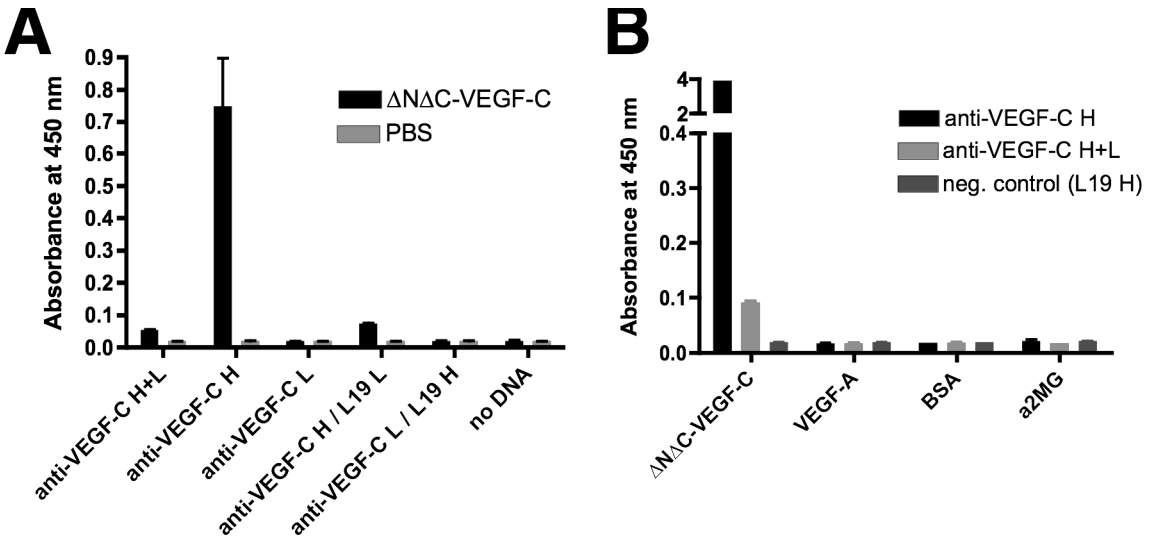

Figure 3.26. ELISA analysis of supernatants from CHO cells transfected with different IgG-vector combinations. (A) Binding specificities of different heavy and light chain combinations towards ΔNΔC-VEGF-C. (B) Cross-reactivity of anti-VEGF-C heavy chain and anti-VEGF-C heavy and light chain towards VEGF-A, BSA or alpha-2-macroglobulin (a2MG). L19, anti-EDB antibody (neg. control); H, heavy chain vector; L, light chain vector.

3.6.4. The V_H domain of anti-VEGF-C heavy chain binds to VEGF-C

To express the variable heavy domain (V_H) of VC2.2.2-scFv, the variable light (V_L) domain as well as the linker between V_H and V_L were removed from the pHEN1-VC2.2.2-scFv plasmid by SOE PCR. Bacterial supernatants from IPTG-induced cultures expressing VC2.2.2 V_H or a control V_H were checked by ELISA for reactivity against ΔNΔC-VEGF-C. Binding to ΔNΔC-VEGF-C was observed, while no unspecific stickiness to alpha-2-macroglobulin was seen. Detection with protein-A was also successful, indicating a generally correct folding of the V_H, since protein-A binds to a conformational epitope on the opposite face of the former dimerization interface of V_H (Fig. 3.27).

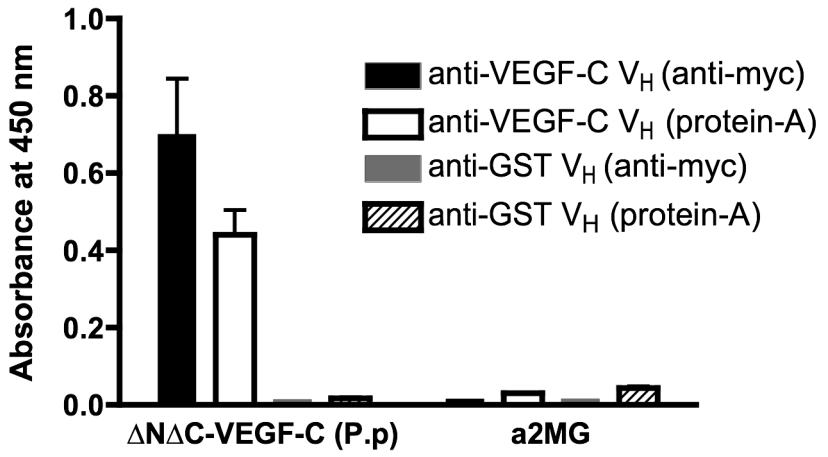

Figure 3.27. ELISA analysis of V_H binding to VEGF-C or alpha-2-macroglobulin (a2MG).

3.6.5. Anti-VEGF-C heavy-chain-only antibody strongly binds soluble VEGF-C

Loss of binding to VEGF-C during presence of the light chain lead us to the hypothesis that light chains cannot assemble correctly with the heavy chain. This incorrect assembly could lead to an obstruction of the antigen recognition by the heavy chain. Incompatible pairing of V_H and V_L has been described before, where a single V_H isolated from a patient and capable of binding to a melanoma-specific antigen lost its binding capability when randomly paired with V_L domains (Cai *et al.* 1996). To test this hypothesis, we decided to construct a heavy chain antibody (HcAb) devoid of the light chain. To avoid prevention of secretion by BiP, we removed the C_{H1} domain from the heavy chain. The C_{H1} domain is recognized by BiP and when removed, the heavy chain should be secreted without the normally necessary pairing with a light chain.

Vectors lacking the C_{H1} domain were prepared, verified by sequencing and transiently transfected into suspension CHO cells. By SDS-PAGE and immunoblotting, a band of 76 kDa under non-reducing and 38 kDa under reducing

conditions was observed, corresponding to the calculated molecular masses (Fig. 3.28 A,B). Cell supernatant strongly reacted against *P. pastoris* and mammalian cell-derived ΔNΔC-VEGF-C but not against VEGF-A as tested by ELISA (Fig. 3.28 C).

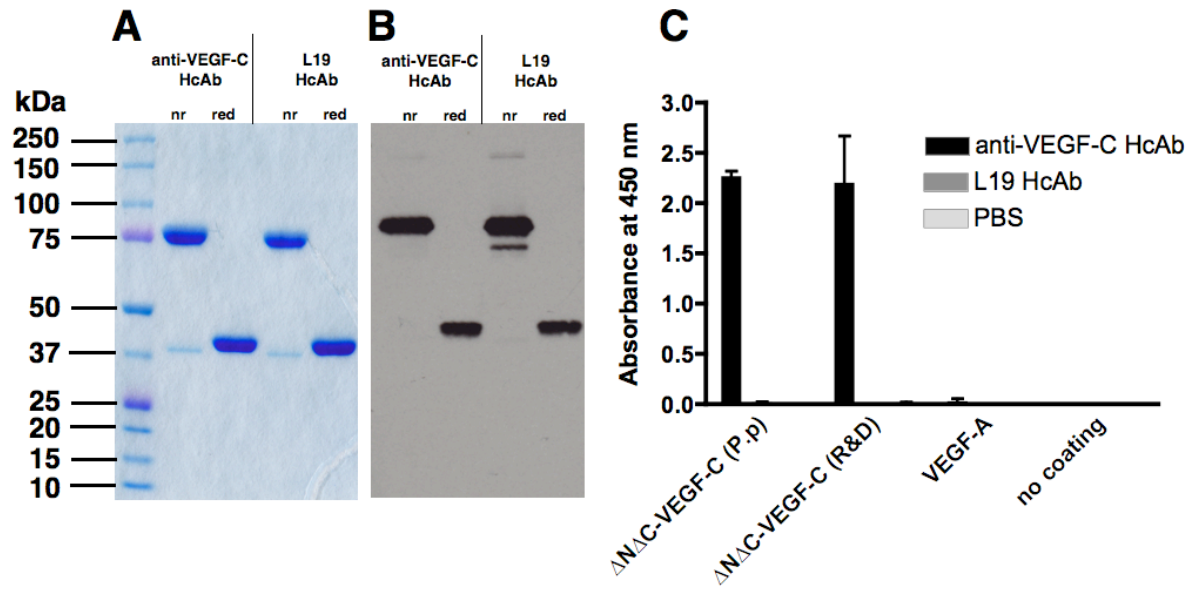

Figure 3.28. Analysis of HcAbs. (A) Supernatants of CHO-S cells transiently transfected with HcAb-vectors were separated on a 4-12% SDS-PAGE gel. (B) Proteins from the gel prepared as in (A) were transferred to a nitrocellulose membrane and immunoblotted using an anti-Fc antibody. (C) Crude supernatants from CHO-S cells transfected with the indicated HcAb vectors were tested for reactivity against the indicated antigens by ELISA. L19 HcAb, anti-EDB heavy chain only antibody (neg. control); P.p, *P. pastoris*-derived ΔNΔC-VEGF-C; R&D, mammalian cell-derived ΔNΔC-VEGF-C.

Protein-A purified HcAbs were further checked by SEC on a Superdex 200 column. Anti-VEGF-C HcAb eluted in a pattern showing 4 peaks, while the L19 HcAb eluted as a single peak (Fig. 3.29). The good solubility and sharply defined monomeric nature of the L19 HcAb is somewhat surprising, since L19 still contains the hydrophobic residues in the former dimerization interface.

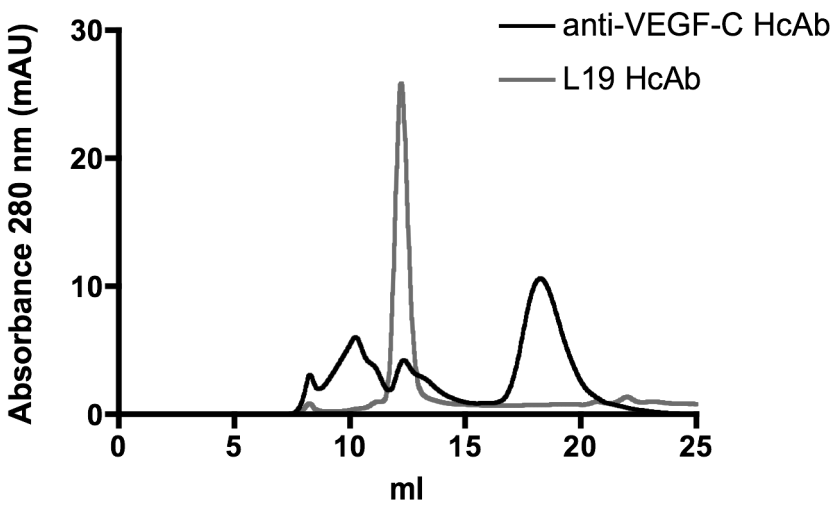

Figure 3.29. SEC profiles of HcAbs. Anti-VEGF-C HcAb and L19 HcAb were analyzed on a Superdex 200 10/300 GL column under a flow of 0.5 ml/min.

Fractions containing the individual peaks were then analyzed by BIAcore on a ΔNΔC-VEGF-C coated sensorchip. All 4 fractions bound to VEGF-C (data not shown). The anti-VEGF-C HcAb was subsequently bound to an anti-Fc sensorchip and soluble ΔNΔC-VEGF-C derived from *P. pastoris* and mammalian cells was injected over the chip. Strong binding with a very slow dissociation of the bound ΔNΔC-VEGF-C from the anti-VEGF-C HcAb was observed (which is due to avidity effects of binding of bivalent HcAbs to dimeric soluble ΔNΔC-VEGF-C), while an anti-VEGF-C IgG coated anti-Fc sensorchip did not react with soluble ΔNΔC-VEGF-C at all (Fig. 3.30 A,B). Binding to immobilized ΔNΔC-VEGF-C was only observed with the HcAb but not with IgG from TGE (Fig. 3.30 C).

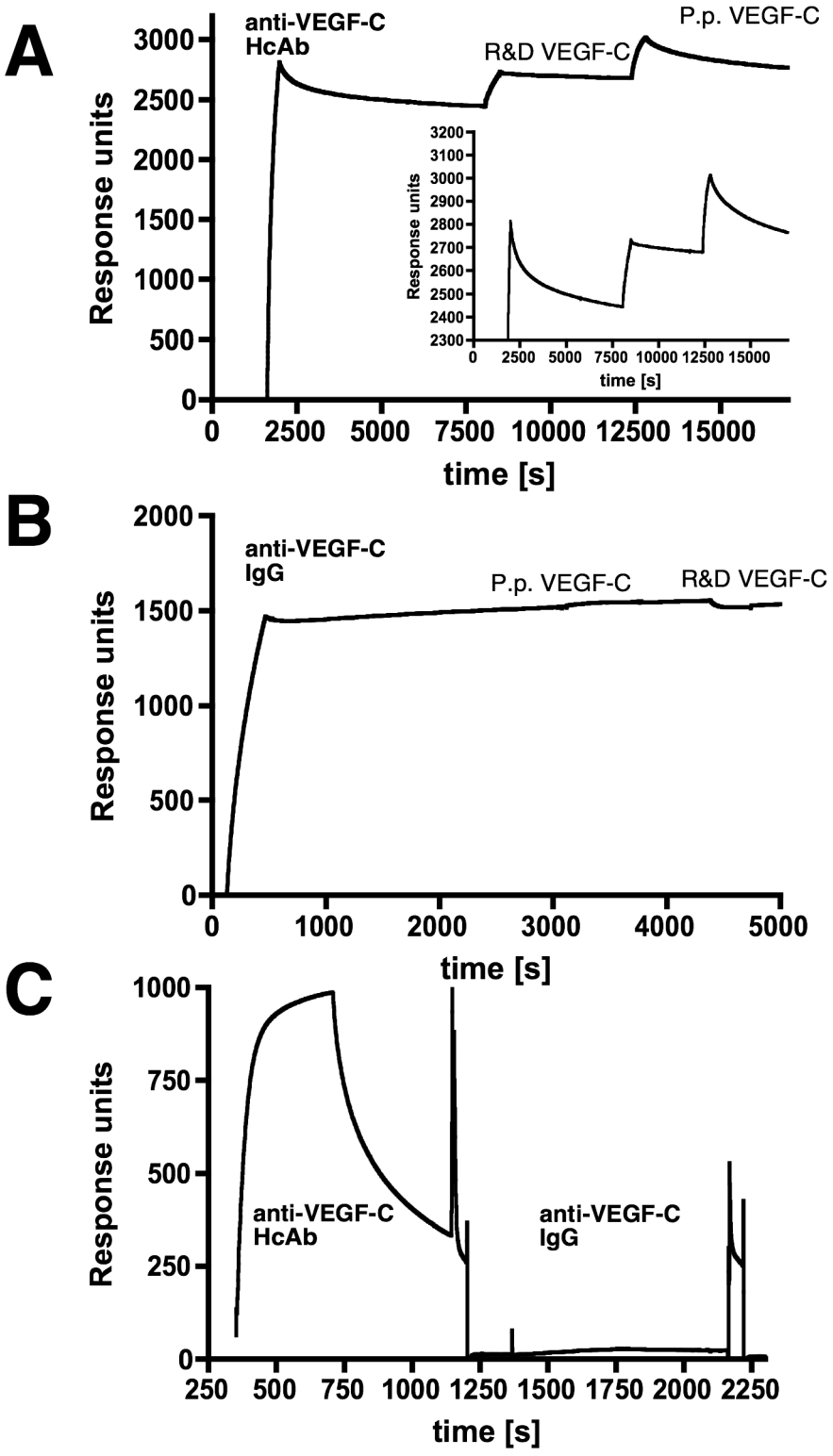

Figure 3.30. Binding profiles of anti-VEGF-C HcAb and IgG. (A,B) *P. pastoris* (P.p) or mammalian cell-derived (R&D) soluble ΔNΔC-VEGF-C was injected over immobilized (A) anti-VEGF-C HcAb or (B) anti-VEGF-C IgG (from TGE) and binding was measured. (C) Anti-VEGF-C HcAb or IgG were injected over immobilized mammalian cell-derived ΔNΔC-VEGF-C.

3.7. Anti-VEGF-C scFvs contain hydrophilic camelid V_HH-like mutations in the V_H:V_L dimerization interface

Upon reexamination of the anti-VEGF-C scFvs, mutations in the framework region 2 (FR2) and adjacent regions of the heavy chain were identified. In VC2 and its daughter clone VC2.2.2, residue 44 was mutated from glycine (as encoded in the ETH-2 Gold library) to glutamic acid (Table 3.6), by a purinic single nucleotide transitional mutation from GGG to GAG, making it more hydrophilic.

	CDR-H1			FR2		CDR-H2	CDR-H3					
Clone	31	32	33	44	45	64	95	96	97	98	99	100
Library	S	Y	A	G	L	K	X	X	X	X	(X)	(X)
VC1	S	Y	A	G	**P**	K	E	S	S	M	-	-
VC2	S	Y	A	**E**	L	K	E	S	L	P	-	-
VC3	S	Y	A	G	L	**E**	E	S	L	P	-	-
VC4	S	Y	A	G	L	K	W	P	A	T	G	-
VC2.2.2	Q	N	Y	E	L	K	E	S	L	P	-	-

Table 3.6. Heavy chain amino acid sequences of anti-VEGF-C scFvs. Numbering according to Chothia *et al.* 1989. VC1 to VC4: first generation anti-VEGF-C scFv; VC2.2.2 affinity matured VC2. X denotes amino acids that are randomized in the library.

The FR2 region lies within the dimerization interface of the V_H and V_L domains. Replacement of hydrophobic residues in this region with hydrophilic residues might prevent correct assembly of the V_H:V_L fragment (Fig. 3.31). Likewise, loss of the V_L domain leads to resurfacing of hydrophobic residues within the former dimerization interface and could lead to decreased solubility and enhanced aggregation of the single V_H fragment.

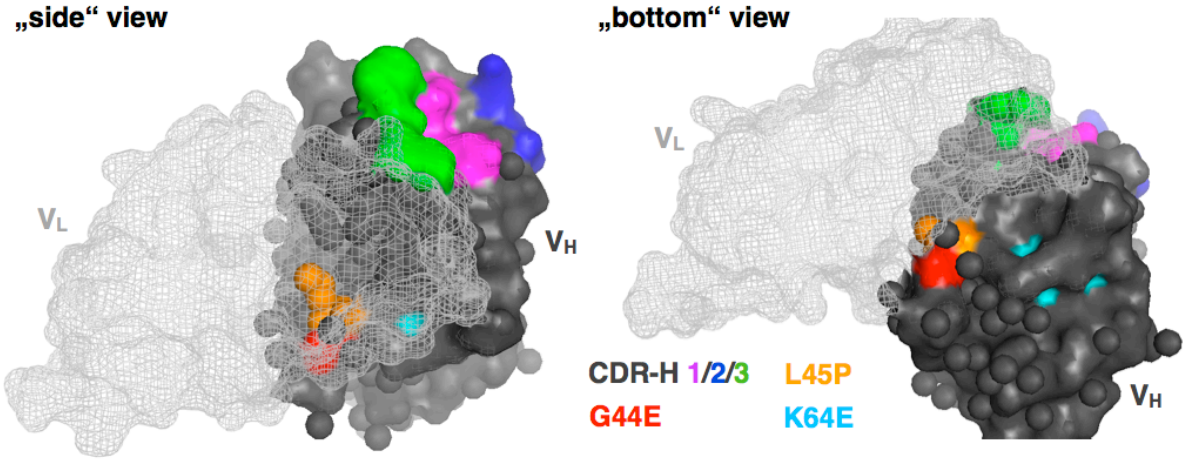

Figure 3.31. Spatial localization of the V_HH-like mutations in the V_H-domain. The V_H-mutations (G44E in red, L45P in orange, K64E in cyan) identified in the anti-VEGF-C scFvs are collectively shown projected on the V_H (dark grey) of a human anti-polyhydroxybutyrate Fv (pdb-file 2D7T, modeled with MacPyMol). The V_L-domain is shown as light grey mesh. For orientation, the heavy-chain CDR1/2/3 are colored in pink, blue and green, respectively.

The G44E substitution and other hydrophilic substitutions in the FR2 region are therefore a hallmark of the variable heavy domain V_HH in camelid heavy chain antibodies, naturally occurring immunoproteins devoid of light chains (Hamers-Casterman *et al.* 1993; Muyldermans *et al.* 1999) (Fig. 3.32). VC1 contains a mutation in the FR2 region where the hydrophobic leucine at position 45 is replaced by the less hydrophobic proline, caused by a CTG to CCG transition mutation (Table 3.6 and Fig. 3.32). L45 is also one of the typical residues altered in camelid V_HH, although the canonical residue there is the hydrophilic arginine. However, the CGG arginine codon can only be reached from the CTG proline codon by a T to G pyrimidine / purine transversion, but transversions are about an order of magnitude less frequent than purinic (A/G) or pyrimidinic (C/T) transitions (Vogel *et al.* 1977; Kondo *et al.* 1993). For a single pyrimidinic transition, proline is the most hydrophilic residue “reachable” from the leucine codon CTG. VC3 contains a mutation in the C-

terminal end of CDR-2, where the already hydrophilic lysine at position 64 is substituted by the similarly hydrophilic glutamic acid, by a AAG to GAG transition mutation (Table 3.6 and Fig. 3.32). VC4, which binds only to *P. pastoris*-derived ΔNΔC-VEGF-C but not to mammalian cell-derived ΔNΔC-VEGF-C, does (outside CDR-3s) not deviate from the aa sequence encoded in the library (Table 3.6).

```
anti-VEGF-C VC2.2.2   EVQLLESGGGLVQPGGSLRLSCAASGFTFSQNYMSWVRQAPGKELEWVSAISGSGGSTYY 59
anti-VEGF-C VC1       EVQLLESGGGLVQPGGSLRLSCAASGFTFSSYAMSWVRQAPGKGPEWVSAISGSGGSTYY 59
anti-VEGF-C VC3       EVQLLESGGGLVQPGGSLRLSCAASGFTFSSYAMSWVRQAPGKGLEWVSAISGSGGSTYY 59
ETH-2 Gold library    EVQLLESGGGLVQPGGSLRLSCAASGFTFSSYAMSWVRQAPGKGLEWVSAISGSGGSTYY 59
canonical human VH3   EVQLVESGGGLVQPGGSLRLSCAASGFTFSXXXXXWVRQAPGKGLEWVSXXXXXXXXXXY 59
camel VHH             EVQLVESGGGSVQAGGSLRLSCAASGYTYSXXXXGWFRQAPGKEREGVSXXXXXXXXXXY 59
                      ****:***** **.************:*:*     *.******  * **          *

anti-VEGF-C VC2.2.2   ADSVKGRFTISRDNSKNTLYLQMNSLRAEDTAVYYCAKESLP--FDYWGQGTLVTVSS 113
anti-VEGF-C VC1       ADSVKGRFTISRDNSKNTLYLQMNSLRAEDTAVYYCAKESSM--FDYWGQGTLVTVSS 113
anti-VEGF-C VC3       ADSVEGRFTISRDNSKNTLYLQMNSLRAEDTAVYYCAKESLP--FDYWGQGTLVTVSS 113
ETH-2 Gold library    ADSVKGRFTISRDNSKNTLYLQMNSLRAEDTAVYYCAKXXXXXXFDYWGQGTLVTVSS 113
canonical human VH3   ADSVKGRFTISRDNSKNTLYLQMNSLRAEDTAVYYCARXXXX--XXXWGQGTLVTVSS 113
camel VHH             ADSVKGRFTISQDNAKNTVYLQMNSLKPEDTAIYYCAAXXXX--XXXWGQGTQVTVSS 113
                      **** ******:**:***:*******:.****:****          ***** *****
```

Figure 3.32. Comparison of human and camel variable heavy chain sequences. Variable heavy chain sequences of anti-VEGF-C scFvs and the ETH-2 Gold library as well as the canonical sequences of the human VH3 subfamily (which contains the DP-47 heavy chain sequence that was used for construction of the ETH-2 Gold library) and camel V_HH were aligned using ClustalW. Typical aa substitutions of camel V_HH are colored yellow, orange and red. The G44E substitution occurring in anti-VEGF-C VC2.2.2 is colored in red, the L45P substitution occurring in VC1 in orange. The K64E substitution occurring in VC3 is colored in blue. X denotes variable amino acids in the CDR regions. Numbering is according to the Chothia 89-97 numbering scheme (Chothia *et al.* 1989).

3.8. Anti-VEGF-C scFvs with camelid-like mutations show unfavorable gel-filtration profiles, but the single V_H is partly stabilized

When analyzed on a Superdex 75 SEC column, the anti-VEGF-C scFvs VC1, VC2 and VC3 as well as the VC2 daughter VC2.2.2 elute with several peaks, indicating presence of dimers, multimers or higher aggregates (Fig. 3.33 A-C, E).

The monomeric peak at about 11 ml is markedly reduced when compared to a control scFv (Fig 3.33 F). VC4, which does not contain any deviation from the ETH-2 Gold library sequence but does only bind to *P. pastoris*-derived ΔNΔC-VEGF-C shows a more favorable elution profile (Fig. 3.33 D). Several peaks with later elution time-points are also present in VC1 to VC4 as well as VC2.2.2, indicating probable proteolytic products (Fig. 3.33 A-E).

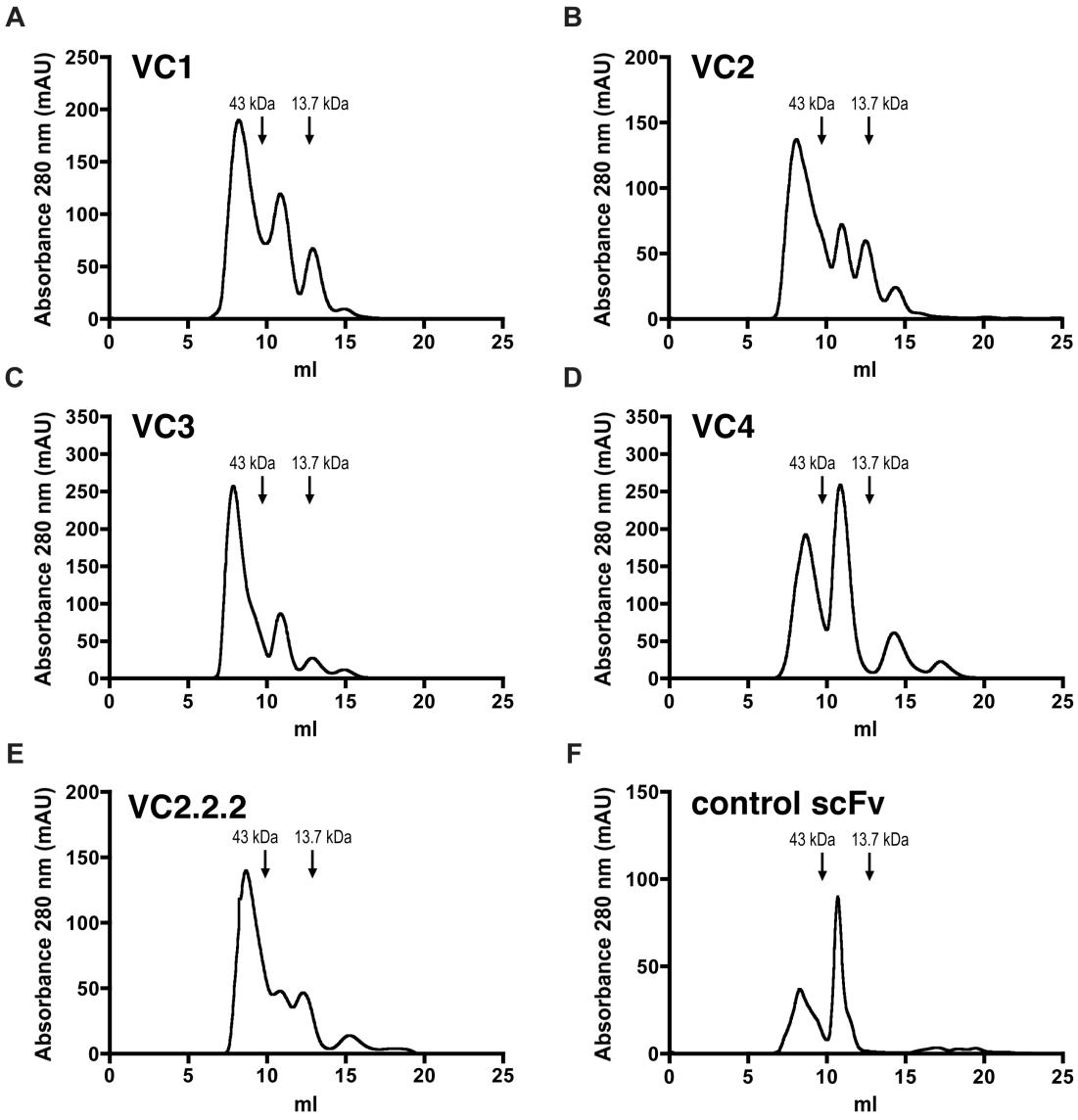

Figure 3.33. Size-exclusion gel-filtration profiles of anti-VEGF-C scFv. ScFv antibody fragments and control proteins (ovalbumin, 43 kDa, and ribunuclease A, 13.7 kDa) were analyzed on a Superdex 75 10/300 GL column under a flow rate of 0.5 ml/min.

As determined by SDS-PAGE and anti-myc immunoblot, protein-A purified myc-tagged VC2.2.2 V_H and anti-GST V_H both run at about 12 kDa (Figure 3.34 A, B), although their molecular masses are calculated from their primary amino acid sequences as 14.6 kDa. When subjected to size-exclusion gel-filtration, the VC2.2.2 V_H showed a partly stabilized behavior with a major peak at 15 ml, corresponding to the putative V_H monomer (Barthelemy et al. 2008), eluting just after the 13.7 kDa marker (Fig. 3.34 C). The non-"camelized" anti-GST V_H showed peaks corresponding to higher molecular weights (Fig. 3.34 D), indicating partial aggregation.

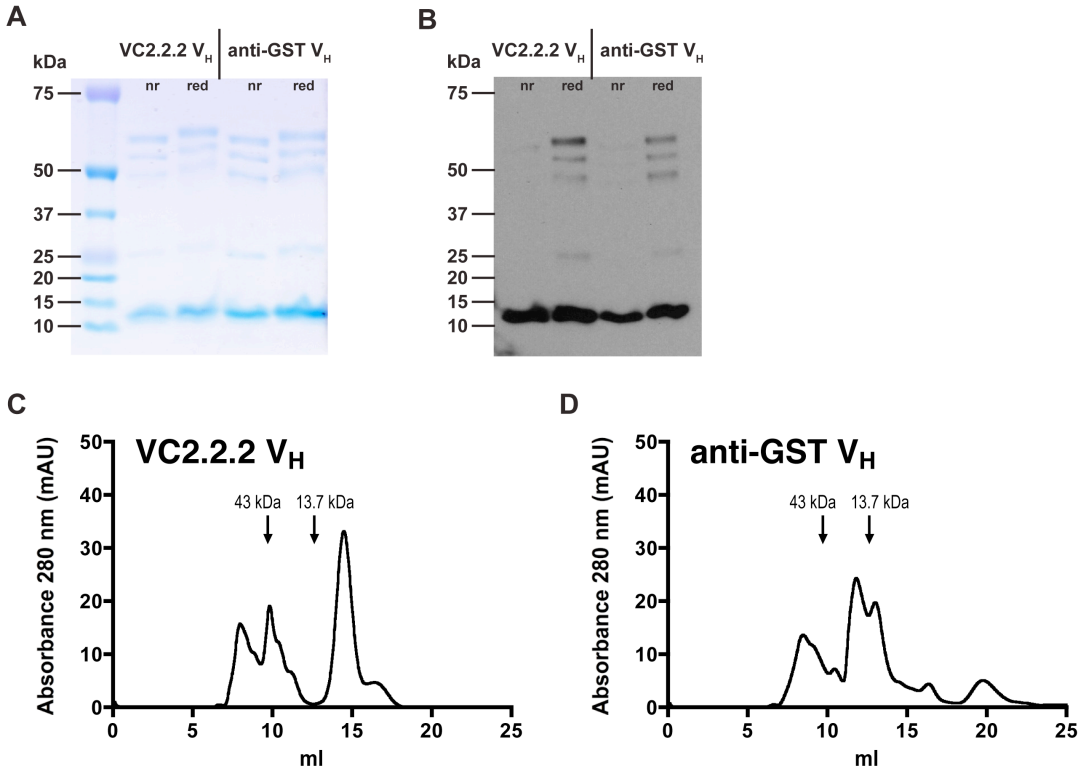

Figure 3.34. SDS-PAGE and immunoblot analysis as well as SEC gel-filtration profiles of anti-VEGF-C VC2.2.2 V_H and anti-GST V_H. Protein-A purified V_H under non-reducing (nr) and reducing (red) conditions were separated by SDS-PAGE and (A) stained using Coomassie-Blue or (B) immunoblotted using an anti-myc antibody followed by anti-mouse HRP. Protein-A purified (C) anti-VEGF-C VC2.2.2 V_H or (D) anti-GST V_H were injected on a Superdex 75 10/300 GL size-exclusion gel-filtration column. Markers represent the major elution peaks of the molecular mass standards ovalbumin (43 kDa) and ribonuclease A (13.7 kDa).

4. Discussion

Discussion

This thesis describes the development and characterization of function-blocking monoclonal antibody fragments against human ΔNΔC-VEGF-C. The blocking capabilities were confirmed on the molecular level using BIAcore and competitive ELISA. Antibody phage-display was used to select 4 lead binders from the ETH-2 Gold library, a fully human synthetic antibody library comprising 3 billion individual antibody clones (Silacci *et al.* 2005). From these 4 binders, one was specific for an epitope only present on *P.pastoris*-derived ΔNΔC-VEGF-C, which was used for selection, while the other 3 clones bound to an epitope in the conserved region of ΔNΔC-VEGF-C (Fig. 3.4 A). Binding to the His-tag could be excluded, since ΔNΔC-VEGF-D, to which the scFv are not binding, also contains a His-tag.

Via affinity maturation of clone VC2, daughter clones with up to 4-fold improved affinity (22 nM, clone VC2.2.2) were obtained (Fig. 3.10 and Table 3.4). The affinities of these daughter clones are in the same range as described for VD1, a function-blocking mouse IgG against human ΔNΔC-VEGF-D (Achen *et al.* 2000).

The molecular assays used to test for a function-blocking capability of VC2.2.2 anti-VEGF-C scFv showed that the affinity of VC2.2.2-scFv is high enough to prevent binding of ΔNΔC-VEGF-C to both of its receptors, VEGF-R2 and VEGF-R3. With a Kd value of 135 pM for VEGF-R3 and 410 pM for VEGF-R2, VEGF receptors possess an affinity to ΔNΔC-VEGF-C about two orders of magnitude higher than VC2.2.2-scFv with 22 nM. It is therefore not surprising that molar excesses in the range of 30 to 100 times more VC2.2.2-scFv, as observed in the competitive ELISA, are needed to significantly block ΔNΔC-VEGF-C binding to its receptors.

Results obtained from competitive ELISA suggest that VC2.2.2 anti-VEGF-C scFv is indeed capable of blocking the action of VEGF-C over a longer time frame. With a high enough molar excess of scFv, the equilibrium of association and dissociation of the scFv – VEGF-C complex and the permanent competition for free VEGF-C binding by the VEGF receptors can obviously be offset.

The blocking of VEGF-C-binding to both VEGF-R2 and VEGF-R3 indicates that the epitope for VC2.2.2-scFv on ΔNΔC-VEGF-C might be localized in a region that is important for binding to both of the receptors. On the other hand, binding of the 27 kDa scFv molecule to the relatively small 21 kDa ΔNΔC-VEGF-C protein (of which a part of the surface is already occupied by the dimerization with another ΔNΔC-VEGF-C monomer) may already be sufficient to block binding to VEGF receptors simply by steric hindrance. However, data generated by the epitope-mapping peptide array experiment hint to a specific binding of VC2.2.2 to the VEGF receptor-binding domain on ΔNΔC-VEGF-C. Recently, the three-dimensional crystal structure of ΔNΔC-VEGF-C in complex with one of its receptors, VEGF-R2, was solved by X-ray diffraction (Leppanen *et al.* 2010). The receptor-binding domains of VEGF-C were mapped to two sites consisting of three loops and part of the N-terminal helix on VEGF-C (Fig. 3.17 A). Site 1 is composed of the N-terminal helix alpha1 (His113 – Thr129) and the loop L2 (Asn167 – Leu171). Site 2 consists of the loops L1 (Asp139 – Pro155) and L3 (Ile188 – Pro196). Site 1 is provided by one VEGF-C monomer, while site 2 comes from the antiparallel second VEGF-C monomer (Leppanen *et al.* 2010). The receptor-binding domains for both VEGF-R2 and VEGF-R3 have also earlier been analyzed by mutational analysis of VEGF-C and these data correlate well with the structural results for VEGF-R2 (Jeltsch *et al.* 2006) (Fig. 3.17 B,C). The VEGF-C sites and residues responsible for binding to

VEGF-R3 are essentially the same as those making contact with VEGF-R2. Furthermore, a stretch around Cys156 was speculated to form the dimerization interface between the two antiparallel VEGF-C dimers. Cys156 is a key determinant for receptor-binding, when mutated to serine, it is responsible for the loss of binding of VEGF-C to VEGF-R2 and when mutated to alanine, it abolishes binding to both VEGF-R2 and VEGF-R3 (Jeltsch *et al.* 2006).

F_{151}FKPPCVSVYRC_{162}, the top-hit peptide from the epitope scan (Table 3.5), maps to loop L1 in site 2 and the presumed dimerization interface of ΔNΔC-VEGF-C. Loop L3 in site 2 and, when dimerized, loop L2 and helix alpha1, that contain other important residues for VEGF receptor binding, are located in the spatial vicinity of the putative epitope. Binding of VC2.2.2 anti-VEGF-C scFv could therefore possibly interfere with dimerization of VEGF-C and sterically hinder VEGF-C loops 1 and 3 from making contacts to the receptor (Fig. 3.17 A-G). Importantly, ΔNΔC-VEGF-D, which is not bound by VC2.2.2-scFv, features two different residues in the FFKPPCVSVYRC region, which might be responsible for the lack of cross-reactivity towards VEGF-D (Fig. 3.16).

The C-terminal sequence SCRCMS to RQVHSIIRRHHHHHH could also be part of the anti-VEGF-C epitope. This region lies in proximity to the loop L2 in the site 1 receptor-binding interface of VEGF-C (Fig. 3.17 A). Binding of anti-VEGF-C to this region could therefore also sterically hinder the binding of VEGF-C to its receptors. In recombinant human VEGF-D, this sequence is much less conserved than the FFKPPCVSVYRC sequence, possibly explaining why VEGF-D is not recognized by the anti-VEGF-C scFv (Fig. 3.16). The His-tag, however, can be excluded as being the actual anti-VEGF-C epitope or being part of the anti-VEGF-C epitope, since (i) the C-terminal His-tag is present in both mammalian-cell derived recombinant VEGF-

C and VEGF-D but rhVEGF-D is not bound and (ii) in the *P.pastoris*-derived ΔNΔC-VEGF-C (which was initially used for panning), the His-tag is present at the N-terminus and thus has different neighboring residues (Fig. 3.16).

The finding that the V_H of VC2.2.2 is sufficient for binding to VEGF-C is intriguing (Fig. 3.27). It might explain why during affinity maturation in the first round, similar advantageous sequences were selected in CDR-H1, while in CDR-L1 no consensus could be observed. Further, it might also explain why additional affinity maturation steps were not successful; obviously, randomizing domains in the CDRs of V_L is useless when V_L is not implicated in binding of the antigen. In this light, identification of mutations in all three scFv binding to mammalian cell-derived ΔNΔC-VEGF-C is perplexing (Table 3.6). Transitional single nucleotide mutations leading to the hydrophilic FR2 substitutions G44E in VC2 (and its daughter clone VC2.2.2) and L45P in VC1 as well as the CDR2 substitution K64E in VC3 obviously lead to a selection advantage during the panning against ΔNΔC-VEGF-C. It can be speculated that ΔNΔC-VEGF-C favors binding of small single V_H domains in contrast to paired Fvs, maybe due to the heavy glycosylation that may obstruct access to proteinaceous epitopes. Hints that V_L and V_H are not paired correctly in the scFvs come from gel-filtration profiles of first and second generation anti-VEGF-C scFvs (Fig. 3.33). The first generation scFv VC1, VC2 and VC3, that contain mutations and bind to mammalian cell-derived ΔNΔC-VEGF-C as well as the VC2 daughter clones all showed unfavorable gel-filtration profiles with an enhanced ratio of scFv multimers or aggregates vs. monomers, while the first generation scFv VC4, that does not contain mutations and binds only to *P.pastoris*-derived ΔNΔC-VEGF-C, shows a more favorable gel-filtration profile with the monomer as the most prominent peak. The mutations could both be the cause to the special binding properties or an

evolutionary adaptation of the scFv-coding gene towards higher solubility of the expressed non-properly folded scFv. Both would result in a selection advantage, either during panning of the scFv-bearing phage or during growth of the phagemid-bearing *E.coli.* Interestingly, camelid V_HHs have been reported to often bind to unusual and hidden protein epitopes, e.g. clefts in enzymes. This has been attributed to their especially long CDR3 loop, which protrudes and is able to insert itself into concave epitopes (Lauwereys *et al.* 1998; Conrath *et al.* 2001; Muyldermans *et al.* 2001). In contrast, normal Fv paratopes are flat or contain a cleft themselves and normally bind to flat or convex epitopes. Interestingly, the FFKPPCSVYRC epitope candidate emerging from the peptide-scan lies partly buried in the dimerization interface between the VEGF-C dimers (Fig. 3.17 D).

Possibly, the folding state of either the scFv or the V_H could be stabilized by either mutating Glu44 back to glycine (to correct the dimerization interface and promote correct assembly of the scFv, although this might disrupt binding to ΔNΔC-VEGF-C at all) or mutating more residues in the dimerization interface into hydrophilic residues to more closely resemble V_HH and to stabilize the V_H (Davies *et al.* 1996). Incorporation of all three observed mutations into one V_H might also be an interesting strategy. The companies Ablynx and Domantis have concentrated on such minimal antibody domains and are actively pursuing applications for treatment of disease. For instance, Ablynx has developed libraries of V_H single-domain antibodies, termed Nanobodies®, and has expedited several nanobodies into clinical development (www.ablynx.com). Single-domain antibodies have several interesting features, among them increased thermal stability, increased stability against proteases as well as extreme pH (making orally delivery for gut-associated diseases possible), simple and fast folding as well as tailorable serum half-life by use of

immunoglobulin or albumin binder technology (van der Linden *et al.* 1999; Muyldermans 2001; Dumoulin *et al.* 2002; Conrath *et al.* 2005; Harmsen *et al.* 2005; Harmsen *et al.* 2006; Ladenson *et al.* 2006).

It has been reported earlier that pairing of an antigen-binding single V_H domain with random V_L domains can lead to loss of binding activity of the resulting scFv. In an interesting study by Cai *et al.* 1996, the melanoma specific V_H domain V86, isolated from a phage display library from a melanoma patient, was paired with random V_L domains. Of 50 V_H-$V_{L\text{-}Lambda}$ fusions, none retained binding capability against melanoma cells and 18 of 68 V_H-$V_{L\text{-}Kappa}$ fusions completely lost their binding capacity.

The surprising finding that VC2.2.2-IgG transiently expressed in CHO-S cells does not bind to ΔNΔC-VEGF-C while VC2.2.2-IgG expressed from clonally selected stable CHO-S cell lines does bind to ΔNΔC-VEGF-C (Fig. 3.24) might be explained as follows. VC2.2.2-IgG molecules from transiently transfected CHO-S cells show the typical IgG pattern of bands to be expected on SDS-PAGE gels, with a strong band at 160-180 kDa (Fig. 3.22). This points to a correct assembly of the IgG molecule, with correct pairing of 2 light chains and 2 heavy chains. In the IgG-format the light chain is held in its place much more strongly than in the scFv format. In the scFv, the V_L pairs with the V_H only due to hydrophobic interactions and may relatively easily dissociate from the V_H (Kd constants of 10^{-6} to 10^{-9} M, (Pluckthun 1992)), especially in the presence of hydrophilic mutations in the dimerization interface. This would result in a “free” V_H with non-obstructed binding capability, while the V_L is still attached via the linker, adopting a non-defined structure (Worn *et al.* 2001). The observation that the V_H is sufficient for binding of VEGF-C (Fig. 3.27) and the non-standard SEC profiles of the anti-VEGF-C scFvs (Fig. 3.33) hint to such

a process. In the case of an IgG, in addition to the non-covalent interactions within the V_H:V_L interface, the light chain is also attached to the heavy chain by hydrophobic interactions and a disulfide bridge within the C_{H1}:C_L interface, leading to more rigidity in the Fab structure than in the scFv structure (Horne *et al.* 1982; Kondo *et al.* 1999). The more rigid placement of V_L in the Fab might lead to an interference of the binding via the V_H, as described above. In the case of VC2.2.2-IgG expressed by clonally selected stably transfected CHO-S cells, a reduced or even totally missing expression of the full size IgG band was observed (Fig. 3.19). This may be due to two reasons. First, FACS-sorting of stably transfected VC2.2.2-IgG-producing CHO-S cells with an anti-Fc antibody actually enriches only for high heavy chain-expression (although heavy chains should not be secreted withouth light chains, but nevertheless are, to some extent). Second, by screening sorted clones for reactivity against ΔNΔC-VEGF-C, producers of functional anti-VEGF-C immunoprotein are selected. Such clones are not necessarily those that secrete full length IgG. In fact, only about half of all FACS-selected viable anti-VEGF-C CHO-S clones actually secreted a product that reacted with ΔNΔC-VEGF-C.

The heavy chain antibody (HcAb) vector used to express the V_H-hinge-C_{H2}-C_{H3} fusion could also be used to construct a new class of IgG-like immunoproteins incorporating both V_H and V_L, encoded by a single polypeptide in the form of V_L-linker-V_H-hinge-C_{H2}-C_{H3}, similar to the small immunoprotein format (Li *et al.* 1997). This simplifies the format conversion from scFv to IgG-like molecules massively. It would obviate the need to titrate the heavy to light chain vector-ratio for optimal secretion, would render higher molar yields due to the smaller size of the immunoprotein compared to full IgGs but would still yield immunoproteins with a size that is above renal excretion limit and thus possess a relatively long serum half-life.

Also, high HcAb secretion yields of approx. 10 mg/l from unoptimized transiently bulk-transfected CHO-S cells were reached.

Surprisingly, reports on neutralizing anti-VEGF-C antibodies are rare. A rabbit monoclonal anti-rat VEGF-C antibody (Reliatech, Wolfenbüttel, Germany), which supposedly cross-reacts with human VEGF-C, was reported to block VEGF-C. This antibody has been used to block suture-induced corneal lymphangiogenesis in the mouse eye (Albuquerque *et al.* 2009) but no tumor studies are available. Some articles report that sc-1881 (Santa Cruz Biotechnology, Santa Cruz, CA), a polyclonal goat antibody raised against the C-terminal propeptide of human VEGF-C, can inhibit processing of the propeptide to fully active ΔNΔC-VEGF-C (Tomanek *et al.* 2002; Timoshenko *et al.* 2007) and activity of this antibody was successfully tested in tube forming and migration assay. Finally, a mouse monoclonal anti-human VEGF-C antibody (Genentech) was reported to block VEGF-C mediated cyclic pressure induced human umbilical vein endothelial cell (HUVEC) proliferation (Shin *et al.* 2002). All of these antibodies are of non-human origin, which limits their use in human cancer therapy due to immunogenicity.

It can be speculated that the scarcity of neutralizing antibodies against VEGF-C, especially against the fully processed ΔNΔC-VEGF-C, may result from its low immunogenicity, since the aa sequence is extremely conserved between different species. For instance, murine ΔNΔC-VEGF-C is identical to the rat sequence and both are identical to the human sequence in 113 out of 115 amino acids (98%). Due to the mechanism of B-cell tolerance, B-cell clones that recognize ΔNΔC-VEGF-C are therefore deleted from the animal's immune system (Sinclair 2004). For VEGF-A, which shares "only" 85% identity between humans and mice, from more than 10 hybridoma monoclonal antibodies raised in mice against human

VEGF-A, none was able to bind murine VEGF-A (Liang *et al.* 2006). To produce animal-derived monoclonal antibodies against such highly conserved self-antigens, more sophisticated methods like the use of B-cell tolerance defective mice are necessary (Zhou *et al.* 2009). In addition, the high degree of glycosylation of ΔNΔ-VEGF-C may further reduce its immunogenicity – as an example, it is known that non-glycosylated forms of therapeutic proteins like GM-CSF (Gribben *et al.* 1990) or IFN-beta (Karpusas *et al.* 1998) greatly enhance their immunogenicity in humans.

Antibody phage-display offers the great advantage of shortcutting the animal's immune system and allows the selection of antibodies against virtually any antigen, including self-antigens, which are normally non-immunogenic. By using antibody frameworks based on human germline V-gene segments, binders with human amino-acid sequences can be obtained and easily be reformatted into fully human IgG formats. This offers the advantage of significantly reduced immunogenicity compared to non-human, chimeric or humanized antibodies, when used in human therapy.

Compared to other inhibitors of the VEGF-C – VEGF-R2/3 axis, an anti-VEGF-C antibody has the main benefit of specifically blocking the action of VEGF-C. This is important, since the VEGF / VEGF receptor interaction network is highly redundant. VEGF receptor blockers, for instance, do only block the action of a VEGF ligand on the one targeted receptor, but not on other VEGF receptors activated by the ligand. At the same time, they do block all interaction with the targeted receptor, indiscriminate of the VEGF ligand. Soluble VEGF-receptors (VEGF-traps) on the other hand, block all ligands that bind to them. This broad-spectrum inhibition (which might be advantageous in cancer therapy) may have impacts on other tissues, where VEGF ligand and receptor expression also occurs. For instance, VEGF-D is

also expressed by osteoblasts, where it regulates bone regeneration in an autocrine manner via VEGF-R3 (Orlandini *et al.* 2006). Interference with the VEGF-D / VEGF-R3 axis might therefore potentially affect bone regeneration.

Conversely, VEGF-C is expressed in osteoclasts, where it enhances bone resorption in an autocrine manner via VEGF-R3 (Zhang *et al.* 2008a). It seems that in the bone, VEGF-C and VEGF-D are counterplayers and blocking VEGF-C could potentially reduce bone degradation.

The high homology between VEGF-C and VEGF-D obviously points to a strong redundancy in function of the two proteins. The individual roles of each protein toward lymphangiogenesis are still largely unknown. The potency of either protein in induction of lymphangiogenesis is also subject to discussion, with most articles reporting fully processed ΔNΔC-VEGF-C as the more potent lymphangiogenic molecule, but some reports designating ΔNΔC-VEGF-D as the more potent one. When strictly looking at affinities to VEGF receptors, ΔNΔC-VEGF-C is more potent (410 pM vs. 56 nM for VEGF-R2, 135 pM vs. 20 nM for VEGF-R3, ΔNΔC-VEGF-C (Joukov *et al.* 1997) and ΔNΔC-VEGF-D (Stacker *et al.* 1999), respectively), although these values must be taken with care, since they come from different analyses. Regarding the importance of VEGF-C and VEGF-D for tumor lymphangiogenesis and metastasis, a high VEGF-C expression seems to be clinically more relevant than a high VEGF-D expression (Rinderknecht *et al.* 2008), with some reports even stating a pathologically positive effect of a high VEGF-D to VEGF-C ratio (Niki *et al.* 2000; George *et al.* 2001).

Taken together, we have selected a human antibody fragment that (i) binds to the receptor-binding region of mature, fully processed human VEGF-C (ΔNΔC-VEGF-C) and (ii) is capable of blocking the interaction of ΔNΔC-VEGF-C with both

VEGF-R2 and VEGF-R3 on the molecular level. The V_H of the selected anti-VEGF-C scFvs contain camelid V_HH-like mutations and VC2.2.2 V_H is sufficient to bind to ΔNΔC-VEGF-C. Upon further engineering of this minimal, less than 14.6 kDa antibody fragment to enhance solubility and stability, it may serve as the basis for development of bulkier fully human neutralizing anti-VEGF-C immunoproteins with improved half-lives in circulation. Such inhibitors could be useful in treatment of cancers that rely on direct VEGF-C signaling such as Kaposi's sarcoma (Stacker *et al.* 2002), acute myeloid or lymphocytic leukemia (Dias *et al.* 2002; Moehler *et al.* 2003) and cancers that metastasize via the lymphatic vasculature (Rinderknecht *et al.* 2009) but also against cancers that have become refractory to anti-VEGF-A treatment. Furthermore, such inhibitors could also be active against VEGF-C-induced bone degeneration and age-related macular degeneration. Finally, neutralizing anti-VEGF-C immunoproteins could also be used as a tool to further dissect the specific role of VEGF-C vs. VEGF-D.

5. Materials and Methods

5.1. Cell lines

Suspension CHO-S cells (Invitrogen, Paisley, UK) were kindly provided by Philochem AG. Cells were grown in suspension using PowerCHO-2 CD medium or ProCHO-4 CD medium (BioWhittaker, Walkersville, MD), both supplemented with 8 mM L-glutamine (Gibco, Paisley, UK), 10 ml/l hypoxanthine/thymidine (Gibco) and antibiotic/antimycotic solution (Gibco). For adherent growth, CHO-S cells were cultured in RPMI 1640 (Cat No A10491, Gibco) supplemented with 10% FBS (Gibco) and antibiotic/antimycotic solution (Gibco). Cells were grown in a humidified atmosphere at 37°C and 5% CO_2.

5.2. Bacterial media

Phage growth medium 2YT consisted of 16 g tryptone (Fluka, Buchs, Switzerland), 10 g yeast extract (Fluka) and 5 g NaCl (Fluka) per liter. For growth of phage infected *E.coli* TG1 on solid agar plates, 2YT was supplemented with 100 µg/ml ampicillin (Sigma-Aldrich, Buchs Switzerland) and 1% (w/v) glucose (Fluka) to give 2YTAG (1%), and was mixed with 17 g of agar (Hänseler, Herisau, Switzerland) per liter.

5.3. Antigens

Human recombinant ΔNΔC-VEGF-C was expressed from a pPICZalpha based expression vector (Invitrogen) in the yeast *Pichia pastoris.* It contains an N-terminal His-tag (Fig. 5.1). Purification to homogeneity was accomplished by IMAC affinity chromatography and gel filtration as described previously (Scheidegger *et al.* 1999). Human recombinant ΔNΔC-VEGF-C and ΔNΔC-VEGF-D, produced in mouse myeloma cells, were purchased from R&D Systems (Abingdon, UK). Human VEGF-

A_{165} was kindly provided by the National Cancer Institute (Bethesda, MD). Alpha-2-macroglobulin was purchased from Sigma.

```
mammalian cell derived ΔNΔC-VEGF-C      ----TEETIKFAAAHYNTEILKSIDNEWRKTQCMPREVCIDVGKEFGVATNTFFKPPCVSVYRCGGCCNSE 67
Refseq human ΔNΔC-VEGF-C               ----TEETIKFAAAHYNTEILKSIDNEWRKTQCMPREVCIDVGKEFGVATNTFFKPPCVSVYRCGGCCNSE 67
P.pastoris-derived ΔNΔC-VEGF-C          EPHHHHHHLVPRGSHYNTEILKSIDNEWRKTQCMPREVCIDVGKEFGVATNTFFKPPCVSVYRCGGCCNSE 71

mammalian cell derived ΔNΔC-VEGF-C      GLQCMNTSTSYLSKTLFEITVPLSQGPKPVTISFANHTSCRCMSKLDVYRQVHSIIRRHHHHHHHHHH 135
Refseq human ΔNΔC-VEGF-C               GLQCMNTSTSYLSKTLFEITVPLSQGPKPVTISFANHTSCRCMSKLDVYRQVHSIIRR 125
P.pastoris-derived ΔNΔC-VEGF-C          GLQCMNTSTSYLSKTLFEITVPLSQGPKPVTISFANHTSCRCMSKLDVYRQVHSIIRR 129
```

Figure 5.1. Amino acid sequences of ΔNΔC-VEGF-C variants used in the study. The region of 100% identity within *P.pastoris*-derived human ΔNΔC-VEGF-C, mammalian cell-derived human ΔNΔC-VEGF-C and Refseq human ΔNΔC-VEGF-C is shown on a grey background.

5.4. Plasmids

The pHEN1 plasmid was used for expression of scFv in *E.coli* as described previously (Silacci *et al.* 2005). For expression of the V_H domain, the V_H sequence was amplified from the VC2.2.2-scFv-encoding pHEN1-based plasmid by PCR using the upstream forward primer LMB3long (attaching 5' of the scFv coding sequence) and the downstream reverse primer VHrev (annealing at the 3' end of V_H) (Table 5.1). The PCR product was then digested with *Nco*I and *Not*I and ligated into the pHEN1-backbone digested with the same enzymes. The resulting plasmid encoding VC2.2.2 V_H from Glu1 to Ser113 (Chothia 89-97 numbering scheme (Chothia *et al.* 1989)) as well as the C-terminal myc-tag and amber stop codon were subsequently verified by sequencing.

For construction of the IgG-vectors, variable heavy and light chains of the scFv were separately amplified by PCR from the pHEN1-scFv plasmid and cloned into separate mammalian expression vectors harboring C_{H1} to C_{H3} or C_V domains, respectively. The V_H domain of VC2.2.2 was amplified from the pHEN1-VC2.2.2 plasmid by PCR with proofreading KOD-polymerase (Toyobo, Osaka, Japan) using

primers LMB3long and DP47XhoIrev, shuttled via the pCRIIblunt topoisomerase vector and cloned via *PpuM*I and *Xho*I into the pcDNA3.1/hygro based heavy chain expression vector pKZ1 (Zuberbuhler *et al.* 2009). The V_L domain was amplified similarly, using the primers LMB3long and DPL16HpaIrev, and cloned into the pcDNA3.1/neo based light chain expression vector via *PpuM*I and *Hpa*I.

Heavy-chain-only antibody vectors were constructed by splicing out the C_{H1} domain from pKZ1-VC2.2.2. The region upstream of the PpuMI site until the end of V_H (350 bp) was amplified from the pKZ1-VC2.2.2 plasmid by proofreading PCR using the primers VHbegin and VHend, attaching part of the hinge region at the 3' end via the VHend primer. The hinge-CH2-CH3 region (720 bp) was similarly amplified from pKZ1-VC2.2.2 by using primers CH2upstream and CH3downstream. Both amplicons were purified by using a PCR purification column (Qiagen) and used as templates annealing to each other via the hinge region in a splicing-by-overlap-extension PCR (see below and Fig. 5.2) for 7 cycles, when the pull-through primers VHbegin and CH3downstream were added for exponential amplification of the annealed and so far linearly amplified VH-Hinge-CH2-CH3 template, essentially as described previously (Silacci *et al.* 2005). All primers were ordered from Sigma.

Primer	**Sequence (5'-3')**	**Reference**
LMB3long	CAGGAAACAGCTATGACCATGATTAC	(Silacci *et al.* 2005)
fdseqlong	GACGTTAGTAAATGAATTTTCTGTATGAGG	(Silacci *et al.* 2005)
VHrev	GAGATGAGTTTTTGTTCTGCGGCCGCactcgagacggtg accagggt (NotI site underlined, annealing site to V_H in lowercase)	This study
DP47XhoIrev	TGGTCGACGCactcgagacggtgaccagggt (XhoI site underlined, annealing site to 3' end of V_H in pHEN1 in lowercase)	This study
DPL16HpaIrev	AGGGGGCAGCCTTGGGCTGgcctaggacggttaacttggtcc (HpaI site underlined, annealing to 3' end of V_L in pHEN1 in lowercase, mutation (g->a) for corrected HpaI site in bold)	This study
VHbegin	CTGGGGGAGGCTTGGTAC	This study
VHend	TGGGCATGTGTGAGTTTTGTCactcgagacggtgaccaggg (annealing site to 3' end of V_H in lowercase, hinge-region-adaptor (DKTHTCP) in UPPERCASE)	This study

CH2upstream	GACAAAACTCACACATGCCCA	This study
CH3downstream	CTAGTCTAGAGCGGGGGCTTGCCGGCC (XbaI site underlined)	This study
DP47CDR1ba	TGGGTCCGCCAGGCTCCAG	(Villa *et al.* 2008)
DP47CDR1for	AGCCTGGCGGACCCAGCTCATMNNMNNMNNGCTAAAGGTGAATCCAGAGGCTGC	(Villa *et al.* 2008)
DPL16CDR1ba	TGGTACCAGCAGAAGCCAGGA	(Brack *et al.* 2006)
DPL16CDR1for	TCCTGGCTTCTGCTGGTACCAGCTTGCMNNMNNMNNTCTGAGGCTGTCTCCTTG	(Brack *et al.* 2006)
VC2.2.2heavybackmutfo	AGCCTGGCGGACCCAGCTCATATAATTCTGGCTAAAGGTGAATCCAGAGGCTGC	This study
VC2.2.3lightbackmutfo	TCCTGGCTTCTGCTGGTACCAGCTTGCAGTATTCTGTCTGAGGCTGTCTCCTTG	This study

Table 5.1. Primers used in this study. M = A/C, N=A/C/G/T

5.5. Splicing-by-overlap-extension (SOE) PCR

SOE PCR was performed as follows:

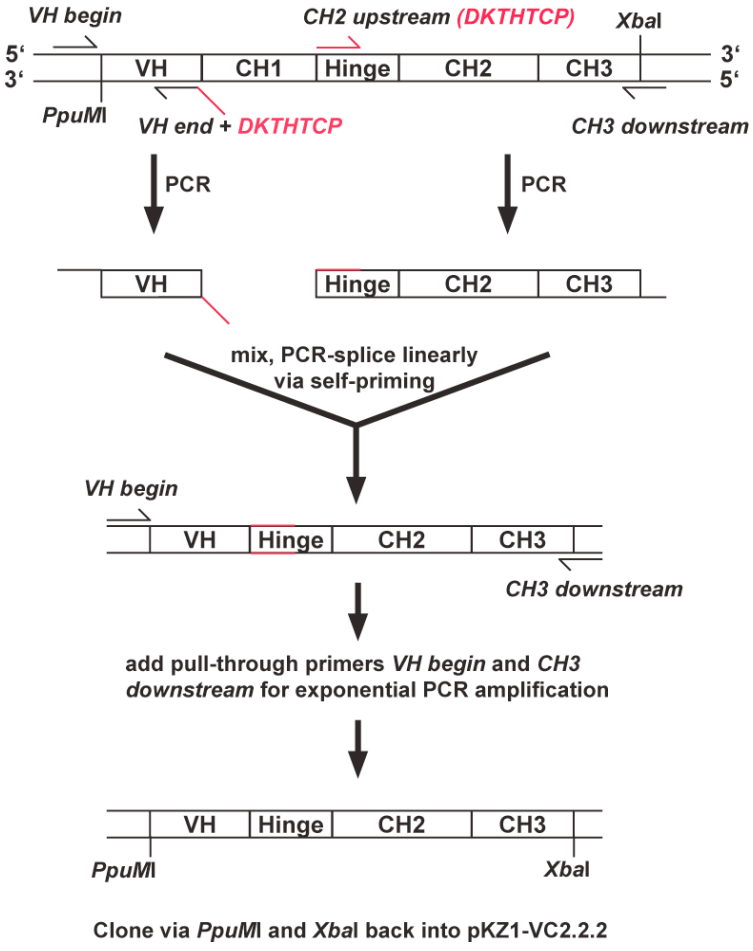

Figure 5.2. Schematic representation of the SOE-PCR principle. Overlaps of the two initial PCR fragments are colored in red.

A typical PCR mix for self-splicing of 2 PCR products consisted of the following components:

PCR product 1	5 µl
PCR product 2	5 µl
KOD polymerase buffer (Toyobo)	2.5 µl
10 mM dNTP (Promega)	0.5 µl
50 mM $MgSO_4$ (Toyobo)	0.75 µl
MilliQ water	10 µl
KOD polymerase (Toyobo)	0.5 µl
Total	25 µl

Linear self-splicing was achieved under the following cycling conditions:

Initial denaturation	95 °C	2 min
Cycle denaturation	95 °C	30 sec
Cycle annealing	56 °C	30 sec
Cycle elongation	70 °C	20 sec
Cycle steps were repeated for 7 times		

After the splicing, pull-through primers, fresh buffer and polymerase were added to the 25 µl of the SOE-PCR reaction as follows:

MilliQ water	15.75 µl
KOD polymerase buffer	2.5 µl
50 mM $MgSO_4$	0.75 µl
10 mM dNTP	0.5 µl
10 µM Primer 1	2.5 µl
10 µM Primer 2	2.5 µl
KOD polymerase	0.5 µl
Total	25 µl

Exponential PCR was achieved under the following cycling conditions:

Initial denaturation	95 °C	2 min
Cycle denaturation	95 °C	30 sec
Cycle annealing	56 °C	30 sec
Cycle elongation	70 °C	20 sec
Storage	4 °C	indef.

Cycle steps were repeated for 30 times

5.6. Transfections

Suspension CHO-S cells (Invitrogen) grown in complete PowerCHO2 as detailed above were transiently transfected with polyethyleneimine (PEI) as follows: CHO-S cells were spun down and respuspended at $2x10^6$ cells/ml in serum-free ProCHO-4 medium. Per 1 ml of cells, 1.25 µg of DNA was diluted in sterile 150 mM NaCl (Fluka) to a final volume of 25 µl and 5 µg of linear 25 kDa PEI (pH 7.0, Polysciences, Eppenheim, Germany) at 1 mg/ml was diluted in 150 mM NaCl. Subsequently, the PEI and DNA solutions were mixed together and incubated for 10 min at RT. The PEI-DNA solution was then added to the cells and the cells were incubated in a roller bottle incubator at 37°C for 4 hours. Then, the cells were diluted 1:1 with complete PowerCHO-2 medium. Cells were incubated for 4 to 6 days, after which the media was collected by centrifugation at 4'000 rpm for 45 min and filtration through a 0.2 µm filter (TPP).

Stable transfections were performed by electroporation. For this, $2x10^6$ CHO-S cells grown in complete PowerCHO-2 were pelleted by centrifugation at 1'100 rpm for 7 min and resuspended in 100 µl of Nucleofector solution V (Lonza, Walkersville, MD). Then, 1.5 µg of plasmid DNA was added, cells were transferred into an Amaxa electroporation cuvette (Lonza) and electroporated with program U-24 in an Amaxa

nucleofector (Lonza). Immediately after electroporation, 500 µl of prewarmed complete RPMI medium was added and the cells were plated onto a 6-well plate. The next day, selection antibiotics were added (300 µg/ml of hygromycin B (Calbiochem, La Jolla, CA) and 750 µg/ml of G418 (Sigma), for pcDNA3.1/hygro and pcDNA3.1/neo based transfection vectors, respectively). After selection for 10 days, the cells were brought into suspension by stepwise transfer into serum-free complete PowerCHO-2 medium, 2 days each in 80% RPMI, 50% RPMI and 20%RPMI.

5.7. SDS-PAGE, Coomassie staining, immunoblotting

Proteins were resolved on either 4-12% gradient or 10% acrylamide bis-tris Novex precast gels in MOPS running buffer, using LDS loading buffer with or without reducing agent as indicated by the manufacturer (all components from Invitrogen). Precision Plus molecular weight standards were from Biorad (Hercules, CA). Staining of SDS-PAGE gels was accomplished using Bio-Safe Coomassie (Biorad). For immunoblotting, the proteins resolved with SDS-PAGE were transferred to nitrocellulose membranes (Biorad) by tank-blotting using transfer buffer (20% (v/v) methanol, 25 mM Tris-base, 192 mM glycine) at 300 mA for 1 h. Membranes were subsequently blocked for 2 h with 5% skimmed milk powder (Coop, Basel, Switzerland) in phospate buffered saline (PBS, Gibco) containing 0.1% (v/v) Tween-20 (Sigma), referred to as MPBST. Immunoblotting was performed using protein-A, HRP-labeled (1:1'000, GenScript, Piscataway, NJ, Cat No M00089) or antibodies againt human VEGF-C (1:400, IBL, Gunma, Japan, Cat No 18415), c-myc (1:1'000, Clone 9E10, Sigma, Cat No M5546), human IgG, Fc specific, HRP-labeled (1:20'000, Leinco Technologies, St. Louis, MO, Cat No H605), penta-His-tag (1:1'000, Qiagen, Hilden, Germany, Cat No 34660) and respective secondary HRP-

labeled antibodies (1:10’000 – 1:20’000, GE Healthcare, Glattbrugg, Switzerland), all diluted in MPBST or according to the manufacturer.

5.8. Mass spectroscopy

Bands from Coomassie-stained SDS-PAGE gels were excised from the gel and cut into small pieces, destained in destaining solution (50% methanol in 100 mM NH_4HCO_3 (Fluka), pH 8) for 3 h at RT and washed in 100 mM NH_4HCO_3 buffer. Subsequently, the proteins in the gel were reduced with 2 mM tris(carboxyethyl)phosphine hydrochloride (TCEP•HCl, Pierce, Rockford, IL) in 100 mM NH_4HCO_3 (pH 8.0 – 8.5) at 37°C for 30 min, 1’000 rpm. The TCEP solution was removed and reduced cysteins were alkylated using 20 mM iodoacetamide (Sigma) in 100 mM NH_4HCO_3 (pH 8.0 – 8.5) for 30 min at RT in the dark. The iodoacetamide was completely removed, washed with 100 µl of MilliQ water and 100 µl of NH_4HCO_3 was added. After 10 min, the NH_4HCO_3 buffer was removed and gel pieces were dehydrated using 100 µl of 80% acetonitrile (ACN, Sigma) / 20% MilliQ water for 10 min. The acetonitrile was completely removed by evaporation in a vacuum concentrator (Eppendorf, Hamburg, Germany). Then, 40 µl of 8 ng/µl sequencing-grade modified trypsin (Promega, Dübendorf, Switzerland) in digestion buffer (50 mM Tris-HCl (Sigma), pH, 8.0, 1 mM $CaCl_2$ (Fluka)) was added and incubated overnight at 37°C, 1’000 rpm). The next day, samples were sonicated twice for 5 min to extract peptides, once in the overnight digestion buffer and once in 40 µl extraction solution (50% ACN, 0.1% trifluoroacetic acid (TFA, Fluka)). Finally, digestion buffer and extraction solution were combined and the sample was lyophilized in a vacuum concentrator. Samples were then redissolved in 30 µl of 0.1% TFA and desalted, purified and concentrated with C18 microcolumns (ZipTip C18; Millipore) according to the manufacturer’s instructions, and again lyophilized.

Lyophilized peptides were redissolved in 70% ACN, 0.1% TFA in MilliQ water, mixed with MALDI matrix (3 mg/ml alpha-cyano-4-hydroxycinnamic acid in 70% ACN, 0.1% TFA in MilliQ water) and spotted on a 384-well MALDI target plate at different protein to matrix ratios ranging from 2:1 to 1:4. Samples were finally subjected to MALDI-TOF/TOF mass-spectroscopy on a 4700 Proteomics Analyzer mass-spectrometer (Applied Biosystems, Rotkreuz, Switzerland). Spectra were processed and analyzed by the Global Protein Server Workstation (Applied Biosystems), which uses internal MASCOT (Matrix Science) software for matching MS and tandem MS data against databases of *in silico* digested proteins.

5.9. Library selections on immobilized antigen

The ETH-2 Gold antibody phage library (Silacci *et al.* 2005) was used to pan on fully processed ΔNΔC-VEGF-C derived from *Pichia pastoris*. A Maxisorp immunotube (Nunc, Wiesbaden, Germany) was coated overnight at room temperature with 50 µg/ml ΔNΔC-VEGF-C in 4 ml of 100 mM carbonate buffer, pH 9.6. As control, another immunotube was incubated with carbonate buffer alone. The next morning, immunotubes were rinsed three times with PBS and blocked with 5 ml of 2% (w/v) of skimmed milk powder in PBS (MPBS) for 2 h at room temperature. After rinsing three times with PBS, approximately 5 x 10^{12} transducing units (tu) of the phage library in 2% MPBS were added to the immunotubes. Subsequently, the immunotubes were incubated on an orbital shaker for 30 min and for another 90 min standing upright at room temperature. Unbound phage was washed away with ten washes of PBST and PBS each. For subsequent panning rounds, washing steps were increased to twenty washes with each buffer. Bound phage was eluted for 15 min by incubating the immunotubes on a rotator with 1 ml of 100 mM glycine pH 2.2, adjusted with HCl. After collecting the eluate, the acidic

elution buffer was neutralized by adding 200 µl 1 M Tris-HCl pH 8.6. The eluted phage was subsequently used to infect 10 ml of exponentially growing *E.coli* TG1 at OD_{600} = 0.5 for 35 min at 37°C. Titration of the eluted phages, phage amplification and colony picking were performed as described previously *(Viti et al. 2000).*

5.10. Biotinylation

ΔNΔC-VEGF-C from *P.pastoris* or mammalian cells was biotinylated with SS- or LC-NHS-Biotin (Pierce). 400 µl of a 500 µg/ml protein solution in PBS (Gibco) was mixed with 80 µl of freshly prepared 1 mg/ml solution of biotinylation agent in MilliQ water and incubated for 1 hour at RT. For removal of unreacted biotinylation agent, the mixture was loaded on a PD10 gel filtration column (GE Healthcare), topped up with 2.12 ml PBS, eluted with 3.5 ml PBS and fractions of 0.5 ml were collected. The protein containing fractions, as measured per spectrophotometric absorbance at 280 nm, were pooled.

To check the biotinylation of the protein, 100 µl of protein solution in PBS were dotted onto a nitrocellulose membrane (Biorad) with an Easy-Titer dot-blot system (Pierce). After drying for 15 min, the membrane was blocked for 1 hour with 3% BSA (Fluka) in PBS at RT. Following washing with PBS-0.1% Tween-20 (PBST), the biotinylated protein on the membrane was detected with streptavidin-HRP (GE Healthcare) 1:20'000 in 3% BSA / PBS. The membrane was then again washed three times for 5 min with PBST, incubated with ECL plus (GE Healthcare) for 5 min and imaged using the GelDoc analysis system (Biorad).

5.11. Affinity selections with biotinylated antigen

For selection of affinity-matured binders from the affinity maturation library, panning in solution with biotinylated antigen was used. This was done to prevent

selection of binders that bind only to denatured VEGF-C. Up to 3 biopanning rounds with different concentrations of biotinylated *P.pastoris*-derived ΔNΔC-VEGF-C (VC2.1 series; 1st round with 3 nM, 30 nM and 300 nM; 2nd round with 30 pM and 3 nM; 3rd round with 30 pM) and biotinylated mammalian cell-derived ΔNΔC-VEGF-C (VC2.2 series; 1st round with 300 pM, 3 nM and 30 nM; 2nd round with 3 nM) were performed. Prior to selection, 50 µl streptavidin coated magnetic beads (M-280 Dynabeads, Dynal Biotech, Oslo, Norway) per selection were blocked with 1 ml 3% BSA in PBS for 1 hour at room temperature and resuspended in 50 µl 2% BSA / PBS. 1 ml of antibody phage library (approximately 10^{12} tu in total) in 2% BSA / PBS was incubated with the biotinylated antigen at the above stated concentrations for 1 hour on a rotator at room temperature. The streptavidin magnetic beads were then added to the phage / antigen mixture and allowed to capture the biotinylated antigen and adhering phages for 15 min on a rotator at room temperature. Using a magnetic rack, the beads were subsequently washed 7 times with 1 ml of PBS-Tween (1%) and 3 times with PBS. Then, the phages were eluted from the magnetic beads with 100 µl of 100 mM glycine pH 2.2, adjusted with HCl, for 10 min at room temperature. The phage-containing supernatant was then removed and neutralized with 1 ml of 1 M Tris-HCl, pH 8.6. Infection of TG1 *E.coli*, titration and amplification was performed as described above.

5.12. ELISA screening

After 2 and 3 rounds of panning, individual bacterial colonies containing the phagemid were picked, inoculated into 150 µl 2YTAG(0.1%) and grown for 3 hours in a 37°C shaking incubator. Then, the cells were induced by addition of 50 µl of 2YTA containing 4 mM isopropyl-thio-galactopyranoside (IPTG; Applichem,

Darmstadt, Germany), to give a final concentration of 1 mM IPTG, and grown overnight for 30°C.

A 96-well maxisorp plate (Nunc) was coated overnight at RT with 50 µg/ml of ΔNΔC-VEGF-C in PBS as described above. The next day, the ELISA plate was washed three times with PBS and blocked with 300 µl 4% MPBS for 2 hours at RT. The plate was then washed again three times with PBS and each well was supplemented with 20 µl of 10% MPBS containing a 1:200 dilution of mouse anti-myc 9E10 antibody (Sigma, Cat No M5546) and 1:200 dilution of anti-mouse horseradish peroxidase labelled sheep antibody (GE Healthcare) as secondary reagents. The bacterial supernatant was centrifuged for 10 min at 1'800 g and 80 µl of supernatant from each well were added to the corresponding ELISA well. The plate was then incubated for 1 hour at RT on an orbital shaker. After three washes each with PBST and PBS using a squirt bottle, 100 µl Blue-POD peroxidase substrate (Roche, Mannheim, Germany) was added to each well and the chromogenic reaction was stopped with 50 µl 1 M H_2SO_4 after 10 min. The plates were then read with a spectrometer at 450 nm and 650 nm. To screen for false positives, the supernatants were also tested on maxisorp plates coated with PBS alone. Since ΔNΔC-VEGF-C derived from *P.pastoris* was used for the panning, the supernatants were also tested on streptawell plates (Roche) coated with 100 µl 10^{-7} M biotinylated ΔNΔC-VEGF-C derived from mammalian cells (R&D Systems) in PBS overnight at 4°C.

5.13. BIAcore analysis

All solutions to be injected into the BIAcore 3000 (GE Healthcare) were filtered using a 0.22 µm filter (Millipore, Zug, Switzerland). A streptavidin-coated sensorchip flowcell (GE Healthcare) was coated at a flowrate of 5 µl/min with 25 µl of

100 nM biotinylated ΔNΔC VEGF-C derived from either *P.pastoris* or mammalian cells in PBS, 0.01% azide, 0.005% surfactant P-20 (GE Healthcare). For both antigens, a stable immobilization level of more than 2'000 RU was achieved. Surface regeneration was done by injection of 5-10 µl 10 mM HCl. Positive supernatants from the ELISA were filtered through a 0.22 µm filter and injected as is.

5.14. Affinity maturation

Parental antibodies obtained after 3 rounds of panning were randomized in the CDR1 at the following positions (numbering according to *Tomlinson et al. 1995*: 31, 32, 33 for V_H, 31, 31a, 32 for $V_{L\text{-}Kappa}$ and 31a, 31b and 32 for $V_{L\text{-}Lambda}$ using degenerate primers DP47CDR1for, DPK22CDR1for and DPL16CDR1for respectively, together with DP47CDR1ba, DPK22CDR1ba, DPL16CDR1ba, LMB3long and fdseqlong respectively (Table 5.1). The three amplicons were assembled by PCR assembly essentially as described (Silacci *et al.* 2005). All primers were purchased from Sigma.

Affinity matured clones that contained a TAG amber stop codon in the mutated CDRs (coding for glutamine in suppressor strains and stop in non-suppressor strains) were backmutated to CAG by using PCR backmutation primers as specified in Table 5.1 and essentially the same assembly procedure as described above.

5.15. Expression and purification of immunoproteins

For scFv or V_H expression, an overnight starter culture of 2YTAG (5%), inoculated with a single colony of phagemid bearing *E.coli* TG1, was diluted 1:100 in 1 l of 2YTAG (0.1%) and grown at 37°C, 225 rpm until OD_{600} = 0.5. The cells were then induced by addition of IPTG (final concentration 1 mM) and grown overnight at

30°C, 225 rpm. Bacterial supernatants were clarified by centrifugation at 5'000 g, 4°C for 45 min and filtered through a 0.2 µm filter (TPP, Trasadingen, Switzerland). Supernatants were then loaded on a Protein-A affinity column (Biorad) using the Profinia automated protein purification system (Biorad) according to the manufacturer's recommendations. The columns were washed with Buffer A (100 mM NaCl, 0.1% Tween-20 (Sigma), 0.5 mM EDTA (Sigma) in PBS) and subsequently Buffer B (500 mM NaCl, 0.5 mM EDTA in PBS). Bound antibody fragments (scFv or V_H) were then eluted with 100 mM triethylamine (Sigma) and immediately neutralized in 1 M Tris-HCl, pH 7.0. The eluate was dialyzed overnight against PBS using Spectra/Por dialysis tubing with a 12-14 kDa cutoff (Spectrum Labs, Breda, The Netherlands) and concentrated to about 1 mg/ ml with Amicon Ultra 15 ultrafiltration devices with a 10 kDa cutoff (Millipore). For sterilization, the preparation was finally filtered through a 0.22 µm filter (Pall, Basel, Switzerland).

IgGs and HcAbs were produced as described in section 5.6 (Transfections) and purified from 0.2 µm-filtered cell culture medium by a similar procedure as described above using Profinia, but washing was performed using PBS only. Bound IgGs or HcAbs were eluted with 100 mM glycine-HCl, pH 2.2 and immediately neutralized with 1 M Tris-HCl, pH 8.0. Dialysis and concentration were performed as described above, using Amicon Ultra 15 devices with a 30 kDa cutoff.

5.16. Size-exclusion chromatography

Size-exclusion chromatography (SEC) and isolation of monomeric scFv and other proteins was performed on an Äkta FPLC system using a Superdex 75 10/300 GL or Superdex 200 10/300 GL column (GE Healthcare) at a flow of 0.5 ml/min.

5.17. FACS sorting and ELISA screening for IgG-expressing CHO-S cells

The procedure was performed essentially as described (Zuberbuhler *et al.* 2009). Recombinant CHO cells grown in suspension were cultured to a density of about $5x10^5$ cells/ml in T75 flasks. For staining, the cell suspension was collected, centrifuged for 5 min at 1'100 rpm and resuspended at $5x10^6$ cells/ml in FACS buffer (PBS supplemented with 2% FBS). Per sample, 200 µl of this cell suspension were added in a round bottom low attachment 96-well plate. The plate was then centrifuged for 3 min at 1'100 rpm and the supernatant was discarded by vigorous inversion. 100 µl of FACS buffer containing 10 µg/ml primary polyclonal rabbit anti-human IgG antibody (Cat No A0423, Dako, Glostrup, Denmark) were added, the cells were resuspended and allowed to incubate for 1 h at RT. Then, the cells were centrifuged for 3 min at 1'100 rpm, the supernatant was discarded and the cells were washed with 200 µl of FACS buffer. The cells were then centrifuged again as above, resuspended in 100 µl FACS buffer containing 1 µg/ml Alexa-Fluor 488-conjugated goat anti-rabbit IgG (Molecular Probes) and incubated for 30 min at RT in the dark. Subsequently, the cells were washed as described above, resuspended in 200 µl FACS buffer containing 1:1'000 diluted 7-amino actinomycin (7-AAD, BD Biosciences) to stain dead cells and transferred to FACS tubes. FACS was performed on a BD FACS-Aria (Becton Dickinson) equipped with FACSDiva software, an argon laser emitting at 488 nm and an automatic cell deposit unit for plate sorting. The 7-AAD staining was used to identify dead (or dying) cells and its emission in the PerCP-Cy5.5 channel was detected using a 695/40 bandpass filter. FITC emission, corresponding to cells stained for membrane-associated human IgGs, was detected using a 530/30 bandpass filter. Cells highly positive for FITC

staining and negative for 7-AAD were single-cell deposited using FACS into 96-well plates containing 200 µl of complete RPMI medium supplemented with 750 µg/ml G418 and 300 µg/ml hygromycin. Clones were subsequently incubated at 37°C and 5% carbon dioxide in a humidified atmosphere for 10 days.

An ELISA plate coated with 3 µg/ml ΔNΔC-VEGF-C produced in *P.pastoris* was prepared as described in ELISA screening. For detection, 20 µl of 10% MPBS containing 0.8 µg/ml horseradish peroxidase-labelled anti-human IgG, Fc-specific (Leinco), was mixed with 80 µl of cell culture supernatant from single-cell sorted CHO cells and incubated for 1 h at RT. Washing and development were performed as described above. The 6 clones exhibiting the strongest signals as compared to the positive control (polyclonal supernatant) and normalized to colony size were selected for further expansion.

5.18. Epitope mapping using peptide array

A peptide array (PepStar; JPT, Berlin, Germany) was used to map the epitope of the anti-VEGF-C antibody. The aa sequence spanning human ΔNΔC-VEGF-C from T103 to R227 and an appended C-terminal 6xHis-tag were used to define 40 overlapping, consecutive 15-mer peptides with 3 residues shift each. Synthesis of the peptides, using SPOT peptide synthesis, and peptide printing on glass slides were conducted at JPT. The myc-tag-epitope AEQLISEEDL, human and murine IgGs as well as *P.pastoris*-derived ΔNΔC-VEGF-C were printed as additional controls. Each slide featured 3 identical subarrays, corresponding to 3 technical replicates per condition.

ScFvs for epitope mapping were fluorescently labelled using Cy3 or Cy5 monoreactive dye (GE Healthcare). Dye aliquots were prepared by dissolving monoreactive Cy3 or Cy5 dye, intended for labeling of 1 mg protein, in 10 µl of

DMSO, dividing into 1 µl aliquots and vacuum-drying in a speed-vac. Dye aliquots were stored at 4°C in a desiccator under vacuum in the dark. Twenty µl of 1 M sodium bicarbonate buffer, pH 9, were added to 200 µl of a 1 mg/ml scFv solution in PBS to bring the final pH between 8.5 and 9.5. Then, this solution was added to 2 aliquots of Cy3 or Cy5 monoreactive dye and left to incubate for 1 hour at room temperature. Non-reacted dye was subsequently quenched with 100 µl Tris buffered saline (TBS), pH 7.5. To separate free dye from the scFv-bound dye and to exchange the buffer to PBS, the solution was loaded on a microcon concentrator column YM-10 (Millipore) with a membrane-cutoff of 10 kDa. The concentrator with the scFv/dye solution was then centrifuged three times at 14 krpm for 30 min and washed with 500 µl PBS between spins. Finally, the dye-labelled scFv was resuspended in 200 µl PBS and the protein concentration as well as the dye absorption were measured using a spectrophotometer (Nanodrop; Thermo Scientific, Wilmington, DE).

Arrays were competitively incubated according to the manufacturer's instructions in a sandwich-like fashion with a Cy3-labelled anti-VEGF-C scFv and a Cy5-labelled irrelevant scFv at 30 µg/ml each, in 300 µl of 0.22 µm filtered binding buffer (TBS containing 3% FBS and 0.5% Tween-20) at 4°C overnight in a humid atmosphere in the dark. Then, the microrarrays were washed 3 times for 6 min with binding buffer and 3 times for 6 min with MilliQ water in the dark. Slides were dried by spinning for 2 min at 300 rpm and scanned using a Genepix 4200A scanner (Axon Instruments, MDS Analytical Technologies, Concord, ON, Canada) with photo-multiplier tube (PMT) gain values for both channels set to prevent saturated pixels and to yield a pixel-count ratio of 1:1 for the two channels. Scanning was done using 2 line averaging and a resolution of 5 µm. Gal-file grids were manually

adjusted observing both colors and Cy3/Cy5 ratios were normalized to human and murine IgG as non-specific controls.

5.19. *In silico* modelling

The localization of the predicted epitope on ΔNΔC-VEGF-C was modeled on the basis of the VEGF-C / VEGF-R2 crystal structure pdb file 2X1X (www.pdb.org). For respresentation of the V_HH-like mutations on the Fv, the crystal structure of the human anti-polyhydroxybutyrate Fv, pdb file 2D7T, was used. Modeling was performed using MacPyMOL (www.pymol.org).

5.20. VEGF-C neutralization assay using BIAcore

Unless otherwise stated, all reagents were from GE Healthcare. A CM5 sensorchip equilibrated overnight with HBS-P was activated by injection of two times 70 µl 1:1 EDC / NHS mixture at a flow rate of 5 µl/min, resulting in a ΔRU of 214. Then, 68 µl of monoclonal anti-Fc antibody at 25 µg/ml diluted in 10 mM sodium acetate pH 5.0 immobilization buffer were injected. After 5 min, 50 µl ethanolamine were injected to deactivate the remaining binding sites. A stable immobilization level of about 16'000 RU was achieved. Surface regeneration between cycles was done by injection of 5 µl of 3 M $MgCl_2$. Injections on the anti-Fc coated CM5 chip were done at a flow rate of 5 µl/min and the different proteins were diluted in HBS-P buffer. For VEGF-C / VEGF-R3 binding experiments, 100 µl of 100 nM VEGF-R3-Fc recombinant protein (R&D Systems), resulting in a response of about 2'500 RU, were immobilized on the anti-Fc coated CM5 chip. For VEGF-C / VEGF-R2 binding experiments, 100 µl of 100 nM VEGF-R2-Fc recombinant protein (R&D Systems), resulting in a response of about 1'200 RU, were immobilized on the anti-Fc coated CM5 chip.

5.21. VEGF-C neutralization assay using competitive ELISA

A maxisorp plate was coated in quadruplicate with 100 µl of 2 µg/ml monoclonal mouse anti-human IgG (Chemicon, Temescula, CA) in PBS overnight at room temperature. The next morning, the plate was washed 3 times with PBS and blocked for 2 hours at room temperature with 200 µl blocking buffer (3% BSA (Probumin; Millipore) in PBS). The plate was then washed again 3 times with PBS and incubated with 100 µl 1 µg/ml VEGF-R2-Fc or VEGF-R3-Fc in blocking buffer for 2 hours at room temperature. After washing with 3 times PBS, 100 µl of a mixture of 2 nM biotinylated *P.pastoris*-derived ΔNΔC-VEGF-C, preincubated for 30 min with a variable concentration of VC2.2.2 anti-VEGF-C scFv or irrelevant scFv in blocking buffer, were added to the ELISA plate for 1 hour at room temperature. Subsequently, the ELISA plate was washed for 2 times with PBST and once with PBS. A mixture of streptavidin-horseradish peroxidase conjugate diluted 1:1'000 in blocking buffer was added and incubated for 1 hour at room temperature. Finally, the plate was washed again 3 times with PBST and 3 times with PBS and developed as detailed above.

6. Curriculum Vitae

Curriculum Vitae

Matthias Rinderknecht
Elisabethenstrasse 24a, 3014 Bern, Switzerland, +41 79 324 44 11
matthiasrinderknecht@gmx.ch

Personal Information

Date of Birth:	23 March 1979
Nationality:	Swiss
Marital Status:	Single

Education

10/2005 – 05/2010 **PhD studies in the group of Prof. Michael Detmar**
„Phage-derived human monoclonal antibody fragments to vascular endothelial growth factor-C that block its interaction with both VEGF receptor-2 and -3"
Institute of Pharmaceutical Sciences, ETH Zurich, Switzerland

10/2005 – 05/2010 **Member of the PhD program in Molecular Life Sciences (MLS)**
University and ETH Zurich, Switzerland

11/2004 **Diploma in Integrative Biology**
ETH Zurich, Switzerland

10/2001 – 06/2002 **ERASMUS Exchange Year**
Attended various practica and courses in medical biology
University of Groningen, The Netherlands

10/1999 – 11/2004 **Undergraduate Studies in Medical Biology and Biotechnology**
ETH Zurich, Switzerland

06/1999 **High school graduation** (Matura Typus C, mathematics & natural sciences)
Kantonsschule Baden, Switzerland

Professional Experience

10/2005 – 05/2010 **Research assistant in the group of Prof. Michael Detmar**
- Applied research in the area of antibody fragment development and characterization
- Supervision of a pharmaceutical science student during her six-month master thesis project
- Teaching of master students during the yearly practicum
- Co-organization of our institute's PhD-symposium
- Peer-review of manuscripts for „Blood"

Institute of Pharmaceutical Sciences, ETH Zurich, Switzerland

11/2004 – 05/2005 **Trainee in Clinical Research**
- Administration of clinical trials
- Evaluation and testing of a patient database
GlaxoSmithKline, Munich, Germany

07/2003 – 01/2004 **Diploma thesis in the group of Prof. Martin Fussenegger**
„Novel Approaches in Biopharmaceutical Manufacturing and Cell and Gene Therapy“
Institute of Biotechnology, ETH Zurich, Switzerland

Additional Education

10/2005 – 03/2006 **Accounting for Managers,** weekly course focused on basic accounting principles
ETH Zurich, Switzerland

10/2006 – 03/2007 **Patent Law and Licensing,** weekly course focused on Swiss and European patent law and different aspects of intellectual property management
ETH Zurich, Switzerland

Scientific Presentations & Posters

09/2009 **„Phage-derived neutralizing monoclonal antibody fragments against VEGF-C“,** poster presentation
7th International Symposium on the Biology of Endothelial Cells, Vienna, Austria

02/2008 **„Fully human monoclonal antibody fragments against VEGF-C”,** oral presentation
4th meeting of the EC FP6 consortium “Anti-tumor targeting”, Zurich, Switzerland

02/2008 **„Phage-derived monoclonal antibodies against VEGF-C and (lymphatic) endothelial cells“,** oral presentation
PhD symposium, Institute of Pharmaceutical Sciences, ETH Zurich, Switzerland

10/2007 **„(Lymphatic) vasculature-specific phage antibodies selected by panning on whole cells”,** poster presentation
ESH meeting “Vascular Targeted Therapies in Oncology”, Mandelieu, France

12/2006 **„Cell-selected (lymphatic) vasculature-specific phage antibodies“** oral presentation
2nd meeting of the EC FP6 consortium “Anti-tumor targeting”, Heidelberg, Germany

10/2006 **„Phage lymphangiomics”,** poster presentation
Annual retreat of the Zurich PhD Program in Molecular Life Sciences (MLS), Chandolin, Switzerland

02/2006 **„Antibody phage-display and the lymphatic endothelium",** oral presentation
1st meeting of the EC FP6 consortium "Anti-tumor targeting", Vienna, Austria

Publications

Rinderknecht M, Villa A, Ballmer-Hofer K, Neri D, and Detmar M: *Phage-derived fully human monoclonal antibody fragments to vascular endothelial growth factor-C block its interaction with VEGF receptor-2 and 3.* PLoS ONE, Vol. 5, No. 8. (2 August 2010), e11941

Proulx S, Luciani P, Derzsi S, **Rinderknecht M**, Mumprecht V, Leroux JC and Detmar M: *Quantitative Imaging of Lymphatic Function with Liposomal Indocyanine Green.* Cancer Res, 2010 Sep 15;70(18):7053-62

Rinderknecht M, Detmar M: *Molecular Mechanisms of lymph node metastasis.* In: Stacker S, Achen M (Eds**).** Lymphangiogenesis in cancer metastasis. Springer, 2009

Rinderknecht M, Detmar M: *Tumor lymphangiogenesis and melanoma metastasis.* J Cell Physiol, 2008, 216:347-354

Weber W, **Rinderknecht M**, Daoud-El Baba M, de Glutz FN, Aubel D and Fussenegger M: *CellMAC – A Novel Technology for Encapsulation of Mammalian Cells in Cellulose Sulfate / pDADMAC Capsules Assembled on a Transient Alginate / Ca^{2+} Scaffold.* J Biotechnol, 2004 Nov 9;114(3):315-26

Weber W, Malphettes L, **Rinderknecht M**, Schoenmakers RG, Spielmann M, Keller B, van de Wetering P, Weber CC and Fussenegger M: *Quorum-Sensing-based Toolbox for Regulatable Transgene and siRNA Expression in Mammalian Cells.* Biotechnol Prog, 2005, 21(1):178-185

7. Acknowledgements

Acknowledgements

I would like to thank Prof. Michael Detmar for giving me the opportunity to work independently on a project that could have direct therapeutic application – this has always motivated me. I have much respect for the patience and optimism he always showed.

I would also like to thank Prof. Dario Neri for being my co-referee and thesis committee member and especially for his extremely valuable guidance and support in questions of antibody phage-display.

I am grateful to Dr. Silvio Hemmi for agreeing to be the third member of my Molecular Life Sciences PhD program thesis committee and his useful comments at the thesis committee meetings.

Also, I would like to thank Prof. Ballmer-Hofer, who was always very willing to share biological materials.

Many thanks go to the people in Prof. Neri's group, especially Dr. Julia Ahlskog, who introduced me to antibody phage display, Dr. Alessandra Villa, who was always very helpful regarding cloning questions and interpretation of BIAcore data as well as Dr. Sarah Wulhfard, Dr. Jörg Scheuermann, Kathrin Zuberbühler and Alessandro Palumbo for support in BIAcore and FPLC and for sharing IgG vectors, cell lines and transfection protocols. Also, Dr. Christoph Rösli has always been very helpful regarding mass-spectroscopy analysis.

All former and present members of the Detmar lab deserve a big thank you as well; they have made my time in the lab an unforgettable experience. My benchmate Viviane deserves to be mentioned especially, I always enjoyed her light heartedness towards life and her sincere dedication to science. Daniela and Martin have performed important experiments for me, I am very grateful to them.

It was a pleasure to work with my master student Yeliz Aydin, who challenged me with interesting questions and quickly learned the wonders of phage display.

Finally, I would to express deep gratitude to my partner Shizuka, my brother and my parents, who always loved and supported me and cheered me up in hard times.

8. References

References

Achen, M. G., M. Jeltsch, E. Kukk, T. Makinen, A. Vitali, A. F. Wilks, K. Alitalo and S. A. Stacker (1998). "Vascular endothelial growth factor D (VEGF-D) is a ligand for the tyrosine kinases VEGF receptor 2 (Flk1) and VEGF receptor 3 (Flt4)." Proc Natl Acad Sci U S A **95**: 548-53.

Achen, M. G., S. Roufail*, et al.* (2000). "Monoclonal antibodies to vascular endothelial growth factor-D block its interactions with both VEGF receptor-2 and VEGF receptor-3." Eur J Biochem **267**: 2505-15.

Albuquerque, R. J., T. Hayashi*, et al.* (2009). "Alternatively spliced vascular endothelial growth factor receptor-2 is an essential endogenous inhibitor of lymphatic vessel growth." Nat Med **15**: 1023-30.

Alitalo, K., T. Tammela and T. V. Petrova (2005). "Lymphangiogenesis in development and human disease." Nature **438**: 946-53.

Ambati, B. K., M. Nozaki*, et al.* (2006). "Corneal avascularity is due to soluble VEGF receptor-1." Nature **443**: 993-7.

Amioka, T., Y. Kitadai, S. Tanaka, K. Haruma, M. Yoshihara, W. Yasui and K. Chayama (2002). "Vascular endothelial growth factor-C expression predicts lymph node metastasis of human gastric carcinomas invading the submucosa." Eur J Cancer **38**: 1413-9.

Arinaga, M., T. Noguchi, S. Takeno, M. Chujo, T. Miura and Y. Uchida (2003). "Clinical significance of vascular endothelial growth factor C and vascular endothelial growth factor receptor 3 in patients with nonsmall cell lung carcinoma." Cancer **97**: 457-64.

Aselli, G. (1627). "De Lactibus Sive Lacteis Venis." Dissertatio Mediolan.

Baert, F., M. Noman, S. Vermeire, G. Van Assche, D. H. G, A. Carbonez and P. Rutgeerts (2003). "Influence of immunogenicity on the long-term efficacy of infliximab in Crohn's disease." N Engl J Med **348**: 601-8.

Baldwin, M. E., B. Catimel*, et al.* (2001). "The specificity of receptor binding by vascular endothelial growth factor-d is different in mouse and man." J Biol Chem **276**: 19166-71.

Baldwin, M. E., M. M. Halford, S. Roufail, R. A. Williams, M. L. Hibbs, D. Grail, H. Kubo, S. A. Stacker and M. G. Achen (2005). "Vascular endothelial growth factor D is dispensable for development of the lymphatic system." Mol Cell Biol **25**: 2441-9.

Baluk, P., T. Tammela*, et al.* (2005). "Pathogenesis of persistent lymphatic vessel hyperplasia in chronic airway inflammation." J Clin Invest **115**: 247-57.

Bando, H., H. A. Weich, S. Horiguchi, N. Funata, T. Ogawa and M. Toi (2006). "The association between vascular endothelial growth factor-C, its corresponding receptor, VEGFR-3, and prognosis in primary breast cancer: a study with 193 cases." Oncol Rep **15**: 653-9.

Bartelds, G. M., C. A. Wijbrandts, M. T. Nurmohamed, S. Stapel, W. F. Lems, L. Aarden, B. A. Dijkmans, P. P. Tak and G. J. Wolbink (2007). "Clinical response to adalimumab: relationship to anti-adalimumab antibodies and serum adalimumab concentrations in rheumatoid arthritis." Ann Rheum Dis **66**: 921-6.

Bartelds, G. M., C. A. Wijbrandts, M. T. Nurmohamed, S. Stapel, W. F. Lems, L. Aarden, B. A. Dijkmans, P. P. Tak and G. J. Wolbink (2010). "Anti-infliximab and anti-adalimumab antibodies in relation to response to adalimumab in

infliximab switchers and anti-tumour necrosis factor naive patients: a cohort study." Ann Rheum Dis.
Barthelemy, P. A., H. Raab, B. A. Appleton, C. J. Bond, P. Wu, C. Wiesmann and S. S. Sidhu (2008). "Comprehensive analysis of the factors contributing to the stability and solubility of autonomous human VH domains." J Biol Chem **283**: 3639-54.
Behring, E. K., S. (1890). "Ueber das Zustandekommen der Diphterie-Immunität und der Tetanus-Immunität bei Thieren." Dtsch. med. Wochenschr. **16**: 1113.
Betsholtz, C., A. Johnsson*, et al.* (1986). "cDNA sequence and chromosomal localization of human platelet-derived growth factor A-chain and its expression in tumour cell lines." Nature **320**: 695-9.
Bjorndahl, M., R. Cao*, et al.* (2005). "Insulin-like growth factors 1 and 2 induce lymphangiogenesis in vivo." Proc Natl Acad Sci U S A **102**: 15593-8.
Brack, S. S., M. Silacci, M. Birchler and D. Neri (2006). "Tumor-targeting properties of novel antibodies specific to the large isoform of tenascin-C." Clin Cancer Res **12**: 3200-8.
Bunone, G., P. Vigneri, L. Mariani, S. Buto, P. Collini, S. Pilotti, M. A. Pierotti and I. Bongarzone (1999). "Expression of angiogenesis stimulators and inhibitors in human thyroid tumors and correlation with clinical pathological features." Am J Pathol **155**: 1967-76.
Burton, J. B., S. J. Priceman, J. L. Sung, E. Brakenhielm, D. S. An, B. Pytowski, K. Alitalo and L. Wu (2008). "Suppression of prostate cancer nodal and systemic metastasis by blockade of the lymphangiogenic axis." Cancer Res **68**: 7828-37.
Byeon, J. S., H. Y. Jung*, et al.* (2004). "Clinicopathological significance of vascular endothelial growth factor-C and cyclooxygenase-2 in esophageal squamous cell carcinoma." J Gastroenterol Hepatol **19**: 648-54.
Cai, X. and A. Garen (1996). "A melanoma-specific VH antibody cloned from a fusion phage library of a vaccinated melanoma patient." Proc Natl Acad Sci U S A **93**: 6280-5.
Cao, R., M. A. Bjorndahl, M. I. Gallego, S. Chen, P. Religa, A. J. Hansen and Y. Cao (2006). "Hepatocyte growth factor is a lymphangiogenic factor with an indirect mechanism of action." Blood **107**: 3531-6.
Cao, R., M. A. Bjorndahl*, et al.* (2004). "PDGF-BB induces intratumoral lymphangiogenesis and promotes lymphatic metastasis." Cancer Cell **6**: 333-45.
Cao, Y., P. Linden, J. Farnebo, R. Cao, A. Eriksson, V. Kumar, J. H. Qi, L. Claesson-Welsh and K. Alitalo (1998). "Vascular endothelial growth factor C induces angiogenesis in vivo." Proc Natl Acad Sci U S A **95**: 14389-94.
Casanovas, O., D. J. Hicklin, G. Bergers and D. Hanahan (2005). "Drug resistance by evasion of antiangiogenic targeting of VEGF signaling in late-stage pancreatic islet tumors." Cancer Cell **8**: 299-309.
Chang, L. K., G. Garcia-Cardena*, et al.* (2004). "Dose-dependent response of FGF-2 for lymphangiogenesis." Proc Natl Acad Sci U S A **101**: 11658-63.
Chen, L., P. Hamrah, C. Cursiefen, Q. Zhang, B. Pytowski, J. W. Streilein and M. R. Dana (2004). "Vascular endothelial growth factor receptor-3 mediates induction of corneal alloimmunity." Nat Med **10**: 813-5.
Chothia, C., A. M. Lesk*, et al.* (1989). "Conformations of immunoglobulin hypervariable regions." Nature **342**: 877-83.

Chung, E. S., S. K. Chauhan, Y. Jin, S. Nakao, A. Hafezi-Moghadam, N. van Rooijen, Q. Zhang, L. Chen and R. Dana (2009). "Contribution of macrophages to angiogenesis induced by vascular endothelial growth factor receptor-3-specific ligands." Am J Pathol **175**: 1984-92.

Ciulla, T. A. and P. J. Rosenfeld (2009). "Antivascular endothelial growth factor therapy for neovascular age-related macular degeneration." Curr Opin Ophthalmol **20**: 158-65.

Cohen, M. H., Y. L. Shen, P. Keegan and R. Pazdur (2009). "FDA drug approval summary: bevacizumab (Avastin) as treatment of recurrent glioblastoma multiforme." Oncologist **14**: 1131-8.

Conrath, K., C. Vincke, B. Stijlemans, J. Schymkowitz, K. Decanniere, L. Wyns, S. Muyldermans and R. Loris (2005). "Antigen binding and solubility effects upon the veneering of a camel VHH in framework-2 to mimic a VH." J Mol Biol **350**: 112-25.

Conrath, K. E., M. Lauwereys, M. Galleni, A. Matagne, J. M. Frere, J. Kinne, L. Wyns and S. Muyldermans (2001). "Beta-lactamase inhibitors derived from single-domain antibody fragments elicited in the camelidae." Antimicrob Agents Chemother **45**: 2807-12.

Cueni, L. N. and M. Detmar (2006). "New insights into the molecular control of the lymphatic vascular system and its role in disease." J Invest Dermatol **126**: 2167-2177.

Currie, M. J., V. Hanrahan, S. P. Gunningham, H. R. Morrin, C. Frampton, C. Han, B. A. Robinson and S. B. Fox (2004). "Expression of vascular endothelial growth factor D is associated with hypoxia inducible factor (HIF-1alpha) and the HIF-1alpha target gene DEC1, but not lymph node metastasis in primary human breast carcinomas." J Clin Pathol **57**: 829-34.

Cursiefen, C., L. Chen*, et al.* (2004). "VEGF-A stimulates lymphangiogenesis and hemangiogenesis in inflammatory neovascularization via macrophage recruitment." J Clin Invest **113**: 1040-50.

Da, M. X., X. T. Wu, J. Wang, T. K. Guo, Z. G. Zhao, T. Luo, M. M. Zhang and K. Qian (2008). "Expression of cyclooxygenase-2 and vascular endothelial growth factor-C correlates with lymphangiogenesis and lymphatic invasion in human gastric cancer." Arch Med Res **39**: 92-9.

Dadras, S. S., B. Lange-Asschenfeldt*, et al.* (2005). "Tumor lymphangiogenesis predicts melanoma metastasis to sentinel lymph nodes." Mod Pathol **18**: 1232-42.

Dadras, S. S., T. Paul*, et al.* (2003). "Tumor lymphangiogenesis: a novel prognostic indicator for cutaneous melanoma metastasis and survival." Am J Pathol **162**: 1951-60.

Davies, J. and L. Riechmann (1996). "Single antibody domains as small recognition units: design and in vitro antigen selection of camelized, human VH domains with improved protein stability." Protein Eng **9**: 531-7.

Davis, S., T. H. Aldrich*, et al.* (1996). "Isolation of angiopoietin-1, a ligand for the Tie2 receptor, by secretion-trap expression cloning." Cell **87**: 1161-9.

Dias, S., M. Choy, K. Alitalo and S. Rafii (2002). "Vascular endothelial growth factor (VEGF)-C signaling through FLT-4 (VEGFR-3) mediates leukemic cell proliferation, survival, and resistance to chemotherapy." Blood **99**: 2179-84.

Dixelius, J., T. Makinen, M. Wirzenius, M. J. Karkkainen, C. Wernstedt, K. Alitalo and L. Claesson-Welsh (2003). "Ligand-induced vascular endothelial growth factor receptor-3 (VEGFR-3) heterodimerization with VEGFR-2 in primary lymphatic

endothelial cells regulates tyrosine phosphorylation sites." J Biol Chem **278**: 40973-9.
Dougher, M. and B. I. Terman (1999). "Autophosphorylation of KDR in the kinase domain is required for maximal VEGF-stimulated kinase activity and receptor internalization." Oncogene **18**: 1619-27.
Dumont, D. J., L. Jussila, J. Taipale, A. Lymboussaki, T. Mustonen, K. Pajusola, M. Breitman and K. Alitalo (1998). "Cardiovascular failure in mouse embryos deficient in VEGF receptor-3." Science **282**: 946-9.
Dumoulin, M., K. Conrath, A. Van Meirhaeghe, F. Meersman, K. Heremans, L. G. Frenken, S. Muyldermans, L. Wyns and A. Matagne (2002). "Single-domain antibody fragments with high conformational stability." Protein Sci **11**: 500-15.
Edelman, G. M., B. A. Cunningham, W. E. Gall, P. D. Gottlieb, U. Rutishauser and M. J. Waxdal (1969). "The covalent structure of an entire gammaG immunoglobulin molecule." Proc Natl Acad Sci U S A **63**: 78-85.
Ehrlich, P. (1891). "Experimentelle Untersuchungen über Immunität. II. Ueber Abrin." Dtsch. med. Wochenschr. **17**: 1281.
Ellis, L. M. and D. J. Hicklin (2008). "VEGF-targeted therapy: mechanisms of anti-tumour activity." Nat Rev Cancer **8**: 579-91.
Favier, B., A. Alam*, et al.* (2006). "Neuropilin-2 interacts with VEGFR-2 and VEGFR-3 and promotes human endothelial cell survival and migration." Blood **108**: 1243-50.
Fischer, C., B. Jonckx*, et al.* (2007). "Anti-PlGF inhibits growth of VEGF(R)-inhibitor-resistant tumors without affecting healthy vessels." Cell **131**: 463-75.
Folkman, J. (1971). "Tumor angiogenesis: therapeutic implications." N Engl J Med **285**: 1182-6.
Forsythe, J. A., B. H. Jiang, N. V. Iyer, F. Agani, S. W. Leung, R. D. Koos and G. L. Semenza (1996). "Activation of vascular endothelial growth factor gene transcription by hypoxia-inducible factor 1." Mol Cell Biol **16**: 4604-13.
Fournier, E., P. Dubreuil, D. Birnbaum and J. P. Borg (1995). "Mutation at tyrosine residue 1337 abrogates ligand-dependent transforming capacity of the FLT4 receptor." Oncogene **11**: 921-31.
Fritz-Six, K. L., W. P. Dunworth, M. Li and K. M. Caron (2008). "Adrenomedullin signaling is necessary for murine lymphatic vascular development." J Clin Invest **118**: 40-50.
Fujio, Y. and K. Walsh (1999). "Akt mediates cytoprotection of endothelial cells by vascular endothelial growth factor in an anchorage-dependent manner." J Biol Chem **274**: 16349-54.
Fukunaga, S., K. Maeda, E. Noda, T. Inoue, K. Wada and K. Hirakawa (2006). "Association between expression of vascular endothelial growth factor C, chemokine receptor CXCR4 and lymph node metastasis in colorectal cancer." Oncology **71**: 204-11.
Funaki, H., G. Nishimura*, et al.* (2003). "Expression of vascular endothelial growth factor D is associated with lymph node metastasis in human colorectal carcinoma." Oncology **64**: 416-22.
Furudoi, A., S. Tanaka, K. Haruma, Y. Kitadai, M. Yoshihara, K. Chayama and F. Shimamoto (2002). "Clinical significance of vascular endothelial growth factor C expression and angiogenesis at the deepest invasive site of advanced colorectal carcinoma." Oncology **62**: 157-66.

Gale, N. W., G. Thurston*, et al.* (2002). "Angiopoietin-2 is required for postnatal angiogenesis and lymphatic patterning, and only the latter role is rescued by Angiopoietin-1." Dev Cell **3**: 411-23.

George, M. L., M. G. Tutton, F. Janssen, A. Arnaout, A. M. Abulafi, S. A. Eccles and R. I. Swift (2001). "VEGF-A, VEGF-C, and VEGF-D in colorectal cancer progression." Neoplasia **3**: 420-7.

Gerli, R., R. Solito, E. Weber and M. Agliano (2000). "Specific adhesion molecules bind anchoring filaments and endothelial cells in human skin initial lymphatics." Lymphology **33**: 148-57.

Gombos, Z., X. Xu, C. S. Chu, P. J. Zhang and G. Acs (2005). "Peritumoral lymphatic vessel density and vascular endothelial growth factor C expression in early-stage squamous cell carcinoma of the uterine cervix." Clin Cancer Res **11**: 8364-71.

Grau, S. J., F. Trillsch, J. Herms, N. Thon, P. J. Nelson, J. C. Tonn and R. Goldbrunner (2007). "Expression of VEGFR3 in glioma endothelium correlates with tumor grade." J Neurooncol **82**: 141-50.

Green, L. L. (1999). "Antibody engineering via genetic engineering of the mouse: XenoMouse strains are a vehicle for the facile generation of therapeutic human monoclonal antibodies." J Immunol Methods **231**: 11-23.

Gribben, J. G., S. Devereux, N. S. Thomas, M. Keim, H. M. Jones, A. H. Goldstone and D. C. Linch (1990). "Development of antibodies to unprotected glycosylation sites on recombinant human GM-CSF." Lancet **335**: 434-7.

Gunningham, S. P., M. J. Currie, C. Han, B. A. Robinson, P. A. Scott, A. L. Harris and S. B. Fox (2000). "The short form of the alternatively spliced flt-4 but not its ligand vascular endothelial growth factor C is related to lymph node metastasis in human breast cancers." Clin Cancer Res **6**: 4278-86.

Hamers-Casterman, C., T. Atarhouch, S. Muyldermans, G. Robinson, C. Hamers, E. B. Songa, N. Bendahman and R. Hamers (1993). "Naturally occurring antibodies devoid of light chains." Nature **363**: 446-8.

Hanauer, S. B., B. G. Feagan*, et al.* (2002). "Maintenance infliximab for Crohn's disease: the ACCENT I randomised trial." Lancet **359**: 1541-9.

Hanrahan, V., M. J. Currie, S. P. Gunningham, H. R. Morrin, P. A. Scott, B. A. Robinson and S. B. Fox (2003). "The angiogenic switch for vascular endothelial growth factor (VEGF)-A, VEGF-B, VEGF-C, and VEGF-D in the adenoma-carcinoma sequence during colorectal cancer progression." J Pathol **200**: 183-94.

Harmsen, M. M., C. B. Van Solt, H. P. Fijten and M. C. Van Setten (2005). "Prolonged in vivo residence times of llama single-domain antibody fragments in pigs by binding to porcine immunoglobulins." Vaccine **23**: 4926-34.

Harmsen, M. M., C. B. van Solt, A. M. van Zijderveld-van Bemmel, T. A. Niewold and F. G. van Zijderveld (2006). "Selection and optimization of proteolytically stable llama single-domain antibody fragments for oral immunotherapy." Appl Microbiol Biotechnol **72**: 544-51.

Harrell, M. I., B. M. Iritani and A. Ruddell (2007). "Tumor-induced sentinel lymph node lymphangiogenesis and increased lymph flow precede melanoma metastasis." Am J Pathol **170**: 774-86.

He, Y., K. Kozaki, T. Karpanen, K. Koshikawa, S. Yla-Herttuala, T. Takahashi and K. Alitalo (2002). "Suppression of tumor lymphangiogenesis and lymph node metastasis by blocking vascular endothelial growth factor receptor 3 signaling." J Natl Cancer Inst **94**: 819-25.

Heidelberger, M. and F. E. Kendall (1929). "A Quantitative Study of the Precipitin Reaction between Type Iii Pneumococcus Polysaccharide and Purified Homologous Antibody." J Exp Med **50**: 809-823.

Hendershot, L. M. (1990). "Immunoglobulin heavy chain and binding protein complexes are dissociated in vivo by light chain addition." J Cell Biol **111**: 829-37.

Hillson, J. L., N. S. Karr, I. R. Oppliger, M. Mannik and E. H. Sasso (1993). "The structural basis of germline-encoded VH3 immunoglobulin binding to staphylococcal protein A." J Exp Med **178**: 331-6.

Hinojar-Gutierrez, A., M. E. Fernandez-Contreras, R. Gonzalez-Gonzalez, M. J. Fernandez-Luque, A. Hinojar-Arzadun, M. Quintanilla and C. Gamallo (2007). "Intratumoral lymphatic vessels and VEGF-C expression are predictive factors of lymph node relapse in T1-T4 N0 laryngopharyngeal squamous cell carcinoma." Ann Surg Oncol **14**: 248-57.

Hirai, M., A. Nakagawara, T. Oosaki, Y. Hayashi, M. Hirono and T. Yoshihara (2001). "Expression of vascular endothelial growth factors (VEGF-A/VEGF-1 and VEGF-C/VEGF-2) in postmenopausal uterine endometrial carcinoma." Gynecol Oncol **80**: 181-8.

Hirakawa, S., L. F. Brown, S. Kodama, K. Paavonen, K. Alitalo and M. Detmar (2007). "VEGF-C-induced lymphangiogenesis in sentinel lymph nodes promotes tumor metastasis to distant sites." Blood **109**: 1010-7.

Hirakawa, S., Y. K. Hong, N. Harvey, V. Schacht, K. Matsuda, T. Libermann and M. Detmar (2003). "Identification of vascular lineage-specific genes by transcriptional profiling of isolated blood vascular and lymphatic endothelial cells." Am J Pathol **162**: 575-86.

Hirakawa, S., S. Kodama, R. Kunstfeld, K. Kajiya, L. F. Brown and M. Detmar (2005). "VEGF-A induces tumor and sentinel lymph node lymphangiogenesis and promotes lymphatic metastasis." J Exp Med **201**: 1089-99.

Hoar, F. J., S. Chaudhri, M. S. Wadley and P. S. Stonelake (2003). "Co-expression of vascular endothelial growth factor C (VEGF-C) and c-erbB2 in human breast carcinoma." Eur J Cancer **39**: 1698-703.

Holliger, P., T. Prospero and G. Winter (1993). ""Diabodies": small bivalent and bispecific antibody fragments." Proc Natl Acad Sci U S A **90**: 6444-8.

Hong, Y. K., B. Lange-Asschenfeldt, P. Velasco, S. Hirakawa, R. Kunstfeld, L. F. Brown, P. Bohlen, D. R. Senger and M. Detmar (2004). "VEGF-A promotes tissue repair-associated lymphatic vessel formation via VEGFR-2 and the alpha1beta1 and alpha2beta1 integrins." Faseb J **18**: 1111-3.

Hoogenboom, H. R. (2005). "Selecting and screening recombinant antibody libraries." Nat Biotechnol **23**: 1105-16.

Horne, C., M. Klein, I. Polidoulis and K. J. Dorrington (1982). "Noncovalent association of heavy and light chains of human immunoglobulins. III. Specific interactions between VH and VL." J Immunol **129**: 660-4.

Huang, H. Y., C. C. Ho, P. H. Huang and S. M. Hsu (2001). "Co-expression of VEGF-C and its receptors, VEGFR-2 and VEGFR-3, in endothelial cells of lymphangioma. Implication in autocrine or paracrine regulation of lymphangioma." Lab Invest **81**: 1729-34.

Hurwitz, H., L. Fehrenbacher*, et al.* (2004). "Bevacizumab plus irinotecan, fluorouracil, and leucovorin for metastatic colorectal cancer." N Engl J Med **350**: 2335-42.

Huston, J. S., D. Levinson*, et al.* (1988). "Protein engineering of antibody binding sites: recovery of specific activity in an anti-digoxin single-chain Fv analogue produced in Escherichia coli." Proc Natl Acad Sci U S A **85**: 5879-83.

Iannello, A. and A. Ahmad (2005). "Role of antibody-dependent cell-mediated cytotoxicity in the efficacy of therapeutic anti-cancer monoclonal antibodies." Cancer Metastasis Rev **24**: 487-99.

Ikeda, Y., Y. Yonemitsu*, et al.* (2006). "The regulation of vascular endothelial growth factors (VEGF-A, -C, and -D) expression in the retinal pigment epithelium." Exp Eye Res **83**: 1031-40.

Ishikawa, M., J. Kitayama, S. Kazama and H. Nagawa (2003). "Expression of vascular endothelial growth factor C and D (VEGF-C and -D) is an important risk factor for lymphatic metastasis in undifferentiated early gastric carcinoma." Jpn J Clin Oncol **33**: 21-7.

Jain, R. K. (2005). "Normalization of tumor vasculature: an emerging concept in antiangiogenic therapy." Science **307**: 58-62.

Jeltsch, M., A. Kaipainen*, et al.* (1997). "Hyperplasia of lymphatic vessels in VEGF-C transgenic mice." Science **276**: 1423-5.

Jeltsch, M., T. Karpanen, T. Strandin, K. Aho, H. Lankinen and K. Alitalo (2006). "Vascular endothelial growth factor (VEGF)/VEGF-C mosaic molecules reveal specificity determinants and feature novel receptor binding patterns." J Biol Chem **281**: 12187-95.

Jennbacken, K., C. Vallbo, W. Wang and J. E. Damber (2005). "Expression of vascular endothelial growth factor C (VEGF-C) and VEGF receptor-3 in human prostate cancer is associated with regional lymph node metastasis." Prostate **65**: 110-6.

Jia, Y. T., Z. X. Li, Y. T. He, W. Liang, H. C. Yang and H. J. Ma (2004). "Expression of vascular endothelial growth factor-C and the relationship between lymphangiogenesis and lymphatic metastasis in colorectal cancer." World J Gastroenterol **10**: 3261-3.

Joukov, V., V. Kumar, T. Sorsa, E. Arighi, H. Weich, O. Saksela and K. Alitalo (1998). "A recombinant mutant vascular endothelial growth factor-C that has lost vascular endothelial growth factor receptor-2 binding, activation, and vascular permeability activities." J Biol Chem **273**: 6599-602.

Joukov, V., K. Pajusola, A. Kaipainen, D. Chilov, I. Lahtinen, E. Kukk, O. Saksela, N. Kalkkinen and K. Alitalo (1996). "A novel vascular endothelial growth factor, VEGF-C, is a ligand for the Flt4 (VEGFR-3) and KDR (VEGFR-2) receptor tyrosine kinases." Embo J **15**: 1751.

Joukov, V., T. Sorsa, V. Kumar, M. Jeltsch, L. Claesson-Welsh, Y. Cao, O. Saksela, N. Kalkkinen and K. Alitalo (1997). "Proteolytic processing regulates receptor specificity and activity of VEGF-C." Embo J **16**: 3898-911.

Juttner, S., C. Wissmann, T. Jons, M. Vieth, J. Hertel, S. Gretschel, P. M. Schlag, W. Kemmner and M. Hocker (2006). "Vascular endothelial growth factor-D and its receptor VEGFR-3: two novel independent prognostic markers in gastric adenocarcinoma." J Clin Oncol **24**: 228-40.

Kabashima, A., Y. Maehara, Y. Kakeji and K. Sugimachi (2001). "Overexpression of vascular endothelial growth factor C is related to lymphogenous metastasis in early gastric carcinoma." Oncology **60**: 146-50.

Kaipainen, A., J. Korhonen, T. Mustonen, V. W. van Hinsbergh, G. H. Fang, D. Dumont, M. Breitman and K. Alitalo (1995). "Expression of the fms-like

tyrosine kinase 4 gene becomes restricted to lymphatic endothelium during development." Proc Natl Acad Sci U S A **92**: 3566-70.
Kajiya, K., S. Hirakawa, B. Ma, I. Drinnenberg and M. Detmar (2005). "Hepatocyte growth factor promotes lymphatic vessel formation and function." Embo J **24**: 2885-95.
Karkkainen, M. J., R. E. Ferrell, E. C. Lawrence, M. A. Kimak, K. L. Levinson, M. A. McTigue, K. Alitalo and D. N. Finegold (2000). "Missense mutations interfere with VEGFR-3 signalling in primary lymphoedema." Nat Genet **25**: 153-9.
Karkkainen, M. J., P. Haiko*, et al.* (2004). "Vascular endothelial growth factor C is required for sprouting of the first lymphatic vessels from embryonic veins." Nat Immunol **5**: 74-80.
Karkkainen, M. J., A. Saaristo*, et al.* (2001). "A model for gene therapy of human hereditary lymphedema." Proc Natl Acad Sci U S A **98**: 12677-82.
Karpanen, T., M. Egeblad, M. J. Karkkainen, H. Kubo, S. Yla-Herttuala, M. Jaattela and K. Alitalo (2001). "Vascular endothelial growth factor C promotes tumor lymphangiogenesis and intralymphatic tumor growth." Cancer Res **61**: 1786-90.
Karpanen, T., C. A. Heckman, S. Keskitalo, M. Jeltsch, H. Ollila, G. Neufeld, L. Tamagnone and K. Alitalo (2006). "Functional interaction of VEGF-C and VEGF-D with neuropilin receptors." Faseb J **20**: 1462-72.
Karpusas, M., A. Whitty, L. Runkel and P. Hochman (1998). "The structure of human interferon-beta: implications for activity." Cell Mol Life Sci **54**: 1203-16.
Kaushal, V., P. Mukunyadzi, R. A. Dennis, E. R. Siegel, D. E. Johnson and M. Kohli (2005). "Stage-specific characterization of the vascular endothelial growth factor axis in prostate cancer: expression of lymphangiogenic markers is associated with advanced-stage disease." Clin Cancer Res **11**: 584-93.
Kawakami, M., T. Furuhata, Y. Kimura, K. Yamaguchi, F. Hata, K. Sasaki and K. Hirata (2003). "Quantification of vascular endothelial growth factor-C and its receptor-3 messenger RNA with real-time quantitative polymerase chain reaction as a predictor of lymph node metastasis in human colorectal cancer." Surgery **133**: 300-8.
Kerjaschki, D., H. M. Regele*, et al.* (2004). "Lymphatic neoangiogenesis in human kidney transplants is associated with immunologically active lymphocytic infiltrates." J Am Soc Nephrol **15**: 603-12.
Kim, K. J., B. Li, K. Houck, J. Winer and N. Ferrara (1992). "The vascular endothelial growth factor proteins: identification of biologically relevant regions by neutralizing monoclonal antibodies." Growth Factors **7**: 53-64.
Kinoshita, J., K. Kitamura, A. Kabashima, H. Saeki, S. Tanaka and K. Sugimachi (2001). "Clinical significance of vascular endothelial growth factor-C (VEGF-C) in breast cancer." Breast Cancer Res Treat **66**: 159-64.
Kishimoto, K., A. Sasaki, Y. Yoshihama, H. Mese, G. Tsukamoto and T. Matsumura (2003). "Expression of vascular endothelial growth factor-C predicts regional lymph node metastasis in early oral squamous cell carcinoma." Oral Oncol **39**: 391-6.
Kitadai, Y., T. Amioka, K. Haruma, S. Tanaka, M. Yoshihara, K. Sumii, N. Matsutani, W. Yasui and K. Chayama (2001). "Clinicopathological significance of vascular endothelial growth factor (VEGF)-C in human esophageal squamous cell carcinomas." Int J Cancer **93**: 662-6.

Kitadai, Y., M. Kodama*, et al.* (2005). "Quantitative analysis of lymphangiogenic markers for predicting metastasis of human gastric carcinoma to lymph nodes." Int J Cancer **115**: 388-92.

Koch, M., D. Dettori*, et al.* (2009). "VEGF-D deficiency in mice does not affect embryonic or postnatal lymphangiogenesis but reduces lymphatic metastasis." J Pathol **219**: 356-64.

Kodama, M., Y. Kitadai, M. Tanaka, T. Kuwai, S. Tanaka, N. Oue, W. Yasui and K. Chayama (2008). "Vascular endothelial growth factor C stimulates progression of human gastric cancer via both autocrine and paracrine mechanisms." Clin Cancer Res **14**: 7205-14.

Kohler, G. and C. Milstein (1975). "Continuous cultures of fused cells secreting antibody of predefined specificity." Nature **256**: 495-7.

Komuro, H., S. Kaneko, M. Kaneko and Y. Nakanishi (2001). "Expression of angiogenic factors and tumor progression in human neuroblastoma." J Cancer Res Clin Oncol **127**: 739-43.

Kondo, H., M. Shiroishi, M. Matsushima, K. Tsumoto and I. Kumagai (1999). "Crystal structure of anti-Hen egg white lysozyme antibody (HyHEL-10) Fv-antigen complex. Local structural changes in the protein antigen and water-mediated interactions of Fv-antigen and light chain-heavy chain interfaces." J Biol Chem **274**: 27623-31.

Kondo, K., T. Kaneko, M. Baba and H. Konno (2007). "VEGF-C and VEGF-A synergistically enhance lymph node metastasis of gastric cancer." Biol Pharm Bull **30**: 633-7.

Kondo, R., S. Horai, Y. Satta and N. Takahata (1993). "Evolution of hominoid mitochondrial DNA with special reference to the silent substitution rate over the genome." J Mol Evol **36**: 517-31.

Koyama, Y., K. Kaneko, K. Akazawa, C. Kanbayashi, T. Kanda and K. Hatakeyama (2003). "Vascular endothelial growth factor-C and vascular endothelial growth factor-d messenger RNA expression in breast cancer: association with lymph node metastasis." Clin Breast Cancer **4**: 354-60.

Kriehuber, E., S. Breiteneder-Geleff, M. Groeger, A. Soleiman, S. F. Schoppmann, G. Stingl, D. Kerjaschki and D. Maurer (2001). "Isolation and characterization of dermal lymphatic and blood endothelial cells reveal stable and functionally specialized cell lineages." J Exp Med **194**: 797-808.

Krzystek-Korpacka, M., M. Matusiewicz, D. Diakowska, K. Grabowski, K. Blachut and T. Banas (2007). "Up-regulation of VEGF-C secreted by cancer cells and not VEGF-A correlates with clinical evaluation of lymph node metastasis in esophageal squamous cell carcinoma (ESCC)." Cancer Lett **249**: 171-7.

Kubo, H., R. Cao, E. Brakenhielm, T. Makinen, Y. Cao and K. Alitalo (2002). "Blockade of vascular endothelial growth factor receptor-3 signaling inhibits fibroblast growth factor-2-induced lymphangiogenesis in mouse cornea." Proc Natl Acad Sci U S A **99**: 8868-73.

Kubo, H., T. Fujiwara*, et al.* (2000). "Involvement of vascular endothelial growth factor receptor-3 in maintenance of integrity of endothelial cell lining during tumor angiogenesis." Blood **96**: 546-53.

Kunstfeld, R., S. Hirakawa*, et al.* (2004). "Induction of cutaneous delayed-type hypersensitivity reactions in VEGF-A transgenic mice results in chronic skin inflammation associated with persistent lymphatic hyperplasia." Blood **104**: 1048-57.

Kurahara, H., S. Takao, K. Maemura, H. Shinchi, S. Natsugoe and T. Aikou (2004). "Impact of vascular endothelial growth factor-C and -D expression in human pancreatic cancer: its relationship to lymph node metastasis." Clin Cancer Res **10**: 8413-20.

Laakkonen, P., M. Waltari*, et al.* (2007). "Vascular endothelial growth factor receptor 3 is involved in tumor angiogenesis and growth." Cancer Res **67**: 593-9.

Ladenson, R. C., D. L. Crimmins, Y. Landt and J. H. Ladenson (2006). "Isolation and characterization of a thermally stable recombinant anti-caffeine heavy-chain antibody fragment." Anal Chem **78**: 4501-8.

Lauwereys, M., M. Arbabi Ghahroudi, A. Desmyter, J. Kinne, W. Holzer, E. De Genst, L. Wyns and S. Muyldermans (1998). "Potent enzyme inhibitors derived from dromedary heavy-chain antibodies." Embo J **17**: 3512-20.

Leppanen, V. M., A. E. Prota*, et al.* (2010). "Structural determinants of growth factor binding and specificity by VEGF receptor 2." Proc Natl Acad Sci U S A **107**: 2425-30.

Leung, D. W., G. Cachianes, W. J. Kuang, D. V. Goeddel and N. Ferrara (1989). "Vascular endothelial growth factor is a secreted angiogenic mitogen." Science **246**: 1306-9.

Li, E., A. Pedraza, M. Bestagno, S. Mancardi, R. Sanchez and O. Burrone (1997). "Mammalian cell expression of dimeric small immune proteins (SIP)." Protein Eng **10**: 731-6.

Li, J. L. and A. L. Harris (2009). "Crosstalk of VEGF and Notch pathways in tumour angiogenesis: therapeutic implications." Front Biosci **14**: 3094-110.

Li, Q., X. Dong, W. Gu, X. Qiu and E. Wang (2003). "Clinical significance of co-expression of VEGF-C and VEGFR-3 in non-small cell lung cancer." Chin Med J (Engl) **116**: 727-30.

Liang, W. C., X. Wu*, et al.* (2006). "Cross-species vascular endothelial growth factor (VEGF)-blocking antibodies completely inhibit the growth of human tumor xenografts and measure the contribution of stromal VEGF." J Biol Chem **281**: 951-61.

Lin, J., A. S. Lalani*, et al.* (2005). "Inhibition of lymphogenous metastasis using adeno-associated virus-mediated gene transfer of a soluble VEGFR-3 decoy receptor." Cancer Res **65**: 6901-9.

Lindenmann, J. (1984). "Origin of the terms 'antibody' and 'antigen'." Scand J Immunol **19**: 281-5.

Liu, X. E., X. D. Sun and J. M. Wu (2004). "Expression and significance of VEGF-C and FLT-4 in gastric cancer." World J Gastroenterol **10**: 352-5.

Liu, Y., P. Hamrah, Q. Zhang, A. W. Taylor and M. R. Dana (2002). "Draining lymph nodes of corneal transplant hosts exhibit evidence for donor major histocompatibility complex (MHC) class II-positive dendritic cells derived from MHC class II-negative grafts." J Exp Med **195**: 259-68.

Loges, S., H. Clausen*, et al.* (2007). "Determination of microvessel density by quantitative real-time PCR in esophageal cancer: correlation with histologic methods, angiogenic growth factor expression, and lymph node metastasis." Clin Cancer Res **13**: 76-80.

Lynch, P. M., F. A. Delano and G. W. Schmid-Schonbein (2007). "The primary valves in the initial lymphatics during inflammation." Lymphat Res Biol **5**: 3-10.

Maeda, K., M. Yashiro*, et al.* (2003). "Correlation between vascular endothelial growth factor C expression and lymph node metastasis in T1 carcinoma of the colon and rectum." Surg Today **33**: 736-9.

Maglione, D., V. Guerriero, G. Viglietto, P. Delli-Bovi and M. G. Persico (1991). "Isolation of a human placenta cDNA coding for a protein related to the vascular permeability factor." Proc Natl Acad Sci U S A **88**: 9267-71.

Makinen, T., T. Veikkola*, et al.* (2001). "Isolated lymphatic endothelial cells transduce growth, survival and migratory signals via the VEGF-C/D receptor VEGFR-3." Embo J **20**: 4762-73.

Mandriota, S. J., L. Jussila*, et al.* (2001). "Vascular endothelial growth factor-C-mediated lymphangiogenesis promotes tumour metastasis." Embo J **20**: 672-82.

Marchio, S., L. Primo, M. Pagano, G. Palestro, A. Albini, T. Veikkola, I. Cascone, K. Alitalo and F. Bussolino (1999). "Vascular endothelial growth factor-C stimulates the migration and proliferation of Kaposi's sarcoma cells." J Biol Chem **274**: 27617-22.

Marks, J. D., H. R. Hoogenboom, T. P. Bonnert, J. McCafferty, A. D. Griffiths and G. Winter (1991). "By-passing immunization. Human antibodies from V-gene libraries displayed on phage." J Mol Biol **222**: 581-97.

Matsumoto, T., S. Bohman*, et al.* (2005). "VEGF receptor-2 Y951 signaling and a role for the adapter molecule TSAd in tumor angiogenesis." Embo J **24**: 2342-53.

Matsuura, M., M. Onimaru, Y. Yonemitsu, H. Suzuki, T. Nakano, H. Ishibashi, K. Shirasuna and K. Sueishi (2009). "Autocrine loop between vascular endothelial growth factor (VEGF)-C and VEGF receptor-3 positively regulates tumor-associated lymphangiogenesis in oral squamoid cancer cells." Am J Pathol **175**: 1709-21.

McColl, B. K., M. E. Baldwin, S. Roufail, C. Freeman, R. L. Moritz, R. J. Simpson, K. Alitalo, S. A. Stacker and M. G. Achen (2003). "Plasmin activates the lymphangiogenic growth factors VEGF-C and VEGF-D." J Exp Med **198**: 863-8.

McColl, B. K., K. Paavonen*, et al.* (2007). "Proprotein convertases promote processing of VEGF-D, a critical step for binding the angiogenic receptor VEGFR-2." Faseb J **21**: 1088-98.

McDonald, N. Q. and W. A. Hendrickson (1993). "A structural superfamily of growth factors containing a cystine knot motif." Cell **73**: 421-4.

Menrad, A. and H. D. Menssen (2005). "ED-B fibronectin as a target for antibody-based cancer treatments." Expert Opin Ther Targets **9**: 491-500.

Mentzel, T. and H. Kutzner (2002). "[Tumors of the lymphatic vessel of the skin and soft tissue]." Pathologe **23**: 118-27.

Miller, K., M. Wang, J. Gralow, M. Dickler, M. Cobleigh, E. A. Perez, T. Shenkier, D. Cella and N. E. Davidson (2007). "Paclitaxel plus bevacizumab versus paclitaxel alone for metastatic breast cancer." N Engl J Med **357**: 2666-76.

Mitsuhashi, A., K. Suzuka, K. Yamazawa, H. Matsui, K. Seki and S. Sekiya (2005). "Serum vascular endothelial growth factor (VEGF) and VEGF-C levels as tumor markers in patients with cervical carcinoma." Cancer **103**: 724-30.

Moehler, T. M., A. D. Ho, H. Goldschmidt and B. Barlogie (2003). "Angiogenesis in hematologic malignancies." Crit Rev Oncol Hematol **45**: 227-44.

Mohammed, R. A., A. Green, S. El-Shikh, E. C. Paish, I. O. Ellis and S. G. Martin (2007). "Prognostic significance of vascular endothelial cell growth factors -A, -C and -D in breast cancer and their relationship with angio- and lymphangiogenesis." Br J Cancer **96**: 1092-100.

Morisada, T., Y. Oike*, et al.* (2005). "Angiopoietin-1 promotes LYVE-1-positive lymphatic vessel formation." Blood **105**: 4649-56.
Muller, N., M. Derouazi, F. Van Tilborgh, S. Wulhfard, D. L. Hacker, M. Jordan and F. M. Wurm (2007). "Scalable transient gene expression in Chinese hamster ovary cells in instrumented and non-instrumented cultivation systems." Biotechnol Lett **29**: 703-11.
Muller, Y. A., C. Heiring, R. Misselwitz, K. Welfle and H. Welfle (2002). "The cystine knot promotes folding and not thermodynamic stability in vascular endothelial growth factor." J Biol Chem **277**: 43410-6.
Muyldermans, S. (2001). "Single domain camel antibodies: current status." J Biotechnol **74**: 277-302.
Muyldermans, S., C. Cambillau and L. Wyns (2001). "Recognition of antigens by single-domain antibody fragments: the superfluous luxury of paired domains." Trends Biochem Sci **26**: 230-5.
Muyldermans, S. and M. Lauwereys (1999). "Unique single-domain antigen binding fragments derived from naturally occurring camel heavy-chain antibodies." J Mol Recognit **12**: 131-40.
Nagy, J. A., E. Vasile*, et al.* (2002). "Vascular permeability factor/vascular endothelial growth factor induces lymphangiogenesis as well as angiogenesis." J Exp Med **196**: 1497-506.
Nakamura, Y., H. Yasuoka, M. Tsujimoto, S. Imabun, M. Nakahara, K. Nakao, M. Nakamura, I. Mori and K. Kakudo (2005). "Lymph vessel density correlates with nodal status, VEGF-C expression, and prognosis in breast cancer." Breast Cancer Res Treat **91**: 125-32.
Nakamura, Y., H. Yasuoka*, et al.* (2003a). "Prognostic significance of vascular endothelial growth factor D in breast carcinoma with long-term follow-up." Clin Cancer Res **9**: 716-21.
Nakamura, Y., H. Yasuoka*, et al.* (2003b). "Clinicopathological significance of vascular endothelial growth factor-C in breast carcinoma with long-term follow-up." Mod Pathol **16**: 309-14.
Niki, T., S. Iba, M. Tokunou, T. Yamada, Y. Matsuno and S. Hirohashi (2000). "Expression of vascular endothelial growth factors A, B, C, and D and their relationships to lymph node status in lung adenocarcinoma." Clin Cancer Res **6**: 2431-9.
Nimmerjahn, F. and J. V. Ravetch (2006). "Fcgamma receptors: old friends and new family members." Immunity **24**: 19-28.
Nishida, N., H. Yano, K. Komai, T. Nishida, T. Kamura and M. Kojiro (2004). "Vascular endothelial growth factor C and vascular endothelial growth factor receptor 2 are related closely to the prognosis of patients with ovarian carcinoma." Cancer **101**: 1364-74.
O-charoenrat, P., P. Rhys-Evans and S. A. Eccles (2001). "Expression of vascular endothelial growth factor family members in head and neck squamous cell carcinoma correlates with lymph node metastasis." Cancer **92**: 556-68.
Ogawa, S., A. Oku, A. Sawano, S. Yamaguchi, Y. Yazaki and M. Shibuya (1998). "A novel type of vascular endothelial growth factor, VEGF-E (NZ-7 VEGF), preferentially utilizes KDR/Flk-1 receptor and carries a potent mitotic activity without heparin-binding domain." J Biol Chem **273**: 31273-82.
Olofsson, B., K. Pajusola*, et al.* (1996). "Vascular endothelial growth factor B, a novel growth factor for endothelial cells." Proc Natl Acad Sci U S A **93**: 2576-81.

Olsson, A. K., A. Dimberg, J. Kreuger and L. Claesson-Welsh (2006). "VEGF receptor signalling - in control of vascular function." Nat Rev Mol Cell Biol **7**: 359-71.

Onogawa, S., Y. Kitadai*, et al.* (2005). "Expression of vascular endothelial growth factor (VEGF)-C and VEGF-D in early gastric carcinoma: correlation with clinicopathological parameters." Cancer Lett **226**: 85-90.

Onogawa, S., Y. Kitadai, S. Tanaka, T. Kuwai, S. Kimura and K. Chayama (2004). "Expression of VEGF-C and VEGF-D at the invasive edge correlates with lymph node metastasis and prognosis of patients with colorectal carcinoma." Cancer Sci **95**: 32-9.

Orlandini, M., L. Marconcini, R. Ferruzzi and S. Oliviero (1996). "Identification of a c-fos-induced gene that is related to the platelet-derived growth factor/vascular endothelial growth factor family." Proc Natl Acad Sci U S A **93**: 11675-80.

Orlandini, M., A. Spreafico, M. Bardelli, M. Rocchigiani, A. Salameh, S. Nucciotti, C. Capperucci, B. Frediani and S. Oliviero (2006). "Vascular endothelial growth factor-D activates VEGFR-3 expressed in osteoblasts inducing their differentiation." J Biol Chem **281**: 17961-7.

Osterborg, A., M. J. Dyer, D. Bunjes, G. A. Pangalis, Y. Bastion, D. Catovsky and H. Mellstedt (1997). "Phase II multicenter study of human CD52 antibody in previously treated chronic lymphocytic leukemia. European Study Group of CAMPATH-1H Treatment in Chronic Lymphocytic Leukemia." J Clin Oncol **15**: 1567-74.

Paavonen, K., N. Horelli-Kuitunen*, et al.* (1996). "Novel human vascular endothelial growth factor genes VEGF-B and VEGF-C localize to chromosomes 11q13 and 4q34, respectively." Circulation **93**: 1079-82.

Paavonen, K., J. Mandelin, T. Partanen, L. Jussila, T. F. Li, A. Ristimaki, K. Alitalo and Y. T. Konttinen (2002). "Vascular endothelial growth factors C and D and their VEGFR-2 and 3 receptors in blood and lymphatic vessels in healthy and arthritic synovium." J Rheumatol **29**: 39-45.

Paavonen, K., P. Puolakkainen, L. Jussila, T. Jahkola and K. Alitalo (2000). "Vascular endothelial growth factor receptor-3 in lymphangiogenesis in wound healing." Am J Pathol **156**: 1499-504.

Pajusola, K., O. Aprelikova, G. Pelicci, H. Weich, L. Claesson-Welsh and K. Alitalo (1994). "Signalling properties of FLT4, a proteolytically processed receptor tyrosine kinase related to two VEGF receptors." Oncogene **9**: 3545-55.

Partanen, T. A., K. Alitalo and M. Miettinen (1999). "Lack of lymphatic vascular specificity of vascular endothelial growth factor receptor 3 in 185 vascular tumors." Cancer **86**: 2406-12.

Partanen, T. A., J. Arola, A. Saaristo, L. Jussila, A. Ora, M. Miettinen, S. A. Stacker, M. G. Achen and K. Alitalo (2000). "VEGF-C and VEGF-D expression in neuroendocrine cells and their receptor, VEGFR-3, in fenestrated blood vessels in human tissues." Faseb J **14**: 2087-96.

Pluckthun, A. (1992). "Mono- and bivalent antibody fragments produced in Escherichia coli: engineering, folding and antigen binding." Immunol Rev **130**: 151-88.

Porter, R. R. (1967). "The structure of the heavy chain of immunoglobulin and its relevance to the nature of the antibody-combining site. The Second CIBA Medal Lecture." Biochem J **105**: 417-26.

Potter, K. N., Y. Li, V. Pascual and J. D. Capra (1997). "Staphylococcal protein A binding to VH3 encoded immunoglobulins." Int Rev Immunol **14**: 291-308.

Presta, L. G., H. Chen, S. J. O'Connor, V. Chisholm, Y. G. Meng, L. Krummen, M. Winkler and N. Ferrara (1997). "Humanization of an anti-vascular endothelial growth factor monoclonal antibody for the therapy of solid tumors and other disorders." Cancer Res **57**: 4593-9.

Radstake, T. R., M. Svenson, A. M. Eijsbouts, F. H. van den Hoogen, C. Enevold, P. L. van Riel and K. Bendtzen (2009). "Formation of antibodies against infliximab and adalimumab strongly correlates with functional drug levels and clinical responses in rheumatoid arthritis." Ann Rheum Dis **68**: 1739-45.

Randolph, G. J., V. Angeli and M. A. Swartz (2005). "Dendritic-cell trafficking to lymph nodes through lymphatic vessels." Nat Rev Immunol **5**: 617-28.

Reichert, J. M. (2001). "Monoclonal antibodies in the clinic." Nat Biotechnol **19**: 819-22.

Riechmann, L., M. Clark, H. Waldmann and G. Winter (1988). "Reshaping human antibodies for therapy." Nature **332**: 323-7.

Rinderknecht, M. and M. Detmar (2008). "Tumor lymphangiogenesis and melanoma metastasis." J Cell Physiol **216**: 347-54.

Rinderknecht, M. and M. Detmar (2009). Molecular mechanisms of lymph-node metastasis. Lymphangiogenesis in Cancer Metastasis. S. A. A. Stacker, M. G., Springer Netherlands. **13:** 55-82.

Ristimaki, A., K. Narko, B. Enholm, V. Joukov and K. Alitalo (1998). "Proinflammatory cytokines regulate expression of the lymphatic endothelial mitogen vascular endothelial growth factor-C." J Biol Chem **273**: 8413-8.

Roberts, N., B. Kloos, M. Cassella, S. Podgrabinska, K. Persaud, Y. Wu, B. Pytowski and M. Skobe (2006). "Inhibition of VEGFR-3 activation with the antagonistic antibody more potently suppresses lymph node and distant metastases than inactivation of VEGFR-2." Cancer Res **66**: 2650-7.

Scheidegger, P., W. Weiglhofer, S. Suarez, B. Kaser-Hotz, R. Steiner, K. Ballmer-Hofer and R. Jaussi (1999). "Vascular endothelial growth factor (VEGF) and its receptors in tumor-bearing dogs." Biol Chem **380**: 1449-54.

Schietroma, C., F. Cianfarani, P. M. Lacal, T. Odorisio, A. Orecchia, J. Kanitakis, S. D'Atri, C. M. Failla and G. Zambruno (2003). "Vascular endothelial growth factor-C expression correlates with lymph node localization of human melanoma metastases." Cancer **98**: 789-97.

Schliemann, C., A. Palumbo, K. Zuberbuhler, A. Villa, M. Kaspar, E. Trachsel, W. Klapper, H. D. Menssen and D. Neri (2009). "Complete eradication of human B-cell lymphoma xenografts using rituximab in combination with the immunocytokine L19-IL2." Blood **113**: 2275-83.

Schonthaler, H. B., R. Huggenberger, S. K. Wculek, M. Detmar and E. F. Wagner (2009). "Systemic anti-VEGF treatment strongly reduces skin inflammation in a mouse model of psoriasis." Proc Natl Acad Sci U S A **106**: 21264-9.

Shida, A., S. Fujioka, K. Kobayashi, Y. Ishibashi, H. Nimura, N. Mitsumori and K. Yanaga (2006). "Expression of vascular endothelial growth factor (VEGF)-C and -D in gastric carcinoma." Int J Clin Oncol **11**: 38-43.

Shimizu, K., H. Kubo*, et al.* (2004). "Suppression of VEGFR-3 signaling inhibits lymph node metastasis in gastric cancer." Cancer Sci **95**: 328-33.

Shin, H. Y., M. L. Smith, K. J. Toy, P. M. Williams, R. Bizios and M. E. Gerritsen (2002). "VEGF-C mediates cyclic pressure-induced endothelial cell proliferation." Physiol Genomics **11**: 245-51.

Shin, J. W., M. Min*, et al.* (2006). "Prox1 promotes lineage-specific expression of fibroblast growth factor (FGF) receptor-3 in lymphatic endothelium: a role for FGF signaling in lymphangiogenesis." Mol Biol Cell **17**: 576-84.

Shintani, S., C. Li, T. Ishikawa, M. Mihara, K. Nakashiro and H. Hamakawa (2004). "Expression of vascular endothelial growth factor A, B, C, and D in oral squamous cell carcinoma." Oral Oncol **40**: 13-20.

Siegfried, G., A. Basak, J. A. Cromlish, S. Benjannet, J. Marcinkiewicz, M. Chretien, N. G. Seidah and A. M. Khatib (2003). "The secretory proprotein convertases furin, PC5, and PC7 activate VEGF-C to induce tumorigenesis." J Clin Invest **111**: 1723-32.

Silacci, M., S. Brack, G. Schirru, J. Marlind, A. Ettorre, A. Merlo, F. Viti and D. Neri (2005). "Design, construction, and characterization of a large synthetic human antibody phage display library." Proteomics **5**: 2340-50.

Sinclair, N. R. (2004). "B cell/antibody tolerance to our own antigens." Front Biosci **9**: 3019-28.

Sipos, B., M. Kojima*, et al.* (2005). "Lymphatic spread of ductal pancreatic adenocarcinoma is independent of lymphangiogenesis." J Pathol **207**: 301-12.

Skobe, M., L. F. Brown, K. Tognazzi, R. K. Ganju, B. J. Dezube, K. Alitalo and M. Detmar (1999). "Vascular endothelial growth factor-C (VEGF-C) and its receptors KDR and flt-4 are expressed in AIDS-associated Kaposi's sarcoma." J Invest Dermatol **113**: 1047-53.

Skobe, M., T. Hawighorst*, et al.* (2001). "Induction of tumor lymphangiogenesis by VEGF-C promotes breast cancer metastasis." Nat Med **7**: 192-8.

Smyth, M. J., E. Cretney*, et al.* (2005). "Activation of NK cell cytotoxicity." Mol Immunol **42**: 501-10.

Soumaoro, L. T., H. Uetake, Y. Takagi, S. Iida, T. Higuchi, M. Yasuno, M. Enomoto and K. Sugihara (2006). "Coexpression of VEGF-C and Cox-2 in human colorectal cancer and its association with lymph node metastasis." Dis Colon Rectum **49**: 392-8.

Stacker, S. A., M. E. Baldwin and M. G. Achen (2002). "The role of tumor lymphangiogenesis in metastatic spread." Faseb J **16**: 922-34.

Stacker, S. A., C. Caesar*, et al.* (2001). "VEGF-D promotes the metastatic spread of tumor cells via the lymphatics." Nat Med **7**: 186-91.

Stacker, S. A., K. Stenvers*, et al.* (1999). "Biosynthesis of vascular endothelial growth factor-D involves proteolytic processing which generates non-covalent homodimers." J Biol Chem **274**: 32127-36.

Stearns, M. E., M. Wang, Y. Hu, G. Kim and F. U. Garcia (2004). "Expression of a flt-4 (VEGFR3) splicing variant in primary human prostate tumors. VEGF D and flt-4t(Delta773-1081) overexpression is diagnostic for sentinel lymph node metastasis." Lab Invest **84**: 785-95.

Steplewski, Z., M. D. Lubeck and H. Koprowski (1983). "Human macrophages armed with murine immunoglobulin G2a antibodies to tumors destroy human cancer cells." Science **221**: 865-7.

Strutzenberger, K., N. Borth, R. Kunert, W. Steinfellner and H. Katinger (1999). "Changes during subclone development and ageing of human antibody-producing recombinant CHO cells." J Biotechnol **69**: 215-26.

Su, J. L., J. Y. Shih, M. L. Yen, Y. M. Jeng, C. C. Chang, C. Y. Hsieh, L. H. Wei, P. C. Yang and M. L. Kuo (2004). "Cyclooxygenase-2 induces EP1- and HER-2/Neu-dependent vascular endothelial growth factor-C up-regulation: a novel

mechanism of lymphangiogenesis in lung adenocarcinoma." Cancer Res **64**: 554-64.
Summers, J., M. H. Cohen, P. Keegan and R. Pazdur (2010). "FDA drug approval summary: bevacizumab plus interferon for advanced renal cell carcinoma." Oncologist **15**: 104-11.
Suzuki, K., T. Morita and A. Tokue (2005). "Vascular endothelial growth factor-C (VEGF-C) expression predicts lymph node metastasis of transitional cell carcinoma of the bladder." Int J Urol **12**: 152-8.
Takahashi, A., K. Kono, J. Itakura, H. Amemiya, R. Feng Tang, H. Iizuka, H. Fujii and Y. Matsumoto (2002). "Correlation of vascular endothelial growth factor-C expression with tumor-infiltrating dendritic cells in gastric cancer." Oncology **62**: 121-7.
Takahashi, H., S. Hattori, A. Iwamatsu, H. Takizawa and M. Shibuya (2004). "A novel snake venom vascular endothelial growth factor (VEGF) predominantly induces vascular permeability through preferential signaling via VEGF receptor-1." J Biol Chem **279**: 46304-14.
Takahashi, H. and M. Shibuya (2005). "The vascular endothelial growth factor (VEGF)/VEGF receptor system and its role under physiological and pathological conditions." Clin Sci (Lond) **109**: 227-41.
Takahashi, T., S. Yamaguchi, K. Chida and M. Shibuya (2001). "A single autophosphorylation site on KDR/Flk-1 is essential for VEGF-A-dependent activation of PLC-gamma and DNA synthesis in vascular endothelial cells." Embo J **20**: 2768-78.
Takeuchi, H., A. Bilchik, S. Saha, R. Turner, D. Wiese, M. Tanaka, C. Kuo, H. J. Wang and D. S. Hoon (2003). "c-MET expression level in primary colon cancer: a predictor of tumor invasion and lymph node metastases." Clin Cancer Res **9**: 1480-8.
Tammela, T., A. Saaristo*, et al.* (2005). "Angiopoietin-1 promotes lymphatic sprouting and hyperplasia." Blood **105**: 4642-8.
Tamura, M. and Y. Ohta (2003). "Serum vascular endothelial growth factor-C level in patients with primary nonsmall cell lung carcinoma: a possible diagnostic tool for lymph node metastasis." Cancer **98**: 1217-22.
Timoshenko, A. V., S. Rastogi and P. K. Lala (2007). "Migration-promoting role of VEGF-C and VEGF-C binding receptors in human breast cancer cells." Br J Cancer **97**: 1090-8.
Tjandra, J. J., L. Ramadi and I. F. McKenzie (1990). "Development of human anti-murine antibody (HAMA) response in patients." Immunol Cell Biol **68 (Pt 6)**: 367-76.
Tomanek, R. J., J. S. Holifield, R. S. Reiter, A. Sandra and J. J. Lin (2002). "Role of VEGF family members and receptors in coronary vessel formation." Dev Dyn **225**: 233-40.
Tomlinson, I. M., G. P. Cook, N. P. Carter, R. Elaswarapu, S. Smith, G. Walter, L. Buluwela, T. H. Rabbitts and G. Winter (1994). "Human immunoglobulin VH and D segments on chromosomes 15q11.2 and 16p11.2." Hum Mol Genet **3**: 853-60.
Tomlinson, I. M., J. P. Cox, E. Gherardi, A. M. Lesk and C. Chothia (1995). "The structural repertoire of the human V kappa domain." Embo J **14**: 4628-38.
Tschopp, J., D. Masson and K. K. Stanley (1986). "Structural/functional similarity between proteins involved in complement- and cytotoxic T-lymphocyte-mediated cytolysis." Nature **322**: 831-4.

Ueda, M., Y. C. Hung*, et al.* (2005). "Vascular endothelial growth factor-C expression and invasive phenotype in ovarian carcinomas." Clin Cancer Res **11**: 3225-32.

Ueda, M., Y. Terai, Y. Yamashita, K. Kumagai, K. Ueki, H. Yamaguchi, D. Akise, Y. C. Hung and M. Ueki (2002). "Correlation between vascular endothelial growth factor-C expression and invasion phenotype in cervical carcinomas." Int J Cancer **98**: 335-43.

Valtola, R., P. Salven*, et al.* (1999). "VEGFR-3 and its ligand VEGF-C are associated with angiogenesis in breast cancer." Am J Pathol **154**: 1381-90.

Van den Eynden, G. G., M. K. Vandenberghe, P. J. van Dam, C. G. Colpaert, P. van Dam, L. Y. Dirix, P. B. Vermeulen and E. A. Van Marck (2007). "Increased sentinel lymph node lymphangiogenesis is associated with nonsentinel axillary lymph node involvement in breast cancer patients with a positive sentinel node." Clin Cancer Res **13**: 5391-7.

van der Linden, R. H., L. G. Frenken*, et al.* (1999). "Comparison of physical chemical properties of llama VHH antibody fragments and mouse monoclonal antibodies." Biochim Biophys Acta **1431**: 37-46.

Van Trappen, P. O., D. Steele*, et al.* (2003). "Expression of vascular endothelial growth factor (VEGF)-C and VEGF-D, and their receptor VEGFR-3, during different stages of cervical carcinogenesis." J Pathol **201**: 544-54.

Vassar, R., M. Rosenberg, S. Ross, A. Tyner and E. Fuchs (1989). "Tissue-specific and differentiation-specific expression of a human K14 keratin gene in transgenic mice." Proc Natl Acad Sci U S A **86**: 1563-7.

Veikkola, T., L. Jussila*, et al.* (2001). "Signalling via vascular endothelial growth factor receptor-3 is sufficient for lymphangiogenesis in transgenic mice." Embo J **20**: 1223-31.

Vihinen, P. P., J. Hilli, M. S. Vuoristo, K. J. Syrjanen, V. M. Kahari and S. O. Pyrhonen (2007). "Serum VEGF-C is associated with metastatic site in patients with malignant melanoma." Acta Oncol **46**: 678-84.

Villa, A., E. Trachsel, M. Kaspar, C. Schliemann, R. Sommavilla, J. N. Rybak, C. Rosli, L. Borsi and D. Neri (2008). "A high-affinity human monoclonal antibody specific to the alternatively spliced EDA domain of fibronectin efficiently targets tumor neo-vasculature in vivo." Int J Cancer **122**: 2405-13.

Viti, F., F. Nilsson, S. Demartis, A. Huber and D. Neri (2000). "Design and use of phage display libraries for the selection of antibodies and enzymes." Methods Enzymol **326**: 480-505.

Vitt, U. A., S. Y. Hsu and A. J. Hsueh (2001). "Evolution and classification of cystine knot-containing hormones and related extracellular signaling molecules." Mol Endocrinol **15**: 681-94.

Vogel, F. and M. Kopun (1977). "Higher frequencies of transitions among point mutations." J Mol Evol **9**: 159-80.

Von Marschall, Z., A. Scholz*, et al.* (2005). "Vascular endothelial growth factor-D induces lymphangiogenesis and lymphatic metastasis in models of ductal pancreatic cancer." Int J Oncol **27**: 669-79.

Weng, W. K. and R. Levy (2003). "Two immunoglobulin G fragment C receptor polymorphisms independently predict response to rituximab in patients with follicular lymphoma." J Clin Oncol **21**: 3940-7.

White, J. D., P. W. Hewett, D. Kosuge, T. McCulloch, B. C. Enholm, J. Carmichael and J. C. Murray (2002). "Vascular endothelial growth factor-D expression is

an independent prognostic marker for survival in colorectal carcinoma." Cancer Res **62**: 1669-75.
Willett, C. G., Y. Boucher*, et al.* (2004). "Direct evidence that the VEGF-specific antibody bevacizumab has antivascular effects in human rectal cancer." Nat Med **10**: 145-7.
Worn, A. and A. Pluckthun (2001). "Stability engineering of antibody single-chain Fv fragments." J Mol Biol **305**: 989-1010.
Wulhfard, S., S. Tissot, S. Bouchet, J. Cevey, M. De Jesus, D. L. Hacker and F. M. Wurm (2008). "Mild hypothermia improves transient gene expression yields several fold in Chinese hamster ovary cells." Biotechnol Prog **24**: 458-65.
Yamada, Y., J. Nezu, M. Shimane and Y. Hirata (1997). "Molecular cloning of a novel vascular endothelial growth factor, VEGF-D." Genomics **42**: 483-8.
Yan, C., J. Zhang*, et al.* (2004a). "Vascular Endothelial Growth Factor C Expression in Gastric Carcinoma and Its Relationship with Lymph Node Metastasis." The Chinese-German Journal of Clinical Oncology **3**: 74-77.
Yan, C., Z. G. Zhu*, et al.* (2004b). "Expression of vascular endothelial growth factor C and chemokine receptor CCR7 in gastric carcinoma and their values in predicting lymph node metastasis." World J Gastroenterol **10**: 783-90.
Yang, A. D., T. W. Bauer, E. R. Camp, R. Somcio, W. Liu, F. Fan and L. M. Ellis (2005). "Improving delivery of antineoplastic agents with anti-vascular endothelial growth factor therapy." Cancer **103**: 1561-70.
Yasuoka, H., Y. Nakamura, H. Zuo, W. Tang, Y. Takamura, A. Miyauchi, M. Nakamura, I. Mori and K. Kakudo (2005). "VEGF-D expression and lymph vessels play an important role for lymph node metastasis in papillary thyroid carcinoma." Mod Pathol **18**: 1127-33.
Yokoyama, Y., D. S. Charnock-Jones*, et al.* (2003). "Expression of vascular endothelial growth factor (VEGF)-D and its receptor, VEGF receptor 3, as a prognostic factor in endometrial carcinoma." Clin Cancer Res **9**: 1361-9.
Yonemura, Y., Y. Endo*, et al.* (1999). "Role of vascular endothelial growth factor C expression in the development of lymph node metastasis in gastric cancer." Clin Cancer Res **5**: 1823-9.
Yu, X. M., C. Y. Lo, W. F. Chan, K. Y. Lam, P. Leung and J. M. Luk (2005). "Increased expression of vascular endothelial growth factor C in papillary thyroid carcinoma correlates with cervical lymph node metastases." Clin Cancer Res **11**: 8063-9.
Yuan, L., D. Moyon, L. Pardanaud, C. Breant, M. J. Karkkainen, K. Alitalo and A. Eichmann (2002). "Abnormal lymphatic vessel development in neuropilin 2 mutant mice." Development **129**: 4797-806.
Yuanming, L., G. Feng, T. Lei and W. Ying (2007). "Quantitative analysis of lymphangiogenic markers in human gastroenteric tumor." Arch Med Res **38**: 106-12.
Zhang, J., J. Ji, F. Yuan, L. Zhu, C. Yan, Y. Y. Yu, B. Y. Liu, Z. G. Zhu and Y. Z. Lin (2005). "Cyclooxygenase-2 expression is associated with VEGF-C and lymph node metastases in gastric cancer patients." Biomed Pharmacother **59 Suppl 2**: S285-8.
Zhang, Q., R. Guo*, et al.* (2008a). "VEGF-C, a lymphatic growth factor, is a RANKL target gene in osteoclasts that enhances osteoclastic bone resorption through an autocrine mechanism." J Biol Chem **283**: 13491-9.

Zhang, X. H., D. P. Huang, G. L. Guo, G. R. Chen, H. X. Zhang, L. Wan and S. Y. Chen (2008b). "Coexpression of VEGF-C and COX-2 and its association with lymphangiogenesis in human breast cancer." BMC Cancer **8**: 4.

Zhao, B., A. Ma, J. Cai and M. Boulton (2006). "VEGF-A regulates the expression of VEGF-C in human retinal pigment epithelial cells." Br J Ophthalmol **90**: 1052-9.

Zhao, B., G. Smith, J. Cai, A. Ma and M. Boulton (2007). "Vascular endothelial growth factor C promotes survival of retinal vascular endothelial cells via vascular endothelial growth factor receptor-2." Br J Ophthalmol **91**: 538-45.

Zhou, H., Y. Wang, W. Wang, J. Jia, Y. Li, Q. Wang, Y. Wu and J. Tang (2009). "Generation of monoclonal antibodies against highly conserved antigens." PLoS One **4**: e6087.

Zorzetto, N. L., W. Ripari, V. De Freitas and G. Seullner (1977). "Anatomical observations on the ending of the human thoracic duct." J Morphol **153**: 363-9.

Zu, X., Z. Tang, Y. Li, N. Gao, J. Ding and L. Qi (2006). "Vascular endothelial growth factor-C expression in bladder transitional cell cancer and its relationship to lymph node metastasis." BJU Int **98**: 1090-3.

Zuberbuhler, K., A. Palumbo, C. Bacci, L. Giovannoni, R. Sommavilla, M. Kaspar, E. Trachsel and D. Neri (2009). "A general method for the selection of high-level scFv and IgG antibody expression by stably transfected mammalian cells." Protein Eng Des Sel **22**: 169-74.